Genetic Factors affecting the RNA interference pathway of *Aedes aegypti* mosquitoes

Mary Etna Richter Haac

Dissertation submitted to the faculty of the Virginia Polytechnic Institute and State University in partial fulfillment of the requirements for the degree of

Doctor of Philosophy
In
Entomology

Zach N. Adelman, Chair
Kevin M. Myles
Richard D. Fell
Xiang-Jin Meng
Liqing Q. Zhang

December 5, 2013
Blacksburg, VA

Keywords: mosquito, *Aedes aegypti*, RNA interference

Genetic Factors affecting the RNA interference pathway of *Aedes aegypti* mosquitoes

Mary Etna Richter Haac

Abstract

Aedes aegypti mosquitoes are the vectors of many significant arboviruses that cause tremendous social and economic impact. RNA interference (RNAi) plays a crucial role in the vector competence of mosquitoes and is often targeted in studies involving mosquito innate immunity, genetics-based vector control strategies, and the development of viral-resistant transgenic mosquitoes. In general, RNA interference is induced by double stranded RNA (dsRNA) and results in the inhibition of cognate gene expression. There are several different RNA interference pathways, with distinct functions and mechanisms. The micro RNA pathway is important for endogenous gene regulation and development. The endogenous small interfering RNA (endo-siRNA) pathway functions in gene regulation and protection of the genome from the deleterious effects of transposable elements. The exogenous siRNA (exo-siRNA) pathway is a major contributor to mosquito innate immunity and vector competence by limiting viral replication during infection. Lastly, the piwi RNA (piRNA) pathway primarily functions in protecting the genome from the deleterious effects of transposable elements.

While the structure and function of many genes involved in *Drosophila* RNAi have been characterized, the corresponding mosquito orthologs have only been peripherally described or remain unknown. Thus, the overall purpose of this study is to improve the understanding of mosquito RNAi mechanisms by identifying and analyzing genetic factors involved in the various pathways. This research especially focuses on characterizing and analyzing putative double-

stranded RNA binding proteins (dsRBPs) important to the function of the RNAi initiator and effector complexes. Two genes, *r2d2* and *r3d1* are orthologs of *Drosophila* genes known to have important roles in the RNAi initiator complex. A third member of the same family, which we refer to as *extra loquacious* (*exloqs*), appears to have no known orthologs outside of the *Aedes* genus. Structural characterization of these genes included identification of single nucleotide polymorphisms (SNPs), novel exons and alternative splice variants. RT-PCR assays were utilized to examine differential expression of all three genes in specific tissues and developmental stages. Sub-cellular fractionation assays enabled intracellular localization of the RNAi proteins within *Ae. aegypti* cells. Co-immunoprecipitation of tagged dsRBPs revealed protein-protein interactions between specific dsRBPs and known RNAi factors. In addition, an exo-siRNA sensor was designed and tested *in-vivo* and *in-vitro* with the purpose of facilitating the identification of novel genetic factors involved in this anti-viral pathway. Lastly, TALEN-based gene disruption was successfully employed to knockout the *exloqs* gene in *Ae. aegypti* mosquitoes, enabling further analysis into the function of this gene. The research described in this document provides further insight into mosquito innate immunity and gene regulation, which is important to the advancement of genetics-based vector control strategies.

Acknowledgements

I would like to thank everyone who has made this accomplishment possible. I thank my husband, Ryan for his endless love and support, and for helping me find balance by motivating me to try new things and delve deeper into the fields I love. My brother, Luis Carlos, our many conversations on life and spirituality have helped me maintain perspective and kept me from getting too lost in on-going challenges and doubts. My parents, Charles and Etna, for the love, encouragement, confidence, patience, and wisdom they have imparted throughout my life. Without them, I would not be here today. I am also very grateful to my friends and family outside of work. Thank you for believing in me and brightening my life. Jen and Allegra, for sharing the gift of dance with me, including its many spiritual and physical aspects. These things have been essential to my mental and physical health, without which I could never have made it this far.

I thank my advisor, Dr. Adelman, for his guidance and mentorship throughout the last five years, for answering my many questions, and considering my ideas in regards to my research. I also thank my advisory committee, Dr. Myles, Dr. Meng, Dr. Fell, and Dr. Zhang, for their advice, diverse perspectives, and interesting conversations that have facilitated my research and professional growth. In addition, I am thankful to Dr. Fell and Dr. Zajac for the opportunity to work in their labs as an undergraduate, fueling my initial interests in biological research. This is what ultimately drove me to return graduate school for a Ph.D.

I am also very grateful to the all the members of the Adelman lab for making the lab a great place to work. Michelle, Sanjay, and Azadeh have been wonderful friends and lab-mates

throughout this process. When I first started working in the lab, Michelle patiently taught me most of the molecular biology techniques I needed for my research. She has helped me with countless projects, helped me troubleshoot challenges, and brainstorm ideas. Sanjay has also helped me through questions and ideas, listened to me vent and made me laugh. To Azadeh, I am grateful for our many conversations on life, culture, and science. I also thank Justin and the many undergraduates for their tremendous help in the insectary with mosquito maintenance, giving me the time to focus on my many experiments.

Last but not least, and whether they know it or not, I am tremendously thankful to the many furry friends in my life, past and present. Their many years of love and companionship helped me maintain my sanity, comforted me when I needed it the most, made me laugh, and warmed my lap (and feet) as well as my heart. I am truly a better person for having them in my life.

Table of Contents

Table of Figures

List of Tables

Chapter 1 - Introduction

Ae. aegypti mosquitoes are the vectors of many arboviruses that pose significant social and economic burdens throughout the world. Mosquito vector control has long been attributed as the most effective means for reducing the prevalence of the diseases they transmit. Issues in traditional strategies combined with the emergence of transgenic technologies have led to an increasing interest in genetics-based vector control strategies, such as population suppression and population replacement. A thorough understanding of mosquito biology is essential to the success of these strategies.

RNAi plays a crucial role in mosquito gene regulation and vector competence. RNAi is often targeted in studies involving mosquito innate immunity, genetics-based vector control strategies, and the development of viral-resistant transgenic mosquitoes. The RNA interference pathway is induced by double stranded RNA (dsRNA) and results in the inhibition of cognate gene expression. In the case of viral infection, this could result in inhibition of viral replication. While RNAi mechanisms have been thoroughly studied in model organisms such as *C. elegans* and *Drosophila*, the factors involved in mosquito RNAi have only been peripherally described, and are generally assumed to be similar to the drosophilid mechanisms. Given the obvious differences between culicid and drosophilid biology, notably the reliance of a blood-meal for egg production, it is likely that mosquito antiviral immunity (such as RNAi) may exhibit important differences from that of *Drosophila*. Hence, the nature of the research presented in this document is to explore the genetic factors involved in mosquito RNAi. The objectives of this research are two-fold: First, two characterize dsRBPs important to RNAi in *A. aegypti*

mosquitoes; and Second, to develop a new sensor for assessing the function of the exo-siRNA pathway utilizing a Nodamura virus expression system.

Chapter 2 - Literature Review

Public health significance

Arthropod-borne viruses pose a significant burden in much of the developing world and continually threaten re-emergence in many developed countries. *Aedes aegypti* mosquitoes are the vectors of several pathogens of global health importance, including dengue viruses, chikungunya virus, and yellow fever virus.

An estimated 50 million cases of dengue occur every year and 2.5 billion people are at risk worldwide (1). While dengue fever is typically characterized as a non-fatal, though often severely debilitating febrile illness, over 500,000 cases of the more severe forms (dengue hemorrhagic fever and dengue shock syndrome) are reportedly annually (1). Over 19,000 dengue-related deaths occur each year (1). In the most severely affected countries of Asia and the Americas, the disease burden is estimated at 1,300 disability-adjusted life years (DALYs) per million population and the number is continually expanding (2).

The dengue viruses are classified into four distinct serotypes (types 1 through 4) belonging to the *Flavivirus* genus of the *Flaviviridae* family of viruses. Infection with one dengue serotype produces long term immunity to that particular serotype, however results in only limited cross-protection against the others. This immune-mediated cross-reactivity appears to increase the pathogenicity of subsequent infection by a different serotype, most notably type 2 (3). Thus dengue hemorrhagic fever and dengue shock syndrome is more likely to develop when individuals infected by one serotype are later super-infected with another (3).

Chikungunya is an acute febrile illness characterized by severe polyarthralgia and myalgia. Due to similarities in clinical symptoms, it is often misdiagnosed as dengue or malaria in regions where these diseases are endemic. Chikungunya virus belongs to the *Alphavirus* genus in the *Togaviridae* family. Chikungunya virus is transmitted by *Aedes* genus mosquitoes, with *Ae. aegypti* and *Ae. albopictus* as the principle vectors to humans. Chikungunya virus was first identified in Tanzania in 1952, and has since been described in several African and Asian countries during sporadic outbreaks (4). Chikungunya virus recently drew significant attention, due to its largest historical outbreak. In 2004, chikungunya virus re-emerged in Kenya (5). The disease then spread east throughout countries in and around the Indian Ocean. In 2006, 266,000 cases were reported in La Reunión (65% of the population), followed by 1.45 million cases reported in India (6). In 2007, over 800 imported cases were reported in Europe, and several in the US and Caribbean (6,7). By September of that year, nearly 300 cases in Europe were suspected of resulting from indigenous transmission of the virus by local *Aedes albopictus* mosquitoes (5,6).

Yellow fever was the first identified human virus, the etiology of which was described by Colonel Walter Reed and his commission in the very early 20th century (8). Like the dengue viruses and chikungunya virus, yellow fever virus is a member of the *Flavivirus* genus and, in an urban setting, is principally transmitted to humans by *Aedes aegypti* mosquitoes. Along with its principle vector, yellow fever virus originated in the African continent and spread throughout the tropics during the expansion of shipping and commercial industries in the 17th and 18th centuries (9). In humans, the virus causes an acute, often lethal, hemorrhagic fever. The 'yellow" in the name refers to the jaundice experienced by some patients with the disease. An estimated 500 million people are considered at risk for yellow fever, with over 200,000 cases occurring each

year at a 28% case fatality rate (10). Despite the presence of an effective vaccine, resurgence of yellow fever epidemics have occurred over the past 30 years in Africa and the American tropics, with the latter at the highest risk of urban epidemics (9).

Transmission of arboviruses is dependent on the establishment of a persistent viral infection within the mosquito host, with minimal repercussions to the organism and its blood-feeding behavior (11). Thus, a thorough understanding of the vector's immune response to viral infection is critical to developing effective means of preventing and controlling disease transmission.

The re-emergence and rapidly expanding global range of arboviruses raises a significant alarm for global health. The diseases caused by these viruses are often devastating and have tremendous social and economic impacts. Control and prevention of arboviral epidemics requires a multi-faceted approach, involving both traditional and novel methods.

Vector control strategies

Vector control strategies remain the foundation of worldwide prevention/intervention campaigns for vector-borne diseases. Traditional mosquito control strategies employ targeted pesticide usage as well as integrated management of larval habits near human dwellings (12). Nonetheless, issues such as resistance, program sustainability, behavioral modification, and financial feasibility indicate a need for alternative strategies of control. Rapid advances in molecular biology, including transgenic technologies, vector genome sequencing, and the identification of target genes have led to an increasing interest in genetics-based control strategies (12-15). Genetic control strategies of disease vectors have two general classifications: population suppression and population replacement strategies (12).

A population elimination strategy functions through the introduction of a deleterious gene into the native population, with the final goal of causing population demise. A highly successful example of this strategy is the sterile insect technique (SIT), which was used to eradicate a severe agricultural pest, the screwworm fly, from North and Central America (16). SIT is based on the mass release of males of the target species that have been artificially sterilized in a breeding factory. The insects carry dominant lethal mutations in their reproductive cells, such that any wild females that mate with the transgenic males lay non-viable eggs. Despite the tremendous efforts and expense required by the campaign, it resulted in several billion dollars of savings to the U. S. and Mexican agricultural industries (17). Stemming from SIT, another strategy known as "release of insects carrying a dominant lethal (RIDL)" is currently undergoing its first field studies, involving *Aedes aegypti* mosquitoes (18). RIDL mosquitoes carry a tetracycline-repressible transgenic element resulting in a flightless female phenotype. Thus, transgenic males mating with wild-type females would result in flightless, non-viable female progeny and viable male progeny (18).

In contrast, population replacement strategies aim to replace the pathogen-susceptible vector population with a more harmless refractory population. Transgenics released for this strategy would carry a gene-drive mechanism to establish the target transgenes into the population, resulting in pathogen-refractory phenotypes. Rapid developments in recombinant DNA technology, and identification of target genes have made this an attractive option. However various issues in feasibility, ethics, public perception, and the biological risks involved remain hindrances to this type of strategy (12). Nonetheless, a population replacement strategy involving the use of *Wolbachia pipientis* is currently undergoing field trials. *Wolbachia* is an intracellular, maternally transmitted bacterium that enhances its own vertical transmission via

cytoplasmic incompatibility (19). *Ae. aegypti* mosquitoes transinfected with *Wolbachia* from other insect hosts are resistant to dengue virus infection (19,20). Thus, male *Ae. aegypti* mosquitoes infected with *Wolbachia* can be released into susceptible populations to mate with wild-type females and drive the *Wolbachia*-driven viral resistance phenotype into the population. Field trials utilizing *Wolbachia* are currently underway in Australia, as well as several countries in Southeastern Asia (21,22).

RNA interference

RNA interference (RNAi) is a highly conserved mechanism of post-transcriptional gene regulation in eukaryotic organisms. In mosquitoes, there are several variations of RNAi pathways, all of which are initiated by a protein complex recognizing double stranded RNA (dsRNA) and ultimately result in the degradation of homologous mRNA and inhibition of cognate gene expression. The origin and characteristics of precursor dsRNA generally determine which pathway's initiator complex processes the dsRNA into small RNA intermediates, which are then loaded into distinct effector complexes that function in silencing target mRNAs. The various pathways can also be distinguished by unique characteristics of the small RNA products, such as strand length and base complementarity. For the purposes of this document, I will primarily focus on the micro RNA (miRNA) pathway, and the endogenous and exogenous small interfering RNA pathways (endo- and exo-siRNA pathways, respectively).

The miRNA pathway (Figure 2.1A) functions in regulating endogenously expressed genes, and is especially important during embryogenesis and development (23). The pathway begins when a small hairpin RNA (pri-miRNA) is transcribed from the genome, which is recognized by a microprocessor complex in the nucleus, consisting of Drosha and Pasha proteins

(24). The complex binds and co-transcriptionally cleaves the pri-miRNA into a ~70 nucleotide (nt) stem-loop structure with a 2 nucleotide (nt) overhang on the 3' end, known as a pre-mRNA. Exportin-5 recognizes the overhang and transports the pre-miRNA to the cytoplasm via the Ran-GTPase nuclear-transport mechanism (25). Once in the cytoplasm, a complex consisting of Dicer-1 (DCR1) and a dsRNA-binding protein (dsRBP) further processes the hairpin into a mature miRNA duplex, 22 nt in length (25). The two miRNA strands are then separated and one is loaded in the RNA-induced silencing complex (RISC) along with Argonaute-1 (AGO1) (25). This AGO1 effector complex functions in promoting degradation and inhibiting translation of the target mRNA messages.

Unlike the miRNA pathway, processing of dsRNAs for the siRNA pathways (Figure 2.1B and C) begins in the cytoplasm when an initiator complex, consisting of Dicer-2 (DCR2) and a dsRBP, binds to and "dices" long dsRNAs into 21 nucleotide (nt) siRNA duplexes, leaving a 2 nt overhang on the 3' end (26). The siRNA is then loaded into the Argonaute-2 (AGO2) RISC complex (27). The RISC complex unwinds the siRNA and uses one strand, known as the guide strand, to detect homologous mRNA by base complementarity, while the other strand, known as the passenger strand is discarded from the complex. Gene silencing occurs when the guide strand pairs with complementary mRNA and induces cleavage by AGO2.

As the name implies, dsRNA targeted by the endo-siRNA pathway (Figure 2.1C) generally originates from the genome. Thus, this pathway largely functions in silencing dsRNAs that arise from convergent transcription products, structured genomic loci, and transposable elements (27).

In contrast, the exo-siRNA pathway (Figure 2.1B) targets exogenous RNAs replicating in the cytoplasm, such as dsRNA intermediates that occur during replication of RNA viruses.

Thus, exo-siRNAs plays a major role in viral defense in invertebrate organisms (28-31). Indeed, many viruses encode RNAi suppressor proteins as a method of circumventing a host's exo-siRNA-based innate immune response (32,33). In regards to arboviral transmission, the link between RNA interference and anti-viral defense in mosquitoes is well established (30,31,34-36). Therefore, RNAi directly affects mosquito vector competence. In order for arboviral transmission to occur arboviruses must maintain a delicate homeostasis with the vector's RNAi defense mechanism. The virus must circumvent RNAi-based immunity efficiently enough to achieve and establish a persistent infection, while still minimizing pathogenesis to the mosquito (30). Consequently, the exo-siRNA pathway is often targeted in studies involving genetic control strategies and the development of viral-resistant transgenic mosquitoes (31,35,37-40).

In addition to the origin of the dsRNAs, the two siRNA pathways also differ in which dsRBP partners with DCR2 in the initiator complex. In *Drosophila*, DCR2/R2D2 functions as the initiator complex for the exo-siRNA pathway (41), while the DCR2/Loquacious-D (LoqsD) complex is important for the endo-siRNA pathway (42). There is some debate as to the specific dynamics of the mechanism in these pathways, such as whether R2D2 and Loqs function separately or sequentially, and their individual roles in loading the RISC complex (43-45).

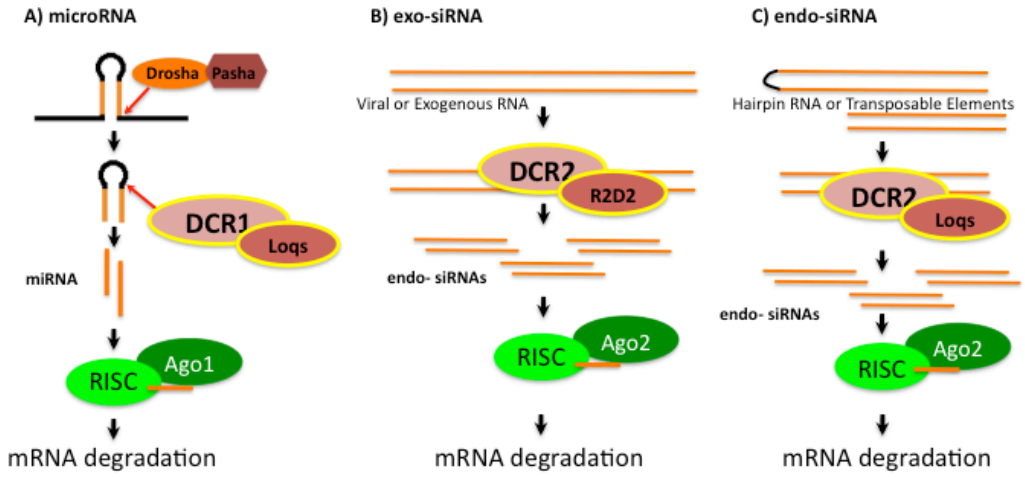

Figure 2.1. Small RNA pathways in *Drosophila melanogaster*

RNA interference is triggered by dsRNA and ultimately results in the degradation of homologous mRNA and inhibition of cognate gene expression. The dsRNA is recognized by a protein complex consisting of a Dicer enzyme and a dsRNA binding protein, such as R2D2 or Loquacious. Small RNAs are loaded into the RNA Induced Silencing Complex (RISC) along with an Argonaute (AGO) protein, ultimately resulting in degradation of homologous mRNA, In Drosophila, different dsRBPs are used in the A) microRNA (miRNA), B) exo-small interfering RNA (siRNA), and C) endo-siRNA pathways [3,4].

Double-stranded RNA binding proteins

Double-stranded RNA-binding proteins share an evolutionarily conserved dsRNA-binding motif (DRM), consisting of approximately 65 amino acids that facilitate interactions with dsRNAs, independent of nucleotide sequence arrangement (46). Eukaryotic dsRBPs may have up to five DRMs, while viral dsRBPs often only have one (47). Although the benefit of a single protein harboring multiple DRMs is not completely clear, different DRMs often have different levels of dsRNA-binding affinity. Thus, it is suspected that the presence of lower-affinity DRMs in conjunction with those of higher affinity may aide in stabilizing dsRBP-dsRNA complexes (48). DsRBPs play diverse roles in many critically important biological mechanisms, including RNAi-based gene regulation and anti-viral defense, embryologic development, and RNA editing and stability (47).

Sources of double-stranded RNA may be either endogenous or exogenous. Endogenous dsRNAs may occur from transcription of complementary mRNAs that anneal to form dsRNA complexes (such as might occur from transcription of convergent gene sequences), or from secondary structures in RNA transcripts (such as hairpin loops, or self-complementarity of highly repetitive sequences) (25,49). RNA viruses comprise the primary exogenous source of dsRNA that may be found in a cell. Viral dsRNAs may occur from viruses with dsRNA genomes, from the dsRNA intermediates that are generated during replication of single-stranded RNA viruses, or from partial complementarity of viral mRNA sequences (28,47). Host immune responses are often activated by viral dsRNAs that are first recognized by key dsRBPs. For example, the mammalian anti-viral interferon and NF-κB responses rely on dsRNA-activation of a dsRBP known as Protein Kinase R (PKR) (50,51). For the purposes of this document, the overview below will focus on dsRBPs that function in RNAi and antiviral immunity.

The RNase III protein family is a highly conserved family of dsRBPs found in prokaryotes, viruses, and eukaryotes. In addition to a DRM, RNase III proteins also have one or more endoribonuclease motifs and are able to bind and cleave dsRNA. The RNase III protein was first described in *E. coli* bacteria by its ability to cleave dsRNA, and was found to function in RNA processing, and gene regulation (47). In eukaryotes, RNase III proteins are important for dsRNA recognition and processing for initiation of RNAi mechanisms. In *Drosophila* and *Caenorhabditis elegans*, the nuclear RNase III protein, Drosha, co-transcriptionally recognizes pri-miRNA stem-loop structures to initiate the miRNA pathway (23). Dicer proteins, also part of the RNase III family, bind to and cleave target dsRNA into small RNA duplexes, which are the hallmark of RNAi-based silencing (24). While humans and *C. elegans* possess only one Dicer protein, two distinct Dicer proteins, DCR1 and DCR2, are found in *Drosophila* (47). DCR1 and DCR2 function in miRNA and siRNA pathways, respectively (24). These Dicers also partner with smaller dsRBPs, known as R2D2 and Loquacious (Loqs, also known as R3D1) (23,41,52). These dsRBPs facilitate dsRNA target recognition and loading of small RNAs into RNAi effector complexes (43,44,53-55).

As its name implies, R2D2 has two DRMs and interacts with DCR2. Gel shift assays by Liu *et al*. demonstrate that, while R2D2 is dispensable for the production of siRNAs, the DCR2/R2D2 complex is essential for loading the siRNAs into the AGO2 RISC (41,53). It is unclear if R2D2 is important for loading both endo and exo-siRNAs (56,57), or only exo-siRNAs (43). This uncertainty is explained in greater depth over the subsequent paragraphs. Studies by Liu *et al*. also demonstrated that the DCR2 stabilizes R2D2 *in vivo*. Depletion of DCR2 results in a decrease of R2D2 protein, while depletion of R2D2 results in a slight reduction of DCR2

(53). Lastly, depletion of R2D2 is known to negatively affect anti-viral immunity in *Drosophila* and mosquitoes (31,58,59).

Four distinct Loqs isoforms have been identified in *Drosophila,* generated from alternative splicing of *loqs* mRNA. Loqs-A and Loqs-B have three DRMs while Loqs-C and Loqs-D have two. The C-terminal DRM in Loqs-A and B enable interaction with Dicer-1, while the unique C-terminal amino acids in Loqs-D facilitate DCR2 binding (60). While both Loqs-A and B partner with DCR1, only Loqs-B is essential to the miRNA pathway and the function of Loqs-A remains unknown (23,60). The *loqs-c* splice variant has only been detected in S2 cells and the protein is not detectably expressed (23,60).

Given that the drosophilid R2D2 and Loqs isoform D (Loqs-D) both partner with DCR2 (53), the importance and specific dynamics by which these two proteins function in the endo- and exo-siRNA pathways remain uncertain. In 2010, Marques *et al*. investigated the effects of *loqs-r2d2* single and double knock-out on endo- and exo-siRNA pathways (44). For the exo-siRNA pathway, siRNA biogenesis and gene silencing was quantified from exogenously and endogenously produced dsRNAs. According to their results, both R2D2 and Loqs are required for efficient silencing by either of the two siRNA pathways. Single depletion of either gene was sufficient to impair siRNA-based silencing, while depletion of both genes resulted in a failure to silence target genes at levels similar to depletion of either DCR2 or AGO2. In addition, single depletion of *loqs* (all isoforms) resulted in drastically reduced processing of dsRNAs in siRNA duplexes, while single depletion of *r2d2* resulted in only a slight decrease in siRNAs. The *r2d2/loqs* double-mutants had no detectable siRNA production, which can be compared to results from DCR2-null mutants. Furthermore, *r2d2* mutants failed to form mature AGO2-RISCs, while the effector complex formation was unaffected by *loqs* depletion. These results

suggest that R2D2, but not Loqs is important to siRNA-RISC loading. Given these results, Marques *et al*. proposed a model suggesting that R2D2 and Loqs-D act sequentially in the endo-siRNA pathway. According to their model, Loqs-D partners with DCR2 to facilitate dsRNA target recognition and binding. After the dsRNAs are cleaved into small RNA duplexes, a DCR2/R2D2 complex binds to the siRNAs and loads them into an AGO2 RISC.

A year later, Hartig and Förstemann proposed a counter model, in which R2D2 and Loqs-D compete for DCR2 binding and act independently in exo and endo-siRNA pathways, respectively (43). Co-immunoprecipitation (co-IP) assays by Hartig and Förstemann indicated that both R2D2 and Loqs-D associate with the helicase domain of DCR2, and likely compete with each other for DCR2 binding. Co-IP assays were also used to assess interaction between endogenous Loqs-D and over-expressed R2D2. Results from this latter assay indicated minimal interaction between the two proteins, further supporting a competition model between R2D2 and Loqs-D (43). It is worth noting that this latter experiment counters results by Miyoshi *et al*., who detected interaction between over-expressed Loqs-D and endogenous R2D2 (45). Hartig and Förstemann used a GFP-based endo-siRNA reporter to further demonstrate that the results presented by Marques *et al*. were likely due to the utilization of mutant flies lacking all *loqs* isoforms, rather than just the *loqs-D* isoform (43,44). Simultaneous depletion of all Loqs isoforms or single depletion of Loqs-D resulted in de-repression of the GFP reporter, where as simultaneous depletion of all loqs isoforms, except Loqs-D, resulted in increased silencing of the GFP reporter. In addition, depletion of R2D2 resulted in increased repression of GFP, suggesting it may antagonize the endo-siRNA-based silencing. Lastly, interactions observed between over-expressed Loqs isoforms appeared dose-dependent and were significantly weaker amongst the endogenous proteins (43,60). Hence, these data support a competition model

between Loqs and R2D2, in which these dsRBPs compete for DCR2 binding and function in distinct pathways (43).

RNAi in the nucleus

In addition to their roles in post-transcriptional gene silencing, several RNAi proteins perform functions in the cell nucleus. The particular function and mode of action varies significantly between different organisms. The overview presented below will provide a brief description of diverse nuclear functions of RNAi-related proteins in various eukaryotes. A recent publication by Castel and Martienssen provides a more complete review of RNAi in the nucleus (61).

In plants and fungi, RNAi-based silencing inhibits not only translation, but also occurs at the transcriptional level by regulating heterochromatin formation. Transcriptional gene silencing (TGS) occurs when epigenetic modifications, such as histone methylation, occur at target genomic loci in response to nuclear RNAi. The specific mechanisms by which RNAi can regulate TGS are not completely known and likely vary by species. However, small RNAs in the nucleus appear to target nascent mRNA by inhibiting elongation by RNA Polymerase (62).

In *Schizosaccharomyces pombe*, co-transcriptional gene silencing (CTGS) directed by RNAi is required for the formation of pericentromeric heterochromatin. The pericentromeric regions consist of repetitive units that are bi-directionally transcribed. DCR1 processes the resulting dsRNAs into siRNAs, which are subsequently loaded into an AGO1 RNA-induced transcriptional silencing complex (RITSC). The siRNA guide strand guides the RITSC to nascent pericentromeric non-coding RNAs, and inhibits transcript elongation by RNA polymerase II (63). After localization of the repeat loci, the RITSC also facilitates H3K9

methylation by recruiting the cryptic loci regulator complex, including the histone methyltransferase, Clr4. Interestingly, the catalytic activity of AGO1 slicing is required for H3K9 methylation to occur. Thus, heterochromatin propagation in *S. pombe* is dependent upon nuclear RNAi activity (64).

In *Arabidopsis thaliana,* RNAi pathways also mediate RNA-directed DNA methylation (RdDM). Of the ten *A. thaliana* Argonaute proteins, three appear to be involved in RdDM, with AGO4 being the most studied in this respect. The siRNAs involved in RdDM are principally derived from RNA polymerase IV transcripts, whereas the target transcripts are generated from intergenic non-coding regions by RNA polymerase V (65). The siRNAs are processed in the cytoplasm by DicerLike-3 protein and loaded onto AGO4, after which the effector complex is transported to the nucleus and guided to target transcripts via base-pair complementarity. This eventually leads to cytosine methylation by the DNA methyltransferase, DRM2, in all sequence contexts, therefore facilitating heterochromatin formation and TGS (66). In addition to RdDM, a study by Enke *et al*. also demonstrated that certain *A. thaliana* siRNAs specifically affect H3K9 methylation as well, thus strengthening the role of RNAi in heterochromatin formation (67).

In *C. elegans*, artificially introduced exogenous dsRNAs can trigger a nuclear RNAi response leading to long-term and even hereditary suppression of target genes. The dsRNAs are processed into primary siRNAs by a Dicer complex in the cytoplasm. Sense and antisense strands from the primary siRNAs are loaded into complexes involving the Rde-1 Argonaute protein and are used to identify target mRNA in the cytoplasm (68). In addition, an RNA-dependent RNA Polymerase (RdRP) uses the primary siRNA strands as templates to generate secondary siRNAs. Some of these secondary siRNAs are recognized by another Argonaute protein, Nuclear RNAi Defective-3 (NRDE-3), which transports them into the nucleus. Once in

the nucleus, another protein, known as NRDE-2, associates with NRDE-3, as the entire effector complex is guided to nascent transcripts targeted by siRNA complementarity (69). As with *S. pombe* CTGS, the complex appears to interact with RNA Polymerase II, inhibiting transcript elongation. Likewise, histone methyltransferases are also recruited to the chromatin at the targeted loci, leading to H3K9 methylation (70).

In *Drosophila*, nuclear RNAi has primarily been associated with the piwi-interacting (piRNA) pathway, which is essential for transposon suppression in the germ line. piRNAs are generated by a process known as the "ping-pong cycle." Precursors for piRNAs are generated from genomic clusters consisting primarily of transposon fragments, which are transcribed into long, single-stranded transcripts (71,72). The precursor piRNAs are cleaved into 23 to 29 nt antisense primary piRNAs in the cytoplasm and then loaded onto Piwi family Argonaute proteins, known as Aubergine and Piwi. These Aubergine and Piwi complexes target transposon mRNA in the cytoplasm for cleavage, producing sense piRNAs, which are loaded onto AGO3. The AGO3 complex then recognizes and induces cleavage of the precursor piRNAs, generating more antisense piRNAs, hence completing the cycle. While this ping-pong cycle occurs in the cytoplasm, the Piwi protein can localize to the nucleus and appears to direct H3K9 methylation to inhibit transposon transcription and mobilization (71,73). A study by Brower-Toland *et al.* demonstrated that Piwi associates with chromatin and interacts directly with Heterochromatin Protein 1, which is a known to be important in heterochromatic gene silencing (74).

Recent evidence suggests that *Drosophila* siRNA components may also play a role in transcriptional regulation. Notably, a publication by Cernilogar *et al.* in *Nature* indicated that both AGO2 and DCR2 associate with RNA polymerase II and transcriptionally active loci in euchromatin to negatively regulate transcription by inhibiting RNA polymerase II activity. In

particular, their research revealed a role for these RNAi components in the heat shock response (75). Additionally, a recent study by Taliaferro *et al*., suggested that depletion of AGO2 affected pre-mRNA splicing patterns, based on genome-wide screens (76).

Sindbis virus

Overview

Sindbis virus (SINV) is a member of the *Togaviridae* family and *Alphavirus* genus. SINV was first described in 1955, when it was isolated from *Culex* mosquitoes captured in the Sindbis health district near Egypt's Nile River delta (77). SINV is an enveloped virus with an icosahedral capsid and positive-sense, non-segmented, single-stranded RNA genome, with a 5' cap and 3' terminal poly-A tract. The viral genome is 11,703 nt in length and is transcribed into genomic (49S) and subgenomic (26S) mRNAs. The 49S mRNA is transcribed from the 5' two-thirds of the genome and encodes for four non-structural proteins, known as nsp1-4. These serve as the viral replicase proteins. The 26S mRNA is transcribed from the 3' third of the genome and encodes the structural proteins (78).

Like other alphaviruses, SINV is an arthropod born virus, replicating in both mosquito and vertebrate hosts. It can also infect a variety of other arthropod and vertebrate species *in vitro* (78). SINV seropositivity in humans and wildlife is widespread throughout the old world (78-80). Despite its wide distribution, human disease resulting from SINV infection is relatively uncommon, but may result in rash, polyarthralgia and chronic rheumatic disease (81).

Symptomatic infections have been documented in Northern Europe (82), South Africa (83), and Australia (84).

SINV is most known for its value in molecular biology and biomedical research. SINV is the type species for the *Alphavirus* genus, yet is relatively less pathogenic than other alphaviruses, such as chikungunya, Ross River and Venezuelan equine encephalitis viruses. Much of what is known about alphavirus biology is based on studies on SINV (78).

Viral replication

SINV viral entry occurs via endocytosis (78). The acidic pH in the endosome triggers fusion of the viral and endosomal membranes, releasing the virion into the cytoplasm (78). The nonstructural proteins are translated directly from the viral genome, giving rise to polyproteins nsp123 and nsp1234, which are eventually cleaved into the four non-structural proteins (78). Along with cleavage intermediates, nsp1-4 regulate transcription and replication of the viral genome. As with other RNA viruses, transcription of the viral RNA produces dsRNA replication intermediates that can be targeted by the host cell's RNAi response(78,85). Transcription from the viral genome results in negative-stranded RNA that functions as a template for replication of the viral genome. In addition, a subgenomic promoter occurring in this negative-strand RNA transcript drives transcription of the 26S mRNA, which is also 5' capped and 3' poly-adenylated. The structural proteins are translated as a polyprotein from the 26S mRNA. The polyprotein is then cleaved into capsid, PE2, 6K, and E1 proteins. The PE2 protein is further cleaved into envelope proteins E2 and E3 during transport in the Golgi network. Virus assembly is completed at the host cell's plasma membrane where the virions are released through budding (78).

Sindbis vectors and expression systems

Rice *et al*. created the first SINV infectious cDNA clones in 1987 (86). Since then, DNA-based SINV expression systems have been created as vectors for gene expression. One of the first of these was an expression plasmid known as pTRCAT, which was based on the SINV viral infectious clone pTOTO1002. The pTRCAT system essentially replaced the structural protein-encoding region with the reporter gene encoding for chloramphenical acetyltransferase (CAT). Thus, electroporation of *in vitro* transcribed pTRCAT, would result in expression of the viral replicon, as well as the CAT-expressing mRNA driven by the subgenomic promoter (87). Low-transfection efficiency was generally the limiting factor in the use of this system, especially in mosquito cells (88).

The development of an infectious, recombinant double-subgenomic SINV (dsSINV) expression system greatly improved the efficiency and versatility of SINV-based gene expression. The dsSINV expression systems, such as the TE/3'2J plasmid, include a full length, viral cDNA, as well as a second subgenomic RNA promoter that can drive transcription of a desired target sequence. Thus, dsSINV expression includes a total of 3 mRNAs: 1) the genomic 49s mRNA, 2) the standard subgenomic 26S mRNA, encoding the viral structural proteins, and 3) the additional subgenomic mRNA expressing the desired heterologous sequence. Since the full viral RNA is transcribed, this system results in the production of infectious virions capable of propagating the recombinant virus to surrounding cells and tissues, thus enabling virtually 100% infection of cells in a culture (89). Since SINV results in no apparent cytotoxicity in mosquito cells, it can be used for long-term expression of a desired gene (either *in vivo* or *in vitro*), although expression will peak in the acute phase of infection (12 to 24 hrs post-infection). In addition, SINV vectors have been recognized as potential tools for gene transfer and targeted

cancer therapy in humans (90-92). The main barrier for this goal is that SINV infection often results in cytotoxicity in mammalian cells. However, manipulation of the virus has drastically reduced much of the toxic effect, or enabled higher specificity of the virus for infection of targeted cells (such as cancer cells) (91,93,94).

Nodamura virus

Overview

Nodamura virus (NoV) belongs to the family *Nodaviridae* and the genus *Alphanodavirus*. Its genome consists of bipartite, single-stranded, positive-sense RNA, with 5' caps and no 3' poly-adenylation (95). The two genomic RNA segments, known as RNA1 and RNA2, encode for the structural and non-structural proteins, respectively. The 3.2kb RNA1 segment encodes the RNA-dependant RNA polymerase (RdRp) protein, known as protein A. The 3' region of RNA1 is also transcribed into a subgenomic mRNA, known as RNA3, which encodes for two additional non-structural proteins known as B1, which is in the same open reading frame (ORF) as protein A, and protein B2 (+2 ORF). The function of B1 is unknown, while B2 functions as an RNAi suppressor protein (96,97).

Nodamura virus is the only Nodavirus that can infect both arthropod and mammalian cells. It was originally discovered in *Culex tritaeniorhynchus* mosquitoes in Japan in 1956, at which time NoV was also found to cause lethality in suckling mice (98). In addition, NoV can infect *Aedes aegypti* and *Aedes albopictus* mosquitoes, and the BHK-21 mammalian cell line (96). Despite its wide range of hosts, it is not a known human pathogen, and no reports of NoV infection in human cells have been reported to date.

Nodamura virus as a molecular tool

Nodamura virus's unique characteristics make it a valuable laboratory tool for creating and expressing heterologous RNAs. The heterologous RNAs can be expressed either in the RNA2 segment (*in trans*) (99), or in the RNA1 segment (*in cis*) (32). Since the RdRP ORF encompasses the entire RNA1 segment, care must be taken for the heterologous sequence not to interfere with the RdRP function. This can be done either by fusing the sequence to the B2 ORF, allowing function of the RNAi suppressor protein, or by replacing most of the B2 ORF with the target sequence. With the latter, not only is the B2 protein essentially eliminated, but the 3' terminal of the RdRP has also been truncated. Nonetheless, a study by Li et al. demonstrated that this method still allows viable NoV replication (32). In theory, the heterologous RNA could also be expressed via a duplicated the subgenomic promoter, similar to the double subgenomic promoter system used in alphaviruses (100). However, a minimal NoV subgenomic promoter for RNA3 has yet to be fully characterized. Depending on the method, expression of target sequences using a NoV-based system may occur either in the presence or absence of the viral RNA suppressor protein, B2. This suggests that an NoV-based expression system could be utilized for assessing the effect of target genes on RNAi (32).

Summary

Arboviruses transmitted by *Ae. aegypti* mosquitoes create a tremendous global health burden, particularly in the developing world. In order for successful transmission to occur from a mosquito to a human host, arboviruses must maintain a homeostatic balance with the

mosquito's immune system. A thorough understanding of mosquito anti-viral immunity is important to the success of genetics-based vector control strategies.

RNAi mechanisms are essential for gene regulation and anti-viral immunity in *Ae. aegypti* mosquitoes. Yet, most of what is known about RNAi in arthropods is based on characterization of the drosophilid mechanisms, while many of the orthologous mosquito RNAi factors remain to be studied. The research presented below primarily focuses on structural and functional characterization of putative dsRBPs important to RNAi in *Ae. aegypti* mosquitoes, as well as the development of a novel tool for assessing the function of the exo-siRNA pathway.

Chapter 3 - Characterization of double-stranded RNA binding proteins important to RNA interference in *Aedes aegypti* mosquitoes

Introduction

Aedes aegypti mosquitoes are vectors of many significant arboviruses, including the dengue viruses, chikungunya virus, and yellow fever virus. Approximately 50 to 100 million cases of dengue occur every year and an estimated 2.5 billion people are at risk (101). Recent outbreaks of chikungunya virus have raised concern over its re-emergence and spread to previously non-endemic areas(7). In addition, an estimated 200,000 cases of yellow fever are thought to occur worldwide (9). Despite the existence of an effective vaccine, the prevalence of yellow fever has been increasing over the last two decades (9).

RNA interference mechanisms are used by eukaryotic organisms for gene regulation, protection from transposable elements, and defense from viral infection (35). In general, RNA interference involves the processing of double stranded RNA precursors into small RNA duplexes, which are then loaded into an effector complex, unwound, and used to detect homologous mRNAs for targeted degradation (35). Most of what is known about arthropod RNAi is based on studies involving *D. melanogaster*. While significant progress has been made in understanding the proteins involved in the various *Drosophila* RNAi pathways, considerably less is known about the mechanisms involved in mosquito RNAi and the degree of similarity between the mosquito and the drosophilid mechanisms. The importance of mosquito RNAi for innate immunity and vector competence has been heavily studied over the last decade (30,31,35). RNAi-induced gene silencing is also commonly used as a laboratory technique for analyzing

mosquito gene function (102-104). Several RNAi pathways exist with distinct functions and characteristics.

The miRNA pathway functions in regulating expression of endogenous genes, and is especially important in germ cell proliferation and embryogenesis (23). miRNAs are derived from genomically transcribed hairpin structures, known as pri-miRNAs (54). In contrast, the long dsRNAs that serve as precursors for siRNAs may be of either genomic or viral origin. The siRNA pathway is important for regulating gene expression, silencing transposable elements, and inhibiting viral replication (27). The siRNAs derived from genomic origin, such as from convergent or hairpin transcripts, or from transposable elements are known as endo-siRNAs, while those of viral origin or experimentally introduced long dsRNAs are known as exo-siRNAs. This distinction is important because biogenesis and processing of miRNAs, endo-siRNAs, and exo-siRNAs depend on different dsRBPs functioning as Dicer binding partners.

In *Drosophila,* alternative splicing of *loqs* mRNA results in four distinct dsRBP isoforms known as Loqs-A, B, C and D. Both Loqs-A and B partner with Dicer-1 (23). Loqs-B is important to miRNA biogenesis and AGO1 loading, while the importance of Loqs-A remains elusive (23). Loqs-D partners with DCR2 and is important to endo-siRNA biogenesis and RISC loading (42,43,60).

Another dsRBP, known as R2D2, also partners with DCR2 and facilitates dsRNA recognition and siRNA RISC loading (53). However, it is unclear if R2D2 is important for loading both endo and exo-siRNAs (56,57), or only exo-siRNAs (43). Furthermore, the specifics of interactions between R2D2, DCR2 and Loqs-D remain uncertain. In 2010, Marques and colleagues published a study utilizing *loqs* and *r2d2* knockout *Drosophila* mutants to propose a model in which R2D2 and Loqs-D act sequentially in both siRNA pathways (56). Their results

suggested Loqs-D functions alongside DCR2 to process long exogenous dsRNAs and endogenous hairpin RNAs into siRNA duplexes, after which R2D2 facilitates loading these siRNAs into RISC. A year later, Hartig and Förstemann proposed a counter model, in which R2D2 and Loqs-D compete for DCR2 binding and act independently in exo and endo-siRNA pathways, respectively (43).

Little is known about mosquito dsRBPs and their roles in the various RNAi pathways. Studies involving knockdown of *Aedes aegypti* R2D2 (R2D2) have indicated that this dsRBP plays a role in limiting dengue virus replication, presumably due to its involvement in the exo-siRNA pathway (31). However, R2D2's association with mosquito exo-siRNA components, such as DCR2 and AGO2, remains to be studied. Likewise, while the distinct drosophilid Loqs isoforms are known to associate with different Dicer and Argonaute proteins (23,42,43,56,60), little is known about the mosquito R3D1 ortholog.

BLAST searches using the drosophilid Loqs protein sequence as a query against the *Ae. aegypti* genome brought our attention to an additional, uncharacterized dsRBP, which we refer to *extra loquacious* (*exloqs*). Due to its similarity to R3D1 and R2D2 sequences, we hypothesized that it is also involved in RNAi. The objective of this study was to characterize the genetic structure and expression profile of three *Aedes aegypti* dsRBPs (*r2d2*, *r3d1*/*loqs*, and *exloqs*) and evaluate the roles of these dsRBPs in the miRNA and siRNA pathways. Through rapid amplification of cDNA ends (RACE) and cDNA sequencing techniques, we identified SNPs, splice variants, novel exons, and transcript initiation and termination loci for these dsRBPs. Tissue-specific expression of each of the dsRBPs was assed using reverse transcriptase PCR (RT-PCR) followed by agarose gel electrophoresis. To assess the importance of the dsRBPs for RNAi, various gene knockdown and co-immunoprecipitation (Co-IP) assays were employed.

Co-IP assays revealed protein-protein interactions between the dsRBPs and DCR and AGO proteins, thus providing indications as to role of these dsRBPs in RNAi. These experiments lay the groundwork for further investigations regarding the specific function of these dsRBPs, as well as provide indications of the potential protein dynamics that are involved in the *Ae. aegypti* RNAi pathways.

Materials and Methods

Phylogenetic analysis

Protein sequences for *D. melanogaster* Loquacious (FBgn0032515) were acquired from FlyBase and used in BLASTP searches on VectorBase or the NCBI databases against *Ae. aegypti, An. gambiae*, and *C. pipiens quinquefasciatus* genomes. Default parameters were used for the queries, and hits with E values $\leq 1x10^{-5}$ were considered significant. For phylogenetic analysis of DRMs, sequences for dsRNA binding domains in Loqs, R2D2, and ExLoqs were identified using Pfam software (105). Evolutionary analyses were performed using MEGA5 software (106) for ClustalW sequence alignment and construction of phylogenetic trees via the neighbor-joining method (107). Evolutionary distances were calculated using the Poisson correction method.

RACE and cDNA sequencing

Transcript sequencing techniques were performed using Liverpool and kh^{w} total RNA templates. Transcript initiation and termination sites for the dsRBPs were determined via 3' and 5' RACE, using the Smart RACE cDNA kit (Clontech). cDNA clones for *r2d2, r3d1*, and

exloqs, were generated by first transcribing total cDNA using the High Capacity Reverse Transcriptase cDNA synthesis kit (Applied Biosystems), and then using these cDNAs as templates to amplify the individual dsRBP sequences using the Platinum Pfx PCR Kit (Invitrogen). The primers used for these PCRs are listed in Table 2.1. Products from both the RACE and cDNA amplification PCRs were cloned into TOPO vector (Invitrogen), sequenced with M13F (5'-GTAAAACGACGGCCAGT-3') and M13R (5'-AACAGCTATGACCATG-3') primers, and compared to the computer-predicted gene sequences listed on VectorBase. The predictions were based on cDNA and EST alignments.

RNA isolation and reverse transcriptase PCR

Total RNA was isolated using TRIzol Reagent (Invitrogen), per the manufacturer's instructions. For RNA extraction from cell culture, TRIzol Reagent was added directly to the cell culture plates for lysis and processing. For analysis of whole mosquitoes or tissues, samples were frozen in liquid nitrogen and stored at -80°C until RNA extraction. Reverse-transcriptase PCR (RT-PCR) was used for analysis of tissue-specific gene expression using 1μg of each RNA template and the One-Step RT-PCR kit (Qiagen), followed by gel electrophoresis. Oligonucleotide primers used for RT-PCR reactions are listed in Table 3.2.

Table 3.1. Oligonucleotide sequences used for RACE and cDNA amplification

Primer Name	Sequence 5' to 3'
R2D2 5'RACE	GGCCAATTCCGCTGCTGGTGAATCCGAGGG
R2D2 3'RACE2	CGGGGAATTCACAAGACGAAGAAAGGGGCC
R2D2 3'RACE4	CGGGACCTTCGCATGCTCCAGAGTTTGAATATGAG
R3D1 5' RACE	CAATCTTCTTGCTCTTGCCCTTGCCCACCTCACGG
R3D1 3'RACE	CCGTGAGGTGGGCAAGGGCAAGAGCAAGAAGATTG
ExLoqs 5'RACE2	CAGGTTTGTTCGCGCTATCGTTGATATACCCA
ExLoqs 3'RACE2	CCGATCACGATTCTGCAGGAGGTTTTGAC
R2D2 ORF F	ATGGCCTCAAAGCCAGTCCTGAGCA
R2D2 R	GCATGTTCTTAAGATACTTGTAGACGCTCTCG
R3D1 F	ATTCCATCGGCCGTGATTTTACAACACCC
R3D1 R3	GTTGTTGGCGGGAGATGGTGTTCCACAAT

Table 3.2. Oligonucleotide sequences used for RT-PCRs

Primer Name	Sequence 5' to 3'
R3D1 4-6 F	GCACGAGCGCCAGTTTACC
R3D1 4-6 R	CTTGGCCGTGCTTCCGCTACC
R3D1 2-7b F	AATCTTAAGCGCCCCGTTCG
R3D1 2-7b R	CGTCGTTTGTTGCGCCAGGTATT
R2D2 F2	CTCGGATTCACCAGCAGCGGAATTG
R2D2 R	GCATGTTCTTAAGATACTTGTAGACGCTCTCG
ExLoqs F	GGTAGAACGAATTCGCCGTCA
ExLoqs R	ACTGAAGAAGTAAACCGTCTTATCCT

Quantitative real-time PCR

Quantitative real-time PCR (qPCR) was used to measure knockdown of *gfp*, *r2d2, r3d1*, *exloqs*, and *dcr2* genes in sensor mosquitoes and Aag2 cells. After isolation (described above), total RNAs were treated with DNAse I, and then purified by phenol/chloroform extraction, followed by ethanol precipitation. cDNAs were synthesized from the DNase-treated total RNA templates using the High Capacity cDNA Reverse Transcriptase Kit (Applied Biosystems). These cDNAs were then used as templates for the qPCR reactions.

Each qPCR reaction was performed in triplicate using primers for the target dsRBP, GFP, and an endogenous housekeeping gene, *elav,* as a control (Table 3.3). The reactions were assembled using *Power* SYBR Green PCR Master Mix (Applied Biosystems), 2µl of the cDNA template, and 250 nM of the primer set. The reactions were run on a Step One Real Time PCR system (Applied Biosystems) with the following program: 95°C for 10 minutes, 40 cycles of: 95°C for 15 seconds, annealing temperature (see Table 3.3) for 30 seconds, and 72°C for the extension time (see Table 3.3), followed by a dissociation curve to verify product melting temperature. The data were analyzed on the 7300 System SDS Software (Applied Biosystems) using the ddCT method, allowing the software to automatically set the Ct threshold and baseline. Statistically significant differences between the ddCT values were determined via One-Way ANOVA. The *elav* values were set as the endogenous control and the uninjected sample functioned as the calibrator for relative quantification of the target sequence.

Table 3.3. Oligonucleotide sequences used for qPCR assays

Primer Name	Sequence 5' to 3'	Annealing temperature/extension time
R2D2 Realtime F4	GCCTCAAAGCCAGTCCT	53°C / 40 seconds
R2D2 Flank R	CTTGCAGCGTCTTAATCATCTC	
R3D1 Realtime Ex2F	CGGGTGGCGAAGAAATC	53°C / 20 seconds
R3D1 Realtime Ex2R	GCGGAAAGTTGGCTCGTGGAC	
ExLoqs PF F2	GACCGGCAAATCCAAGAAG	55°C / 60 seconds
ExLoqs PF R2	GCGAACAACCGCAAGCTAACCATT	
GFP sensor F	AGCTGGACGGCGACGTAAA	51°C / 36 seconds
GFP Sensor R	TCGCCGATGGGGGTGTTCTGC	
ElaV F	AAAGAAGCTGAACGTGCCATTG	(Any of the above)
ElaV R	TCTCCTCCCATCGGTGAAAAG	

Plasmid construction

We designed forward and reverse oligos containing FLAG or HA tag sequences flanked by *NdeI* and *SacI* restriction enzyme sites (Table 3.4). Forward and reverse oligos were annealed and ligated into *NdeI* and *SacI* sites of a pSLfa plasmid. The sites were in a multiple cloning site (MCS) immediately downstream of the *polyubiquitin* (*PUb*) promoter sequence and upstream of a SV40 3'UTR polyadenylation sequence. The resulting plasmids were named *PUb*-HA-MCS and *PUb*-FLAG-MCS. The open reading frames (ORFs) for *r2d2, r3d1a, r3d1b,* and *exloqs* were amplified using the One-Step Reverse Transcriptase PCR Kit (Qiagen) and primers designed to add *NdeI* and *SalI* sites to the 5' and 3' ends, respectively (Table 3.4). The PCR products were digested, purified by low melt agarose gel extraction, and ligated into the *NdeI* and *SalI* sites in the MCS of *PUb*-HA-MCS and/or *PUb*-FLAG-MCS vector plasmids. The resulting plasmids were: *PUb*-HA-R2D2, *PUb*-HA-R3D1A, *PUb*-HA-R3D1B, *PUb*-HA-ExLoqs, *PUb*-FLAG-R3D1A, and *PUb*-FLAG-R3D1B.

For expressing the tagged dsRBPs via recombinant Sindbis viruses, each of the ORFs were amplified from the above plasmids using Platinum *Pfx* (Qiagen) and primers designed to add *AscI* and *PacI* restriction enzyme recognition sites to the 5' end of the tag and 3' end of the ORF, respectively (Table 2.1). After restriction digestion and gel extraction as before, each tagged dsRBP was ligated into the TE/3'2J double subgenomic Sindbis virus vector using *AscI* and *PacI* restriction enzyme recognition sites. The resulting plasmids were named: pTE/3'2J-HA-R2D2, pTE/3'2J-HA-R3D1A, pTE/3'2J-HA-R3D1B, pTE/3'2J-HA-ExLoqs, pTE/3'2J-FLAG-R3D1A, pTE/3'2J-FLAG-ExLoqs, and pTE/3'2J-FLAG-R3D1B.

Recombinant pTE/3'2J constructs for knocking down the dsRBPs were created by amplifying short (255 to 459 bp) fragments from the dsRBP sequence utilizing the One-Step Reverse Transcriptase PCR kit, and primers designed to add *AscI* and *PacI* restriction sites. These dsRBP fragments were cloned into the corresponding restriction sites of pTE3'2J in the antisense direction (Table 2.2), generating pTE/3'2J-r2d2_as, pTE/3'2J-r3d1_as, and pTE/3'2J-exloqs_as.

To create templates for dsRNA synthesis, the *exloqs* ORF, and 5' and 3' halves of *exloqs* were amplified using Platinum Pfx (primers listed in Table 3.6), and cloned directly into pGEM-T easy vector (Promega), per the manufacturer's instructions. A 505 bp fragment of GFP was also amplified using Platinum Pfx (primers listed in Table 3.6) and cloned into *KpnI* and *AvrII* sites of the pLitmus28i vector (NEB).

The miRNA-based R2D2 silencing vector was constructed essentially as described by Haley *et al*. (108), using a modified *Drosophila* pre-*miR-1* backbone. The pre-miR1 backbone was synthesized and cloned into the *XbaI* restriction site in the intron of the *Ae. aegypti PUb* promoter sequence located in a pGL3 plasmid, driving expression of firefly luciferase. This created the plasmid, pGL3-*PUb*-(miR1)-FFluc. The synthetic backbone was also modified to include *NheI* and *EcoRI* recognition sites to enable insertion of a 71 bp oligonucleotide containing the target *r2d2* miRNA sequence. This generated pGL3-*PUb*(miR-R2D2)FFLuc. In order to express the miRNA via the 3xP3 synthetic promoter, the *PUb* intron (including the miRNA) was then amplified using Platinum *Pfx* and primers designed to add *KpnI* and *NcoI* recognition sites to the 5' and 3' ends, respectively. The PCR product was then digested with these restriction enzymes and ligated into the *KpnI* and *NcoI* sites of the pM2-3xP3-BFP plasmid, resulting in pM2-3xP3-(miR-R2D2)BFP.

Table 3.4. Oligonucleotide sequences used to create HA-tagged dsRBPs

Primer Name	Sequence 5' to 3'*
NcoI HA NdeI F	catggagTACCCATACGACGTACCAGATTACGCTca
NcoI HA NdeI R	tatgAGCGTAATCTGGTACGTCGTATGGGTActc
NcoI FLAG NdeI F	catggagGATTACAAGGATGACGATGACAAGca
NcoI FLAG NdeI R	catggagGAACAAAAACTTATTTCTGAAGAAGATCTG
R2D2 NdeI ORF F	ttttcatATGGCCTCAAAGCCAGTCCTGAGCA
R2D2 SalI ORF R	ttttgtcgacTCAATCAATGTAATCGAAATTAAGCATGTTC
ExLoqs NdeI ORF F	ttttcatATGGGTAGAACGAATTCGCCGTCAAATG
ExLoqs SalI ORF R	ttttgtcgacTTAAATAGTGGCATTGGTCAACTCACG
R3D1 NdeI ORF F	ttttcatATGAGTAAGACGGATTTGCCGGCGGT
R3D1AB SalI ORF R	ttttgtcgacTTAGGTCTTGGTCATGATCTTCAGATATTCC
AscI HA F	ttttggcgcgccatgTACCCATACGACGTACCAGATTACGCT
AscI FLAG F	ttttggcgcgccatgGATTACAAGGATGACGATGACAAG
R2D2ORF PacI R	ttttttaattaaTCAATCAATGTAATCGAAATTAAGCATGTTC
ExLoqsORF PacI R	ttttttaattaaTTAAATAGTGGCATTGGTCAACTCACG
R3D1AB ORF PacI R	ttttttaattaaTTAGGTCTTGGTCATGATCTTCAGATATTCC

*lower case letters denote restriction sites

Table 3.5. Oligonucleotide sequences used to create pTE/3'2J dsRBP knockdown constructs

Primer Name	Sequence 5' to 3'*
R2D2 Asc R4	ttttggcgcgccATATTCAAACTCTGGAGCATGCGAAGGTCCCG
R2D2 Pac F2	ttttttaattaaCTCGGATTCACCAGCAGCGGAATTG
R3D1 Asc R2	ttttggcgcgccGTTGTTGGCGGGAGATGGTGTTCCACAAT
R3D1 Pac	ttttttaattaaAACGGTTTGAGGTGACCTACGTTGACATTGAC
ExLoqs Asc R3	ttttggcgcgccTCACGTTGGTTTCCTGCTTTCTG
ExLoqs Pac F2	ttttttattaaACTGGCCGGTGTTGCTTTCTG

*lower case letters denote restriction sites

Table 3.6. Oligonucleotide sequences used to create plasmids for dsRNA-synthesis templates

Primer Name	Sequence 5' to 3'*
ExLoqs NdeI ORF F	ttttcatATGGGTAGAACGAATTCGCCGTCAAATG
ExLoqs 5' R	CAGGTTTGTTCGCGCTATCGTTGATATACCCA
ExLoqs 3' F	CCGATCACGATTCTGCAGGAGGTTTTGAC
ExLoqs SalI ORF R	ttttgtcgacTTAAATAGTGGCATTGGTCAACTCACG
EGFP505 AvrII F	ttttcctaggTTGGTGAGCAAGGGCTAGGAGCTG
EGFP KpnI R	ttttggtaccGGATCTTGAAGTTCACCTTGATG

*lower case letters denote restriction sites

In-situ hybridization

Since *exloqs* was found to be robustly expressed in *Ae. aegypti* ovaries, *exloqs* mRNA was hybridized *in-situ* to a digoxigenin labeled probe in order to further localize the gene's expression within the ovaries. *In-situ* hybridization was performed essentially as described by Juhn and James (109). Templates for generating the sense (control) and antisense *exloqs* mRNA probes were prepared by linearizing pGEM-ExLoqs plasmid DNA using *PstI* or *SacII*, respectively. The digoxigenin-labeled probes were then transcribed *in-vitro* using the DIG mRNA Labeling Kit (Roche) and T7 RNA polymerase, per the manufacturer's instructions. The *in-situ* hybridization technique was performed by Michelle Anderson.

Focus-stacked images of the *in-situ* hybridized ovaries were generated using ImageFuser open-source software to align and merge 30 to 80 photographs taken at various focal depths. The pre-stacked photographs were taken using a Canon Powershot S3 IS digital camera attached to a Leica Dm1000 microscope at 10x magnification.

Virus production and infection of Aag2 cells

pTE/3'2J plasmids were linearized using *XhoI* prior to *in-vitro* transcription. Viral RNAs were transcribed *in-vitro* using SP6 RNA polymerase, and electroporated into BHK-21 cells, as previously described (110). Infectious viruses were harvested, aliquoted and stored at -80°C until use. Viruses were titered by plaque assay in Vero cells.

Cell culture, transfection, and infection

Aag2 cells were maintained at 28 °C in Schneider's *Drosophila* medium (Lonza BioWhittaker) supplemented with 10% FBS, 1% penicillin-streptomycin, and 1% L-glutamine. Cells were transfected in T-25 flasks using Effectene transfection reagent (Qiagen). For each flask, a total of 2.5 µg of plasmid DNA was first mixed with 20 µl Enhancer and 220 µl Buffer EC. After incubating 5 minutes at room temperature, 62.5 µl Effectene transfection reagent was added. After an additional 10-minute incubation, the transfection complex was mixed with 2.5 mL medium and added drop-wise to the flask.

BHK-21 and Vero cells were maintained at 37°C, 5% CO_2 in Dulbecco's Modified Eagle Media (Cellgro), supplemented with 10% FBS, 1% penicillin-streptomycin, and 1% L-glutamine.

For SINV infections, Aag2 cells were seeded into T-25 flasks and allowed to grow to approximately 80% confluency. After removing the growth medium from the cells, virus was added to the flask for a multiplicity of infection of 5 or higher and the volume was brought up to 1 mL using Schneider's medium. Cells were incubated with the virus on a rocker platform for 1 hour, after which an additional 10mL of growth medium was added. Cells were incubated at 28°C until ready to harvest.

Synthesis of dsRNAs

DsRNAs were synthesized using the MegaScript RNAi kit (Ambion), per the manufacturer's instructions. Templates for *exloqs* ORF *in-vitro* transcription reactions were generated by linearizing pGEM-ExLoqsORF via digestion with *SacII* or *PstI* restriction enzymes for anti-sense and sense strands, respectively. Likewise, pGEM-5'ExLoqs and pGEM-3'ExLoqs

were digested with *SacII* or *SalI*, and pLitmus28i-GFP505 was digested with *XhoI* or *KpnI* to generate anti-sense and sense templates, respectively.

Mosquito husbandry and inoculation

All mosquitoes were reared in an insectary with photoperiods consisting of 16 hours of light and 8 hours of darkness. Eggs were hatched in large pans filled with approximately 4 liters of reverse osmosis (RO) purified water, and larvae were fed ground fish food. Adult mosquitoes were fed 10% sucrose solution. Sensor mosquitoes were kept in environmental chambers maintained at 28°C and approximately 90% humidity. Liverpool and kh^w were reared in a "warm-room" maintained at 28°C and 60-70% humidity. For egg collection, female mosquitoes were fed defibrinated sheep blood using an artificial feeder.

For sensor knockdown assays, hemizygous sensor mosquitoes were inoculated via intrathoracic injection with approximately $5x10^5$ pfu of recombinant Sindbis virus. Infected mosquito heads (three biological replicates, each n≥30) were harvested 11 to 17 days post-injection by snap-freezing in liquid nitrogen and storing in a -80°C freezer.

For dsRNA injections, female Lvp strain mosquitoes (n≥10 for each biological replicate) were intrathoracically injected with ~2 μg/μl dsRNA targeting *gfp* or *exloqs* (entire ORF, 5'half, or 3'half). ExLoqs expression was assessed by western blotting ovary lysates at 2, 3, and 4 days post-injection.

miRNA design

Per Haley *et al*., the R2D2 target sequence was selected using Dharmacon's siRNA Design Center (Thermo Scientific), setting GC percentages between 40 and 60%, and selecting

sequences with scores above 70 (108). The selected 21 nt siRNA sequence was used in a BLAST search against the *Aedes aegypti* genome on VectorBase (111) (blastn search, maximum E-Value of 10, word size of 5), to verify target specificity. The 71 bp modified pre-*miR-1* oligonucleotide was designed to include the 21 nt siRNA sequence, with base pair mismatches introduced at nucleotides 5 and 11, from the 5' end of the siRNA sequence. These mismatches were designed to mimic the natural RNA structure of *Drosophila* pre-*mir-1*. RNA structure was verified using RNAfold software (112). The final R2D2 miRNA sense sequence, including the mismatches (lowercase), was: TCGAgAAAGGcCTGAGCGAAA. The 71 bp oligonucleotide was designed with *NheI* and *EcoRI* overhangs to enable insertion into the *PUb* intron, described above.

Generation of miR-R2D2 transgenics and miR-R2D2/sensor crosses

Liverpool strain *Ae. aegypti* embryos were microinjected with 500 ng/μl of the PM2-PUb(miR-R2D2) plasmid along with 300 ng/μl of PGL3-PUb-MosI helper plasmids in 1x injection buffer (113). Embryo injections were performed by Dr. Sanjay Basu. Surviving G0 individuals were pooled into groups of approximated 20 individuals and mated with parental strain mosquitoes to generate the G1 generation. G1 larvae were screened for DsRed+ bodies and BFP+ eyes using a Leica MZ-16FL fluorescent microscope. Positive G1 individuals were mated with Liverpool strain mosquitoes to generate the G2 generation (Table 3.9).

To assess the effect of R2D2 knockdown on sensor GFP expression, miR-R2D2 females were mated with 3xP3-sensor males (genotype Mm-sensor). Female progeny from this cross were screened for DsRed and BFP expression to detect miR-R2D2 positive (miR-R2D2+) individuals (approximately 50%). Since the sensor line is female-linked, all the females of this

cross were also sensor positive (sensor+). Therefore, the resulting progeny were approximately 50% miR-R2D2-/sensor+ (sensor ctrls) and 50% miR-R2D2+/sensor+.

Co-immunoprecipitation, cell fractionation and immunoblotting

For co-IP assays, native lysis and wash buffers were treated with EDTA-free protease inhibitor tablets (Roche). Aag2 cells were harvested by scraping into phosphate buffered saline (PBS) and pelleted by centrifugation at 500 x g for 10 minutes at 4°C. Cells were lysed by resuspending the pellets in native lysis buffer (20 mM HEPES, pH 7.0, 150 mM NaCl, 2.5 mM $MgCl_2$, 0.3% Triton X-100, 30% glycerol) treated with EDTA-free protease inhibitor (Roche) and rotating for 30 minutes at 4°C.

All steps for co-IP assays were performed at 4°C. First, 3 µg of anti-HA or anti-FLAG mouse monoclonal antibodies (GenScript) were incubated with 50 µl Protein G Dynabeads (Invitrogen) and rotated for 30 minutes at 4°C. Excess antibody was removed by washing the beads once with 200 µl PBS-T (0.02% Tween-20). The Aag2 cell lysates were incubated with the antibody-Dynabead complex for 1 hour on a rotator. Once the unbound fraction was removed from the beads, the Dynabead complex was washed 3 times with 200 µl IP Wash Buffer (20 mM HEPES, pH 7.0, 150 mM NaCl, 2.5 mM $MgCl_2$, 0.3% Triton X-100) and once with 100 µl IP Wash Buffer. The entire complex was transferred to a clean tube during this last wash. After removing the remaining wash buffer, the bound complex was denatured in Laemmli sample buffer and stored at -20°C.

Co-IP samples were resolved by SDS-PAGE and transferred to nitrocellulose membranes. For anti-HA or anti-FLAG blots, we used 1:10,000 dilutions of HRP- conjugated mouse monoclonal primary antibodies (GenScript). This facilitated detection of dsRBPs, which

migrate near the heavy antibody chain present in the immunoprecipitates. Custom rabbit polyclonal antibodies to detect *Ae. aegypti* DCR1, DCR2, AGO1, and AGO2 were obtained from GenScript. A complete list of the primary antibody epitopes and dilutions used for immunoblotting is provided in Table 3.7. All primary antibodies were diluted in 3% non-fat milk/TBS-T. For the secondary antibody incubations, we diluted 1:50000 Horseradish Peroxidase (HRP)-conjugated goat anti-rabbit antibody (GenScript) in TBS-T. Chemiluminescent detection was performed using ECL Prime Reagent (Amersham, GE Healthcare) and radiographic film.

For detection of endogenous Exloqs, we used a custom rabbit polyclonal anti-ExLoqs antibody (GenScript), which was generated as described above. Western blots from sugar-fed ovary lysates were probed with a 1:5000 dilution of the anti-Exloqs antibody in 3% non-fat milk/TBS-T. Secondary antibody incubation and chemiluminescent detection was performed as described above.

For cell compartment localization assays, infected and 2 dpi SINV-infected Aag2 cells were fractionated into cytoplasmic, membrane, nuclear, and cytoskeletal fractions using the QProteome Cell Compartment Fractionation Kit (Qiagen), per manufactures instructions. Successful sub-cellular fractionation was verified by immunoblotting with antibodies detecting either β–Actin or Heterochromatin Protein 1 (HP1), which are cytoplasmic and nuclear proteins, respectively. The anti-β-actin antibody was an HRP-conjugated mouse polyclonal antibody obtained from GenScript (diluted 1:5000), while the anti-*Drosophila* HP1 antibody was a mouse monoclonal antibody (diluted 1:500) obtained from the Developmental Studies Hybridoma Bank, developed under the auspices of the NICHD and maintained by The University of Iowa. Following detection of anti-HP1 antibody binding, incubation with HRP-conjugated goat anti-

mouse secondary antibody was performed, using a 1:50000 dilution. Anti-DCR, AGO, FLAG and HA immunoblots were performed as described above.

Table 3.7. Primary antibodies used for immunoblotting

Ab	Epitope	Company	Host/ pAb or mAb	Stock Conc.	Dilution ratio
HA	YPYDVPDYA	GenScript	Mouse/ mAb	0.5 μg/μl	1:10000
FLAG	DYKDDDDK	GenScript	Mouse/mAb	0.5 μg/μl	1:10000
Ago2	CSPANQQKFKLENGT	GenScript (custom)	Rabbit/pAb	1.58 μg/μl	1:3000
Ago1	CPRRPNLGREGRPI	GenScript (custom)	Rabbit/pAb	3.06 μg/μl	1:3000
DCR1	CFDSGSGDGDSDKNY	GenScript (custom)	Rabbit/pAb	1.86 μg/μl	1:5000
DCR2	GKDLDKPLTEGGKRC	GenScript (custom)	Rabbit/pAb	1.63 μg/μl	1:5000
ExLoqsB	CSHDGVPEGFTDKAK	GenScript (custom)	Rabbit/pAb	1.38 μg/μl	1:5000
β-Actin	DDDIAALVVDNGSG	GenScript	Rabbit/pAb	0.5 μg/μl	1:1000
HP1 (C1A9)	(unknown)	DSHB	Mouse/pAb	20 μg/mL	1:500

Results

Phylogenetic analysis

In addition to the expected *Ae. aegypti* R2D2 and R3D1 orthologs identified via BLAST searches on VectorBase and NCBI databases, query results also brought our attention to an additional dsRBP, ExLoqs (AAEL013721), which is an apparent R3D1 paralog. (E value = 4.0E-16, match length = 185 amino acids with 39% identity, score = 191). An additional NCBI BLASTp search using the VectorBase ExLoqs protein sequence further highlighted that ExLoqs does not appear to be found outside the *Aedes* genus and is closely related to the RNAi proteins, R2D2 and R3D1, as well as another dsRBP known as Staufen. This latter dsRBP is important to oocyte development via its function in the localization and regulation of translation of select mRNAs (114).

Phylogenetic analysis of these dsRBP orthologs in *Ae. aegypti, An. gambiae*, and *C. pipiens quinquefasciatus* indicate that ExLoqs is indeed closely related to R3D1 and likely arose from a gene duplication event (Figure 3.1). To further explore the evolutionary history of these dsRBPs, sequences for the DRMs of R2D2, R3D1, and ExLoqs were extracted, aligned with ClustalW; the resultant alignment was used to generate a neighbor-joining phylogenetic tree (Figure 3.2). Both ExLoqs DRMs, as well as the first R2D2 DRM map to the same clade as the first loquacious DRM, whereas the second R2D2 DRM and second R3D1 DRM both share a separate clade. This suggests that both *exloqs* and *r2d2* evolved from separate *r3d1* duplication events. Whereas the 3' region of *r3d1*, including the first two DRMs, may have duplicated to give rise to the precursor for *r2d2*, *exloqs* likely arose from duplication of only first *r3d1* DRM , which was then duplicated a second time, creating the precursors for the two *exloqs* DRMs.

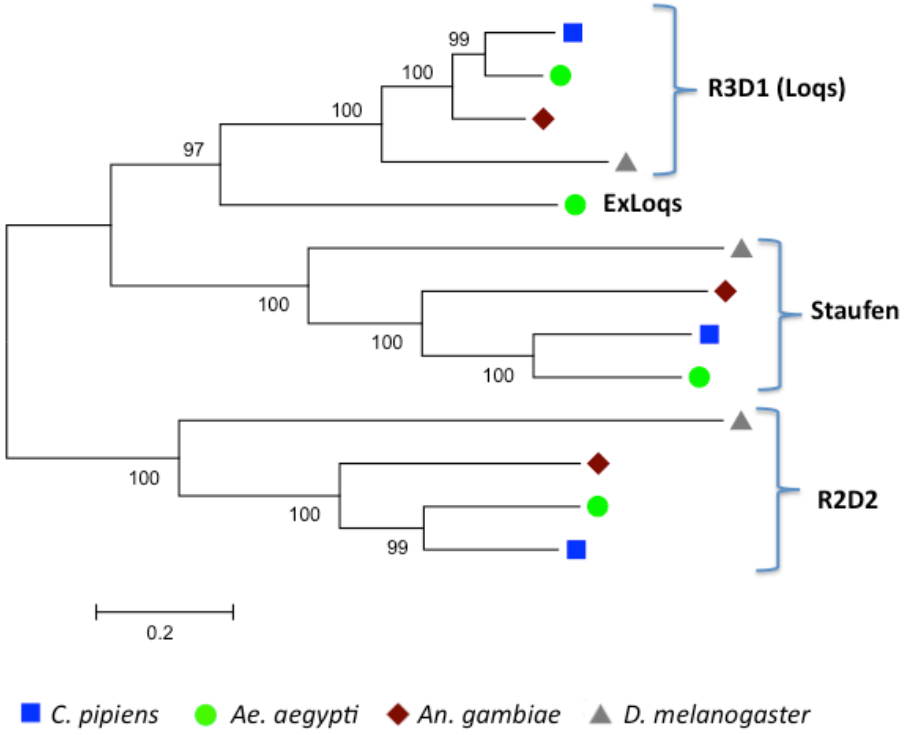

Figure 3.1. Evolutionary relationship of dsRBPs

The neighbor-joining method (107) was used to infer the phylogenetic relationship between R3D1, R2D2, ExLoqs and Staufen protein orthologs in *Culex pipiens, Aedes aegypti, Anopheles gambiae*, and *Drosophila melanogaster*. Bootstrap values (1000 replicates) are shown next to branch points. Evolutionary distances (in number of amino acid substitutions per site) were computed used the Poisson correction method. This phylogenetic analysis was conducted using MEGA5 (106).

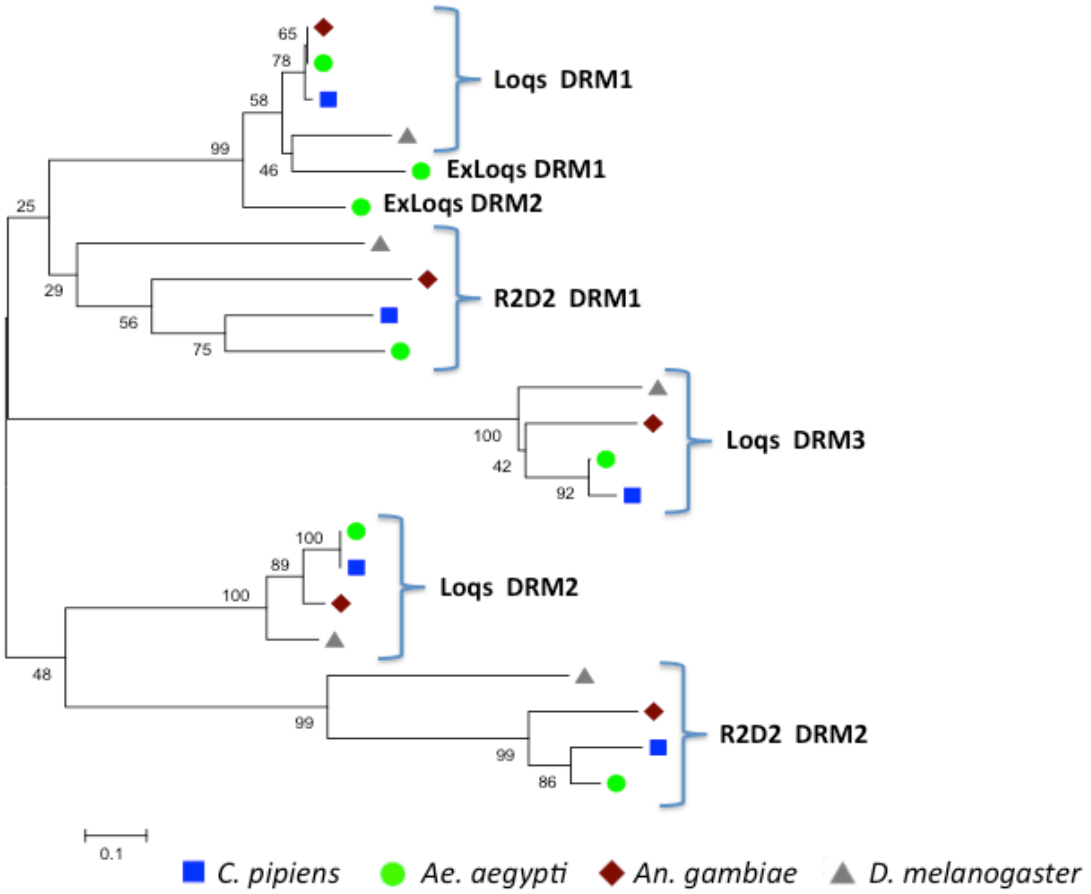

Figure 3.2. Evolutionary analysis of dsRNA binding motifs (DRMs)
Neighbor-joining tree (107) displaying the phylogenetic relationship of the DRMs found in R3D1 (Loqs), R2D2, and ExLoqs. Evolutionary distances (listed as number of amino acid substitutions per site) were computed used the Poisson correction method. Bootstrap values (1000 replicates) are shown next to branch points. This phylogenetic analysis was conducted using MEGA5 (106).

Gene structure and tissue distribution

For *r2d2* (VectorBase gene AAEL011753) a total of six 5' RACE clones were sequenced, all of which revealed a start of transcription exactly 32 bp upstream from the computer-predicted start (AAEL011753-RA). Conversely, the six clones we were able to sequence for *r2d2*'s 3'RACE suggest that transcription termination occurs much sooner than the computational predicted gene model suggests. Poly-A tails for five of the clones occurred between 255 and 290 bp upstream from the predicted stop, and 413 bp upstream for one of the clones. Our experiments did not reveal additional exons or splice variants for this gene as compared with the existing gene model.

For *r3d1* (AAEL008687), 3' and 5' RACE sequencing revealed variability in both transcription start and stop locations. Of the fifteen 5'RACE *r3d1* clones sequenced, thirteen clones began transcription 69 bp upstream of the predicted start, one 111 bp upstream, and one 34 bp upstream. Of the twelve 3' RACE *r3d1* clones sequenced, 1 clone ended at exactly the predicted stop, 3 clones ended 332 bp upstream, 3 clones between 1052 and 1123 bp upstream, 4 clones between 1304 and 1356 bp, and 1 clone ended 1832 bp upstream. Through cDNA sequencing, we confirmed three mRNA splice variants of *Ae. aegypti r3d1*, which we refer to as *r3d1-a*, *b* and c (Figure 3.3A). The *r3d1-a* isoform matches the exon structure of AAEL008687-RA. The *r3d1-b* isoform is similar to *a*, but includes a new exon (exon 5) that increases the distance between the last two of the three predicted dsRNA binding motifs (DRMs 2 and 3). This difference is similar to that of the drosophilid Loqs-A and B isoforms, both of which partner with Dicer-1. The drosophilid isoform, Loqs-D, includes only the first two DRMs and is important to endo-siRNA biogenesis. However, the third *Ae. aegypti* isoform we detected,

R3D1C, does not resemble either of the two remaining drosophilid isoforms, Loqs-C or D, as *Ae. aegypti* R3D1-C includes only the first DRM.

Our experiments also revealed a novel exon in the *exloqs* (AAEL013721) transcript. A 160 bp exon was discovered through 5'RACE sequencing of 12 clones, adding an 18,765 bp intron to the annotated gene (Figure 3.3A). A total of eleven 3' RACE *exloqs* clones were sequenced, all of which ended within 7 bp of the predicted termination site.

Sequencing of *r2d2* cDNA revealed two non-synonymous SNPs between kh^w (n=7) and Lvp (n=5) *r2d2*, including one non-synonymous mutation, K83N. Two of the seven kh^w clones had three additional non-synonymous SNPs. For *r3d1,* three synonymous SNPs between kh^w and Lvp identified, as well as six synonymous SNPs within the Lvp strain. Sequencing of *exloqs* cDNA sequencing enabled identification of18 SNPs between kh^w and Lvp strains, nine of which were non-synonymous changes (Table 3.8).

To determine where *r2d2, r3d1*, and *exloqs* mRNA are expressed in the mosquito body, we performed One-Step RT-PCR reactions using total RNA isolated from *Ae. aegypti* heads, thoraces, midguts, sugar-fed ovaries, blood-fed ovaries, male pupae, female pupae, and L4 larvae (Figure 3.3B). In order to improve the resolution *r3d1a* and *b* expression during agarose gel electrophoresis, we used two sets of PCR primers: one pair that would amplify all three splice variants, and one that would selectively amplify only *r3d1a* and *b* variants. The approximate primer locations are indicated in Figure 3.3A. Our results indicate that *r2d2* is uniformly expressed in all of the tissues analyzed. Likewise, both *r3d1-a* and *r3d1-b* isoforms are detectable in all the tissues analyzed, while *r3d1-c* expression is much weaker and appears slightly stronger in sugar-fed ovaries. In contrast, *exloqs* transcripts appear to be highly enriched

in *Ae. aegypti* ovaries in a bloodmeal independent fashion, and is nearly undetectable in the head and thorax.

To determine if *exloqs* is preferentially expressed in female verse male gonads, we performed and additional RT-PCRs analyzing expression in testes, as well as in the ovary at various time points after blood feeding. Results indicate that *exloqs* is expressed in testes and in ovaries throughout follicular development and that exloqs expression is largely independent of oogenesis (Figure 3.3B).

To determine the spatial distribution of *exloqs* expression within the ovaries, we performed *in-situ* hybridization of endogenous *exloqs* mRNA using *in-vitro* transcribed digoxigenin-labeled anti-sense and sense (as a control) *exloqs* mRNA as a probe (Figure 3.4). *Exloqs* is strongly expressed in the nurse cells and is detectable up to 24 hours post-blood feed (pbf), after which the nurse cells atrophy as part of the ovarian development process. We could not detect *exloqs* in 48 hour or 72-hour pbf follicles. At these time-points, the follicles have reached Christophers' stages IV and V (trophic and post-trophic stages) of development and the nurse cells have fully degenerated (115).

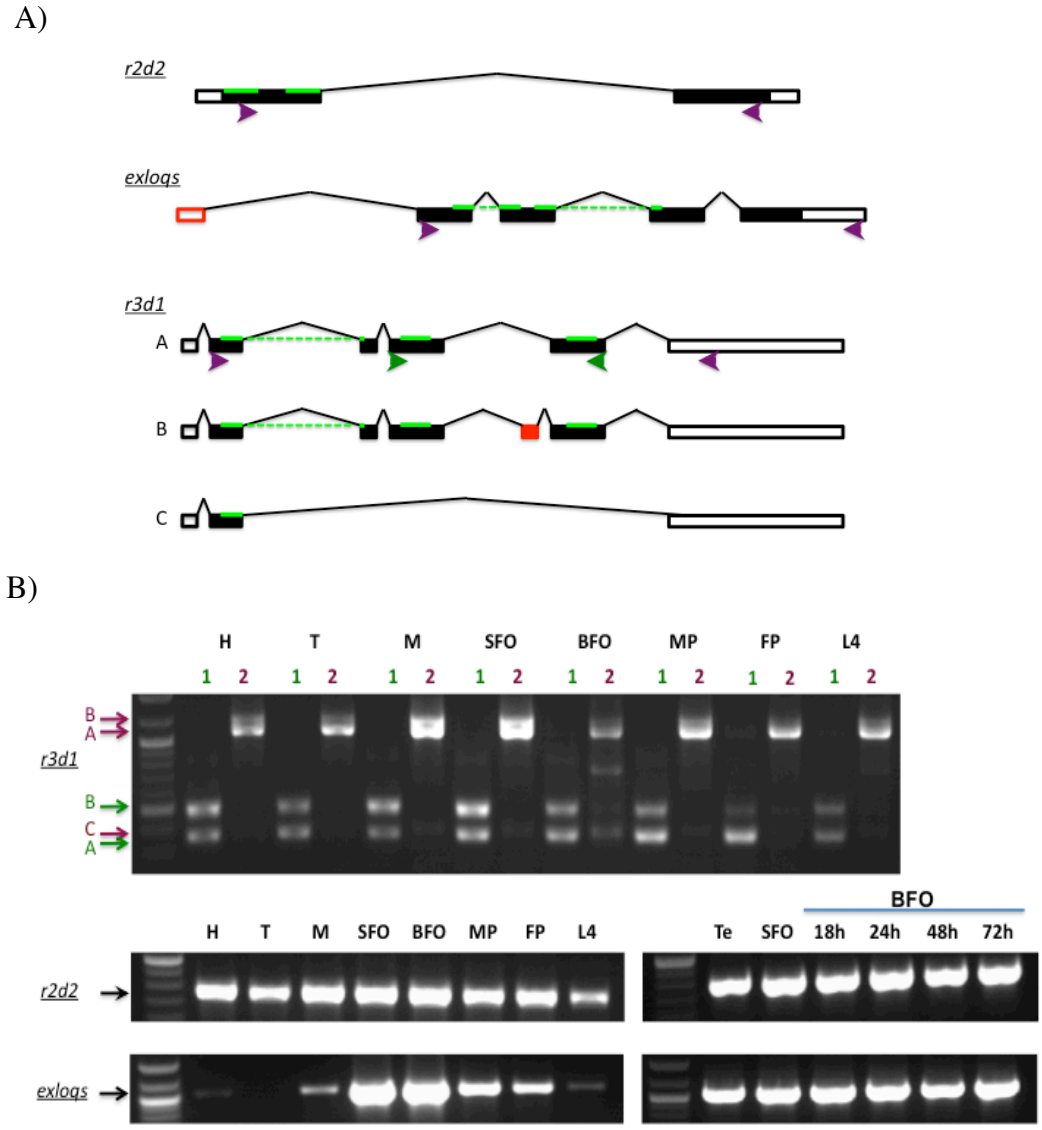

Figure 3.3. Characterization of dsRBP gene structure and expression

A) mRNAs structures of *r3d1* mRNA splice variants, *exloqs* mRNA, and *r2d2* mRNA. Solid boxes represent ORFs, unfilled boxes represent UTRs, red boxes represent new exons, and green lines represent DRMs. Primer locations used for RT-PCR and cDNA sequencing are marked by purple arrows. Additional primer locations used for the second r3d1 RT-PCR assay (B) are marked by green arrows. B) One-step RT-PCRs using head (H), thorax (T), midgut (M), sugar-fed ovaries (SFO), blood-fed ovaries (BFO), male pupae (MP), female pupae (FP), and L4 larvae (L4) total RNA as templates to detect dsRBP transcripts. To determine if *exloqs* is preferentially expressed in the female gonad at specific developmental stages, expression in testes (Te), sugar-fed ovaries and ovaries from various time-points post-blood-meal were analyzed, using r2d2 expression as a control.

Table 3.8. Comparison of SNP identification through cDNA sequencing

Fixed SNPs were variations between the Lvp and *kh*^{w} strains, while polymorphic SNPs were variations identified within a single strain.

dsRBP gene	Gene size (no introns)	Largest ORF	Fixed SNPs (*kh*^{w}/Lvp)	Polymorphic SNPs	Non-syn. SNPs
r3d1	3133 bp	1134 bp	3	6 (Lvp)	0
r2d2	1253 bp	957 bp	2	3 (*kh*^{w})	4
exloqs	1249 bp	870 bp	18	1 (*kh*^{w})	9

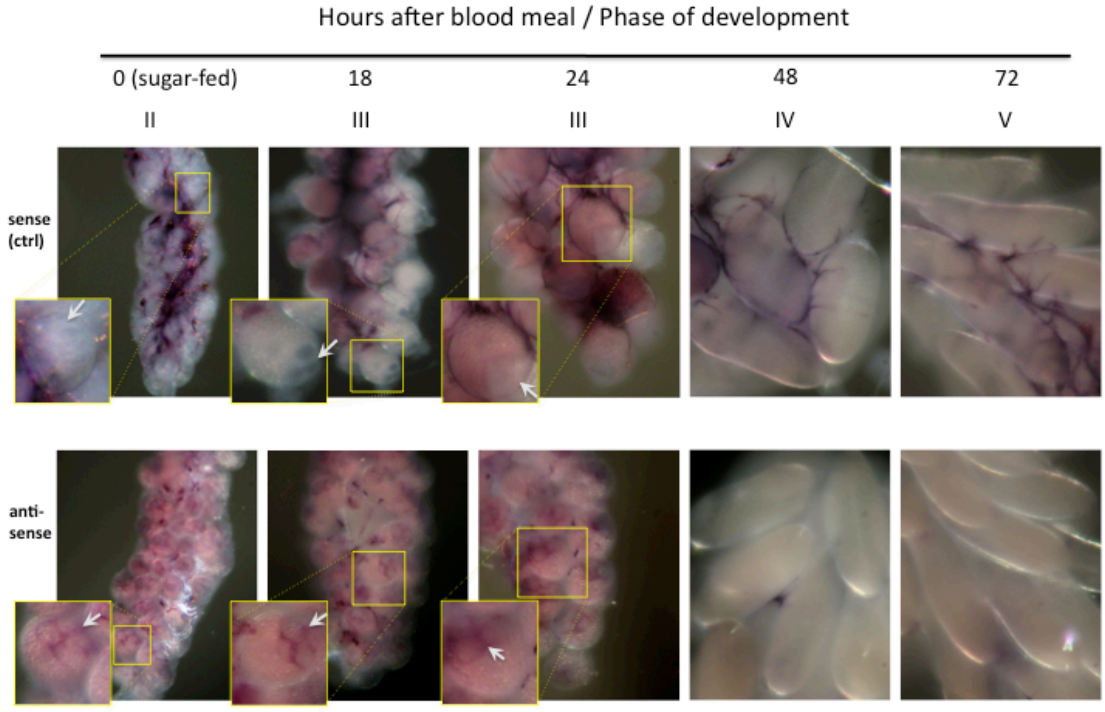

Figure 3.4. *exloqs* RNA *in-situ* hybridization
Ae. aegypti ovaries were dissected at 0, 18, 24, 48, and 72 hours after a blood-feed and hybridized *in-situ* with digoxigenin-labeled sense or anti-sense exloqs mRNA probe. Hybridized *exloqs* transcripts, identified by the purple dye, could be detected in the nurse cells (white arrow) up to the 24 hours post-blood meal.
(In-situ hybridization by Michelle Anderson, focus-stacked images by Mary Etna Haac.)

Subcellular localization of RNAi components

Cellular compartment fractionation assays were used to determine the intracellular localization of R2D2, R3D1-A, R3D1-B, ExLoqs, DCR1, DCR2, AGO1 and AGO2 proteins in cultured mosquito cells (Figure 3.5A). DCR2 was only detected in the cytoplasm, while DCR1 was detectable in all sub-cellular fractions. AGO2 appeared to localize in both cytoplasmic and nuclear fractions. *Ae. aegypti* AGO1 normally appears as doublet band around 112 kilodaltons (KD) in immunoblots using our anti-AGO1 antibody; these doublets were detectable in the cytoplasmic fractions, while a slightly larger band was also detectable in the nuclear fraction of all three replicates of this experiment. No difference in the localization of DCR or AGO proteins could be detected following infection with SINV (Fig. 2.3).

For localization of the dsRBPs, HA or FLAG-tagged EGFP, R2D2, R3D1A, and ExLoqs were individually expressed through infection of Aag2 cells with recombinant double-subgenomic Sindbis virus (TE/3'2J) designed to express the tagged protein or following transfection of an over-expression plasmid. We were unable to obtain HA or FLAG-R3D1B-expressing Sindbis virus, thus this protein was only expressed via plasmid transfection. Cells were harvested 48 hour post infection/transfection, fractionated, and western blotted. EGFP and R2D2 were detected only in cytoplasmic fractions. HA-Exloqs was detected in both cytoplasmic and nuclear fractions, while R3D1A and R3D1B were detectable in all sub-cellular fractions.

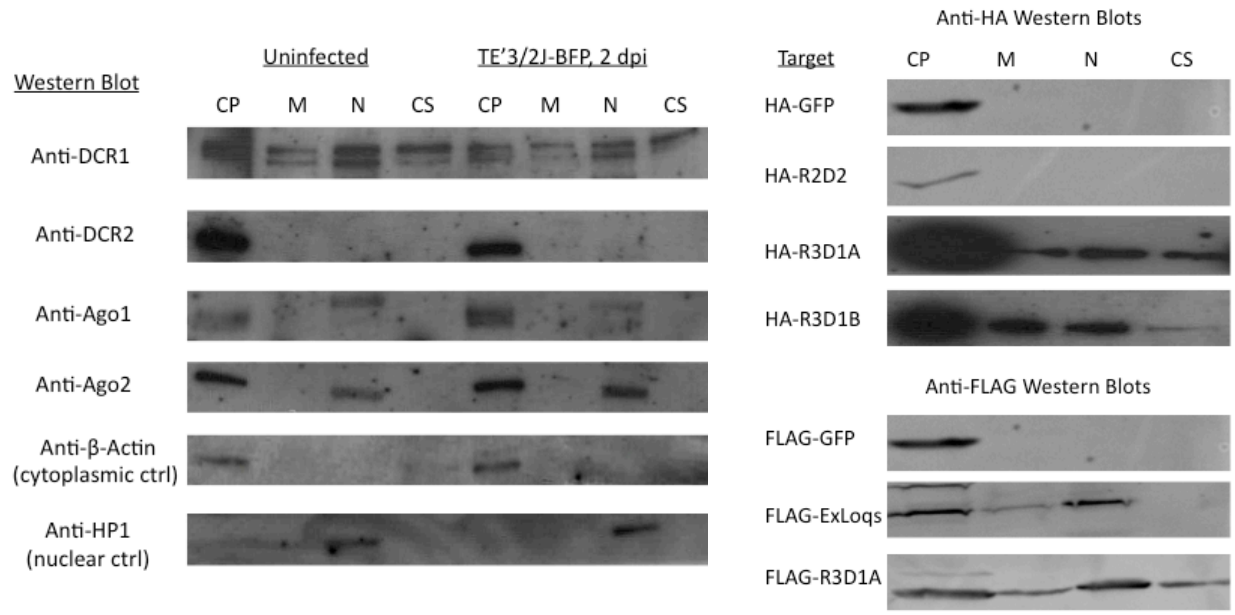

Figure 3.5. Cell localization of RNAi factors

A) Localization of DCR and AGO proteins in uninfected and infected Aag2 cell Fractions: cytoplasm (CP), membrane (M), nucleus (N), and cytoskeleton (CS). B) Localization of expressed HA or FLAG-tagged dsRBPs in Aag2 cell fractions. All tagged-dsRBPs were expressed via dsSINV, except HA-R3D1A and HA-R3D1B, which were expressed via plasmid transfection.

Co-Immunoprecipitation assays

To further explore the relationships of these dsRBPs to the various RNAi pathways, we employed co-immunoprecipitation (Co-IP) assays to test for protein-protein interactions between our three target dsRBPs and DCR1, DCR2, AGO1, and AGO2. In the first set of Co-IP experiments, HA-tagged R2D2, R3D1-A, and ExLoqs were expressed in Aag2 cells via Sindbis virus-based expression or via plasmid transfection (Figure 3.6A). HA-tagged dsRBPs were immunoprecipitated using an anti-HA antibody, and immunoblotted to test for interactions with DCR1, DCR2, AGO1, or AGO2. DCR2 co-immunoprecipitated with HA-R2D2 in both infected and uninfected cells. However, the intensity of the DCR2 band appeared stronger when HA-R2D2 was expressed by recombinant Sindbis virus than when expressed by plasmid (Figure 3.6A,B). HA-R3D1-A was found to interact with both DCR1 and DCR2, as well as with AGO1 and AGO2 proteins. Interestingly, the amount of co-immunoprecipitated AGO1 and AGO2 appeared much stronger in Co-IPs from the cells expressing HA-R3D1-A via plasmid rather than via virus (Figure 3.6A). HA-Exloqs did not appear to associate with either of the Dicer or Argonaute proteins (Figure 3.6A).

To determine if the differences mentioned above were due to viral infection status or due to the method of protein-expression, additional Co-IP experiments were repeated in infected and uninfected Aag2 cells, where over-expression in both cases occurred through plasmid-based transfection (Figure 3.6B). Aag2 cells were transfected with each HA-dsRBP-expressing plasmid and then infected with TE/3'2J-BFP twenty-four hours post-transfection. Anti-HA Co-IPs were performed on the cells 48 hours post-infection and compared with the uninfected cells.

A)

B)

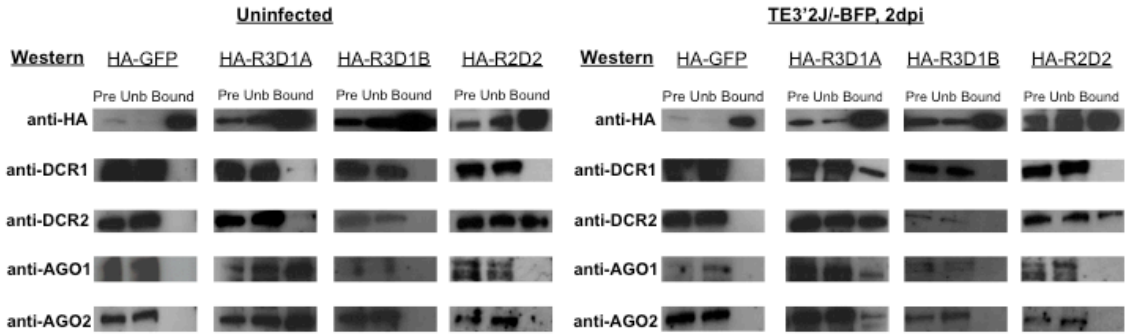

C)

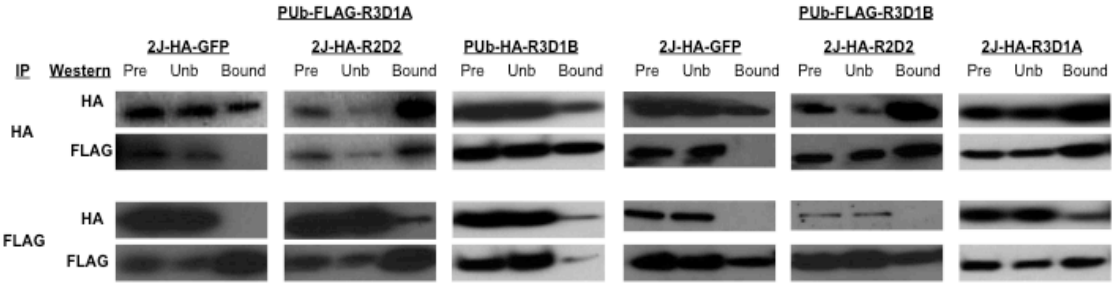

Figure 3.6. Co-immunoprecipitation assays

A) Co-immunoprecipitation of DCR and AGO proteins with HA-tagged dsRBPs. HA-dsRBPs were expected either by plasmid transfection or by infection with recombinant SINV. B) Co-immunoprecipitation of DCR and AGO proteins with HA-tagged dsRBPs in uninfected and infected Aag2 cells. HA-dsRBPs were expressed in Aag2 cells by transfection of plasmid DNA. C) Co-Immunoprecipitation of FLAG-R3D1A or FLAG-R3D1B with HA-tagged proteins.

Once again, Co-IP results indicated associations between R2D2 and DCR2, as well as between R3D1A and both DCR and both AGO proteins. This time the DCR2 band intensity appeared the same with infected and uninfected HA-R2D2 Co-IPs. However, we again observed that R3D1A/AGO1 and R3D1A/AGO2 protein-protein interactions appeared to decrease following viral infection. In contrast, R3D1A/DCR1 and R3D1A/DCR2 interactions appeared to increase in the infected cells. Interestingly, we did not detect any interactions between HA-R3D1B and any of the DCR or AGO proteins tested.

The observation that DCR2 could interact with both R2D2 and R3D1A suggests that both of these proteins could be involved in siRNA biogenesis. This result raises questions about whether these dsRBPs bind DCR2 in tandem, sequentially, or competitively. To test whether R2D2 and R3D1A exist in a complex, additional Co-IP assays were run on lysates from Aag2 cells expressing both HA-R2D2 and FLAG-R3D1A proteins. Initially, we attempted expressing both proteins by co-transfection of the corresponding plasmids. However, this resulted in insufficient HA-R2D2 expression for reliable western blot detection and immunoprecipitation. This is likely because co-transfection of both plasmids required the use of smaller quantities of the *PUb*-HA-R2D2 plasmid (1250 ng) than could be used for single-plasmid transfection (2500 ng). To circumvent this hurdle, we co-expressed the dsRBPs by first transfecting Aag2 cells with *PUb*-FLAG-R3D1A plasmid, followed by TE/3'2J-HA-R2D2 infection at 24 hours post-transfection. Anti-HA and anti-FLAG co-IP assays were run 24 hours post-infection (48 hours post-transfection). As controls, co-IPs assays were also run to assess interactions between HA-R2D2 and FLAG-R3D1B, HA-R3D1A and FLAG-R3D1B, FLAG-R3D1A and HA R3D1B, and HA-GFP and FLAG-R3D1A (Figure 3.6C). Results revealed protein-protein interactions

between HA-R2D2 and FLAG-R3D1A, as well as HA-R2D2 and FLAG-R3D1B. In addition, Co-IP assays indicated interaction between the two tagged-R3D1 isoforms.

Gene knockdown experiments

An *Ae. aegypti* "sensor" strain was developed to enable the expression of a phenotypic marker that "senses" the status of the endo-siRNA pathway in *Ae. aegypti* (Figure 3.7A) (102). The inserted transgene consists of a series of 3 artificial gene cassettes. The first and the second genes in the series code for the red and green fluorescent proteins, DsRed and EGFP, respectively, while the third cassette consists of an inverted repeat sequence (GFPir) designed to express dsRNA homologous to a portion of the EGFP. Each of these genes is individually controlled by the eye-specific 3xP3 artificial promoter, therefore enabling gene expression to be easily detected in the eyes using a fluorescent microscope. Thus, in mosquitoes with a functional endo-siRNA pathway, EGFP expression should be suppressed, whereas those with a compromised RNAi pathway will express EGFP (102). The presence of the sensor transgene is also verifiable by DsRed expression (102).

To assess whether R2D2, R3D1, and/or ExLoqs are important to the endo-siRNA pathway, hemizygous sensor mosquitoes were injected with recombinant dsSINV designed to express dsRNA targeting individual dsRBPs. Knockdown of each dsRBP (Figure 3.7B), as well as the effect on the endo-siRNA pathway was measured by quantitative real time PCR (qPCR) (Figure 3.7C). No change in *gfp* mRNA levels could be detected when either *r2d2* or *r3d1* (all isoforms) were knocked down. We considered that *r2d2* and *r3d1* could have redundant functions in RNAi, and thus created a new virus designed to knockdown both genes simultaneously. Once, again no difference in *gfp* expression could be observed despite

knockdown of both *r2d2* and *r3d1* (Figure 3.7C). Unfortunately, we were unable to successfully knockdown *exloqs* using the dsSINV expression system, despite multiple attempts targeting different locations of the gene's sequence. A recombinant dsSINV targeting DCR2 was used as a positive control (102).

Gene knockdown using a viral-based expression system relies on the exo-siRNA pathway for generating the knockdown phenotype. Since endo and exo-siRNA mechanisms require several overlapping factors, it is possible that using siRNA-based gene knockdown to study a potential siRNA gene may result in a self-limiting phenomenon, in which the degree of gene silencing is limited by the level at which the pathway is still functional. Thus, we also created a series of transgenic R2D2-knockdown mosquito strains using a miRNA-based approach (Figure 3.8A). These strains, which we have named miR-R2D2, include a transgene cassette consisting of the 3xP3 promoter driving transcription of a miRNA targeting *r2d2,* followed by a blue fluorescent protein (mTagBFP) ORF as a marker gene.

After injection of the construct and initial screening of 1st generation mosquitoes, four miR-R2D2 positive (miR-R2D2+) pools were identified, labeled P2, P7, P8, and P9 (Table 3.9). Of these four pools, qPCR data verified significant R2D2 knockdown in P2 (Figure 3.8C). Female miR-R2D2 mosquitoes from each of the four pools were mated with sensor males (a female-linked strain), resulting in sensor positive (sensor+) female offspring. Therefore, of the female progeny, 50% were sensor+/miR-R2D2+ and 50% were sensor+/miR-R2D2- (sensor ctrls). As before, this enabled comparison of *gfp* expression between the two cohorts (Figure 3.8 B and C). Real time PCR assays were used to measure *r2d2* knockdown and the effect on *gfp* silencing. In contrast to the previous results using viral-based knockdown, *gfp* silencing was

significantly enhanced in the R2D2 knockdown sample, as compared to the sensor control (Figure 3.8D). This suggests that R2D2 antagonizes endo-siRNA-based silencing.

Since we were unable to successfully knockdown *exloqs* using the dsSINV expression system, and considering that the primary sites of *exloqs* expression were in germ-line tissues, we reattempted knockdown by injecting female Lvp mosquitoes with dsRNA homologous to the entire *exloqs* ORF. Uninjected mosquitoes and mosquitoes injected with GFP dsRNA were used as controls. Anti-Exloqs immunoblots were run on mosquito lysates 2, 3, and 4 days post-injection (dpi) to assess the level of knockdown (Figure 3.9). While initial results suggested effective knockdown of Exloqs at 4 dpi (Fig. 2.7A), this could not be repeated in two follow-up experiments (Figure 3.9B, C).

A)

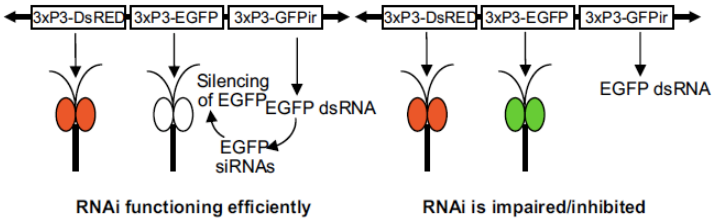

B)

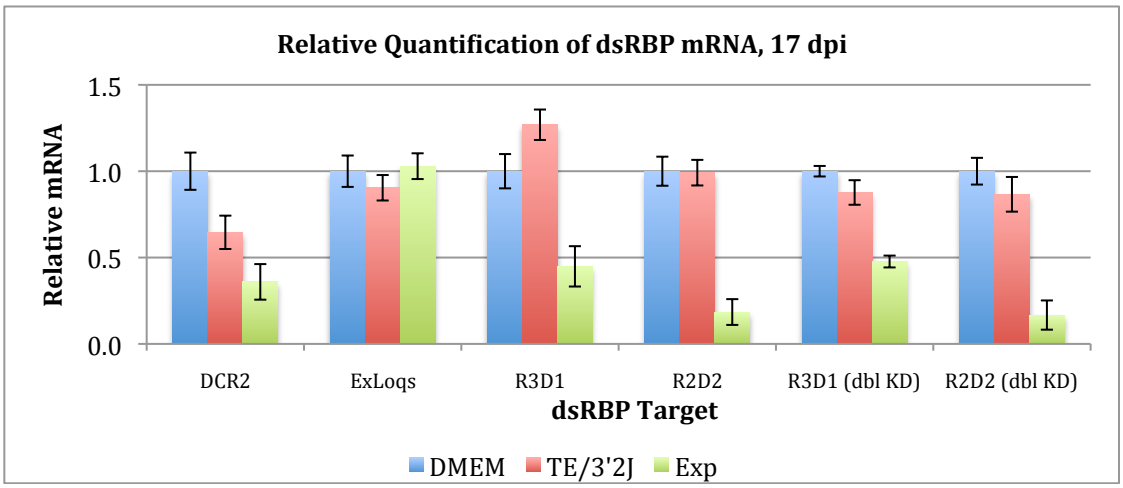

C)

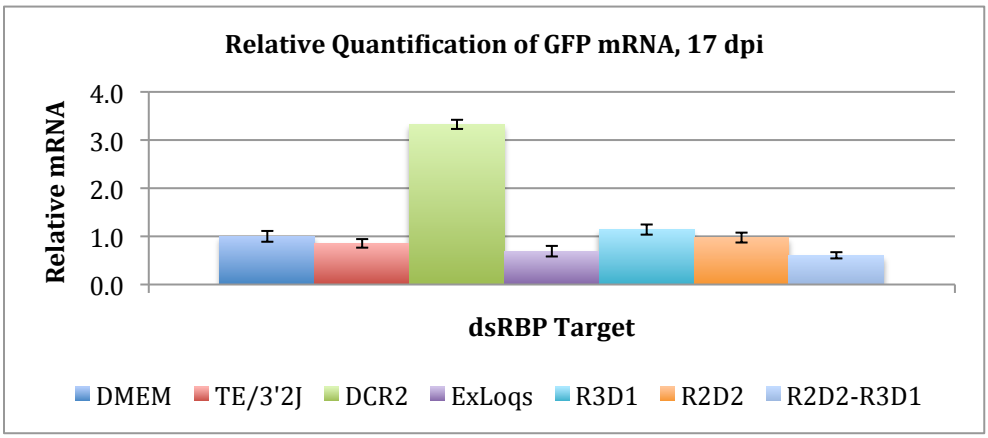

Figure 3.7. Effect of dsRBP knockdown on *gfp* expression of sensor mosquitoes.
A) Figure from Adelman *et al*., 2008 (102), used with permission of Z. N. Adelman. Schematic of 3xP3-Sensor construct showing conditional expression of EGFP. EGFP expression is repressed in mosquitoes with a functional endo-siRNA pathway. EGFP expression increases when the endo-siRNA pathway is impaired. B) Relative quantification of dsRBP mRNA from TE/3'2J-[dsRBP] injected sensor mosquitoes compared to DMEM injected and TE/3'2J injected controls. C) Relative quantification of *gfp* mRNA in dsRBP-knockdown mosquitoes. Error bars represent standard deviation.

A)

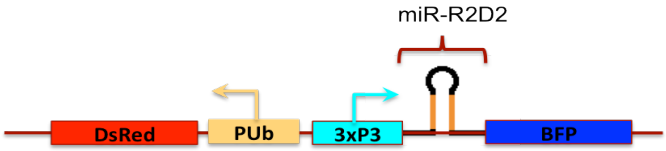

B)

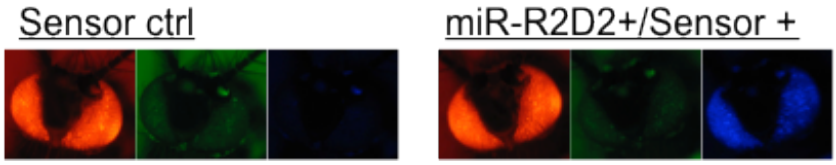

C)

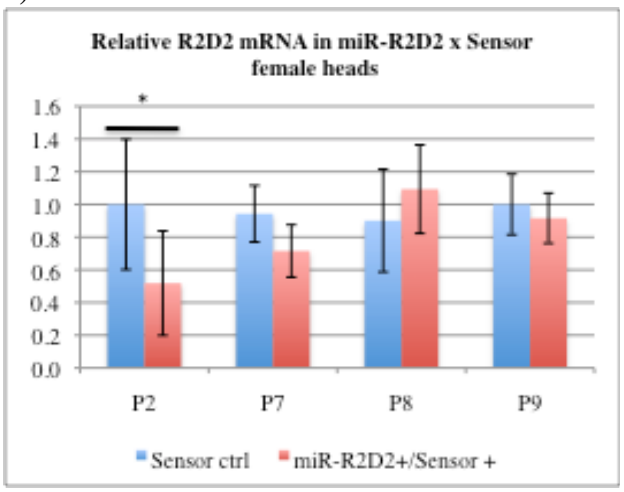

D)

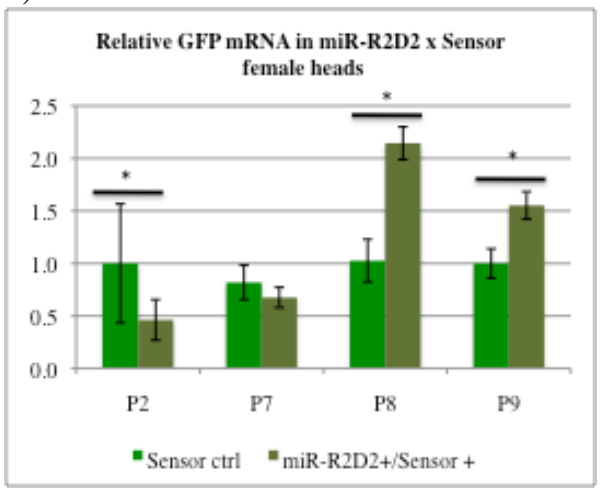

Figure 3.8. miR-R2D2 assay

A) Construct used for generation of the miR-R2D2 mosquito strain. A miRNA targeting *r2d2* mRNA is generated fro the miR-R2D2 sequence in the intron between the 3xP3 promoter and *bfp* ORF

B) Phenotypes of female progeny resulting from crossing miR-R2D2 females by sensor males. The sensor genotype is sex-linked, therefore all female progeny are DsRed+ (sensor+). Of these, 50% are BFP- (sensor ctrl), and 50% are BFP+ (miR-R2D2+/Sensor+). C) Relative quantification of *r2d2* knockdown in miR-R2D2 transgenic pools. Transcript levels in heads were measured by qPCR from miR-R2D2+/sensor+ females compared to sensor ctrl females. D) Relative *gfp* in sensor ctrl and miR-R2D2+/sensor+ females. Error bars represent standard deviation. (* $P<0.05$, based on One-way ANOVA, followed by a Bonferroni post-test)

Table 3.9. Results from miR-R2D2 embryo injections and progeny screening

Mos1 Donor Plasmid	# embryos injected	# G0 survivors	# Pools	#G1 progeny screened	Pools with DsRed+/GFP+ progeny	G2 +/Total (% +)
PM2-PUb-DsRed-3xP3(miR-R2D2)-BFP	970	198 (20.4%)	9	~10930	#P2	197/490 (40.2%)
					#P7	274/314 (87.3%)
					#P8	88/208 (42.3%)
					#P9	222/506 (43.8%)

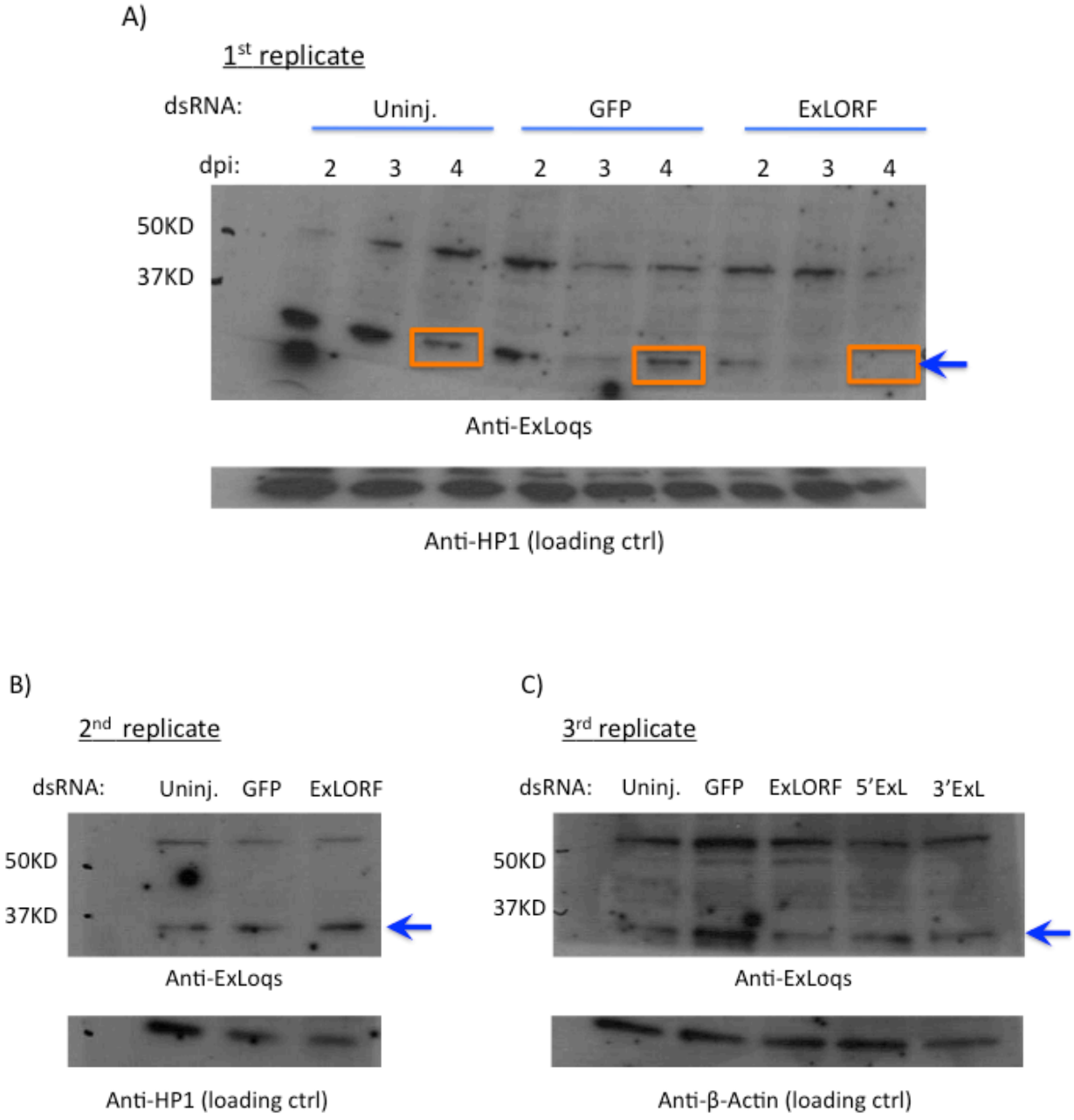

Figure 3.9. ExLoqs expression in ovaries from dsRNA-injected Lvp mosquitoes
A) For the first replicate, Liverpool ovaries were dissected at 2, 3, and 4 dpi. Successful ExLoqs knockdown was detected at 4 dpi in mosquitoes injected with dsRNA targeting the entire ExLoqs ORF, as compared to uninjected mosquitoes and mosquitoes injected with GFP dsRNA. For second (B) and third (C) replicates ovaries were harvested at 4 dpi. B) For the second replicate no difference in ExLoqs expression could be detected between injected and uninjected mosquitoes. C) For the third replicate, additional dsRNAs were included, homologous to specifically the 5' or 3' halves of the ExLoqs ORF. Once again, ExLoqs expression appeared unaffected.

Discussion

RACE and cDNA sequencing reactions improved the annotations of all three of our target dsRBPs, *r2d2, r3d1*, and *exloqs*. Precise annotation of transcription start sites is essential to identification and analysis of gene promoter regions. Compared to the VectorBase predicted sequences, we extended the 5'UTR and identified SNPs for all three genes, and identified novel exons in *r3d1* and *exloqs*. The relatively high number of SNPs in *exloqs* suggests that this gene may be rapidly evolving. Similarly, while only four SNPs were identified for *r2d2*, three of these were non-synonymous. Further studies may reveal whether these could affect the function of the encoded protein. In contrast, all SNPs identified for *r3d1* were synonymous.

Sequencing reactions also revealed three distinct *Ae. aegypti r3d1* splice variants (Figure 3.3A). This is similar to what is seen with the *Drosophila* ortholog, *loquacious*, which has four splice variants, with seemingly distinct functions (42). The drosophilid Loqs-A and –B isoforms both partner with DCR1, but only Loqs-B is essential to miRNA processing (27,42). Likewise, the drosophilid Loqs-D protein partners with DCR 2 and is important to endo-siRNA biogenesis(42). The function for *Drosphila* Loqs-C remains unknown. The *Ae. aegypti* R3D1 isoforms we have labeled A and B are structurally similar to the *Drosophila* A and B isoforms, respectively. This suggests that they may share a similarity in function as well. In *Ae. aegypti* cells, over-expressed R3D1-A co-precipitated with both DCR1 and DCR2, as well as with both AGO1 and AGO2 (Figure 3.6 A and B). Interaction with DCR1 and AGO1 suggests R3D1-A is involved in the miRNA pathway, whereas interaction with DCR2 and AGO2 suggests a role in the siRNA pathway as well. Visual comparison of co-IP results from uninfected and infected Aag2 cells also appear to indicate a decrease in R3D1A/AGO1 and R3D1A/AGO2 protein-protein interactions following viral infection (Figure 3.6B). While these differences are

interesting to note, at this time we hesitate to draw any conclusion regarding these differences without further investigation. Potential future experiments include purification and analysis of small RNAs and mRNAs bound to R3D1A/AGO1 and R3D1A/AGO2 complexes in infected and uninfected cells, as well as anti-AGO1 and AGO2 IPs. It is important to note that the protein-protein interaction that we have observed at this point have involved the use of over-expressed tagged-dsRBPs. Thus, it is also necessary to re-assess these interactions in the endogenous proteins. Unfortunately, we were unsuccessful in our attempts at detecting the endogenous dsRBPs using custom-antibodies designed to detect *Ae. aegypti* R2D2, and R3D1.

HA-R3D1B did not appear to associate with either of the Dicers or Argonautes, suggesting this isoform may not be involved in either of these small RNA pathways in Aag2 cells. However, the over-expressed R3D1-B did appear to interact with R3D1-A, as well as R2D2, suggesting it may have a unique regulatory role or function in a different, but overlapping, pathway (Figure 3.6C). The third isoform we identified, R3D1-C, does not resemble any of the drosophilid isoforms. It is interesting to note that, while we were able to recover several mRNA clones of the *r3d1-c* splice variant, we were unable to detectably express an HA-tagged version of this protein in Aag2 cells, either through recombinant virus or through plasmid transfection. This is somewhat reminiscent of the drosophilid *loqs-c* splice variant, which was only detectable in S2 cells and had no detectable protein product (23,60).

In *Drosophila*, R2D2 partners with DCR2 and enables loading of small interfering viral RNAs (viRNAs) in the AGO2 effector complex. Co-immunoprecipitation of *Ae. aegypti* DCR2 with R2D2 proteins supports the hypothesis that R2D2 plays a similar role in mosquitoes (Figure 3.6A and B). This finding also coincides with previous observations that depletion of R2D2 can increase viral replication in infected mosquitoes (31).

Additional co-IPs to purify and sequence small RNAs bound to the dsRBP complexes may also provide deeper insight into the functions of these dsRBPs. Small RNA libraries from the immunoprecipitation products will enable analysis of the characteristics and origins (viral or genomic) of small RNAs present in dsRBP complexes, thus further aiding in the identification of which pathway each dsRBP is involved in. Additional mechanistic studies analyzing the generation and characteristics of small RNAs following dsRBP-depletion both *in-vivo* and *in-vitro* are also need to define the role of these dsRBPs in specific RNAi pathways.

Analyses of tissue-specific gene expression indicated that *exloqs* is preferentially expressed in the mosquito gonads (Figure 3.3B), suggesting that it may have a function in germline integrity or reproduction. Furthermore, *in-situ* hybridization of ovaries revealed that *exloqs* expression is most prominent in the ovarian nurse cells, as well as undeveloped follicles (Figure 3.4). Thus, it is possible that *exloqs* expression in females is important to nurse cell development or vitellogenesis. Meanwhile, *r2d2* and all *r3d1* splice variants appear to be fairly uniformly expressed in all the tissues analyzed (Figure 3.3B), indicating that their functions are likely of broader benefit, such as anti-viral protection or RNAi-based gene regulation.

Subcellular fractionation assays indicated that *Ae. aegypti* DCR1, AGO2, R3D1A and R3D1B localized to the nucleus, while R2D2 and Exloqs were cytoplasmic (Figure 3.5). For AGO1, we were uncertain if the band appearing in the nuclear fraction resulted from a slightly slower migrating AGO1 protein or from non-specific antibody binding. In several organisms, including *C. elegans,* and *Drosophila*, RNAi components function in co-transcriptional and heterochromatic gene silencing. Notably, recent studies in *Drosophila* reveal that AGO2 and DCR2 may inhibit transcription by RNA polymerase II when bound to euchromatin (75). Our

results from intracellular localization of RNAi components suggest a potential nuclear role for RNAi in *Ae. aegypti* as well.

Gene knockdown experiments to study the effects of dsRBP depletion on the endo-siRNA pathway were largely inconclusive. We were unable to knockdown *exloqs*, despite multiple attempts using dsSINV as well as *exloqs* dsRNA. Single and double knockdown of R2D2 and R3D1 using recombinant SINV in sensor mosquitoes did not reveal any effect on endo-siRNA-based silencing. However, single miRNA-based knockdown of R2D2 in sensor mosquitoes significantly enhanced endo-siRNA-based silencing of the GFP reporter, suggesting that R2D2 antagonized the endo-siRNA pathway. This phenomenon would be compatible with a model in which R2D2 competes for DCR2 binding with a dsRBP important to endo-siRNA based silencing. For example, if R2D2 only functions in the exo-siRNA pathway, but competes with an endo-siRNA dsRBP for DCR2 binding, then depleting R2D2 would liberate more Dicer-2 proteins to partner with the endo-siRNA dsRBP, thus strengthening the endo-siRNA pathway.

It is possible that the conflicting results of the dsSINV and miRNA based knockdown experiments could be attributed to the presence or absence of viral infection in the former and latter experiments, respectively. The exo-siRNA pathway is known to regulate SIV replication in infected mosquitoes (85). Several key proteins involved in the anti-viral, exo-siRNA pathway are also important to endo-siRNA-based silencing (notably, DCR2 and AGO2) (59,116). Thus, in the presence of virus, resources needed for the endo-siRNA pathway may be diverted for exo-siRNA-based anti-viral immunity. Hence, this inhibition of the endo-siRNA pathway may counter its potential up-regulation due to R2D2 depletion. Thus, we are inclined to consider the virus-free, miRNA-based knockdown more reliable for attributing the effects of R2D2 knockdown on the endo-siRNA sensor. Nonetheless, the results remain uncertain. It is also

perplexing that the sensor+/miR-R2D2+ offspring from two of miR-R2D2 pools with seemingly unsuccessful *r2d2* knockdown (P8, P9) had significant de-repression of the endo-siRNA reporter. However, it is possible that we were unable to detect knockdown in these pools due to lingering transcript degradation products that were amplified via the qPCR assay. Unfortunately, a functional antibody detecting the endogenous R2D2 protein was not available to screen for knockdown via western blot.

Conclusion

While the importance of dsRBPs in RNAi-based silencing has been studied in several model organisms, such as *C. elegans* and Drosophila, little is known about how this information translates to RNAi mechanisms in mosquitoes. Given that RNAi plays a direct role in vector competence, a thorough understanding of the process and the genes involved can provide valuable information on virus-vector interactions and the control of major pathogens. Variations in gene sequence and structure affect the function of the encoded proteins and their potential roles in anti-viral defense and gene regulation. Identification of SNPs, new exons, and isoforms facilitates further studies on the function of these genes in RNAi and vector competence. For this study, we improved the gene annotation and identified SNPs for all three of our target dsRBPs, *r2d2*, *r3d1*, and *exloqs*. We also identified three splice variants for the *r3d1* transcript, and novel exons in both *r3d1* and *exloqs*. Additionally, RT-PCR assays provided an expression profile of the transcripts for these genes in various tissues and developmental stages.

Lastly, the Co-IP assays provided further insight into the roles of the dsRBPs in RNA interference. Observed protein-protein interactions between R2D2 and DCR2 support evidence that R2D2 is involved in siRNA biogenesis. Whereas, R3D1-A associated with both Dicers and

both Argonautes studied, suggesting involvement in multiple RNAi pathways. This study provides important insight into the potential roles of dsRBPs essential to RNAi and lays a foundation for future mechanistic studies.

Chapter 4 - Generation of an ExLoqs knockout mosquito

Introduction

Several dsRBPs have been shown to affect fertility and development through roles in gene regulation, germ-line maturation, stem-cell maintenance and proliferation, cell differentiation, mRNA localization and expression, and transposon repression. Of the *Ae. aegypti* dsRBPs, ExLoqs is robustly expressed in mosquito ovaries and testes. Phylogenetic analyses indicate that the protein is most closely related to the RNAi dsRBPs, R3D1 and R2D2 as well as the dsRBP, Staufen, which is involved in the localization of maternal mRNAs in developing oocytes (114). This relation suggests that ExLoqs may function in small RNA pathways or RNA-localization pathways important to fertility and/or development.

In both male and female *Drosophila*, piRNAs are primarily expressed in the germ-line and are important for regulation of germ-line stem cell renewal and protection from transposable elements (71-73). Meanwhile, endo-siRNAs are abundant in both germ-line and somatic tissues and function in gene regulation and transposon silencing (27,117,118). In addition, the miRNA pathway is essential for gene regulation in both somatic and germ cells. Specifically in regards to fertility, miRNAs regulate genes that are important to oocyte development, embryogenesis (119), and gonadal cell differentiation, proliferation and morphology (119-121).

In *Drosophila*, both Loqs-A and Loqs-B interact with DCR-1 and the Loqs-B is required for miRNA biogenesis. Through RT-PCR analysis, Förstemann *et al*. found that the drosophilid *loqs-a* isoform is most abundantly expressed in ovaries while *loqs-b* is the predominant isoform in males (23). An additional isoform, Loqs-D is important to endo-siRNA biogenesis (42). Depletion of *loqs* (all isoforms) results in female infertility, and decreased male fertility (23).

While R2D2 is primarily responsible for exo-siRNA based silencing, it also appears to play a role in the development of ovarian follicles in *Drosophila (122)*.

The dsRBP Staufen functions in the localization and regulation of translation of maternally-derived mRNAs in developing oocytes. In *Drosophila*, Staufen anchors *bicoid* mRNA to the anterior pole and *oskar* to the posterior pole during different stages of development (114,123). The orientation and appropriately timed expression of anterior/posterior-patterned mRNAs is important to the polarity of developing embryos (114,123,124).

Another dsRBP, Blanks is unique to testes and essential for male fertility in *Drosophila*. Knockdown of *blanks* results in complete male sterility due to incomplete spermiogenesis (125). Blanks associates with a unique siRNA/dsRNA binding complex, different from canonical RISCs, that appears to regulate sperm maturation as well as post-transcriptional repression of retro-transposons during later stages of sperm development (125).

To identify a potential role for ExLoqs in *Ae. aegypti* fertility, we attempted *in-vivo* gene knockout experiments. As described in the previous chapter, we were unable to knockdown *exloqs* in *Ae. aegypti* mosquitoes using dsSINV or dsRNA. Thus, we attempted *exloqs* knockout, this time using transcription activator-like effector (TALE) nucleases for targeted gene disruption.

TALEs bind target DNAs in a sequence specific manner mediated by a 34 amino acid repeat region with two hyper-variable residues, which specify an individual nucleotide target (126,127). Consequently, fusion of multiple TALE repeat domains to a *FokI* nuclease enables highly specific cleavage at target DNA sequences (reviewed in (128)). Imperfect DNA repair mechanisms following cleavage by TALE nucleases (TALENs) often result in nucleotide deletions, enabling sequence-specific disruption of target genes (128).

In a recent publication by the Adelman lab, TALENs were successfully utilized to disrupt the kynurenine 3-monoxygenase (KMO) gene, creating a novel strain of white-eyed *Ae. aegypti* mosquitoes, with a kh^{w}-like phenotype, but with the robust Lvp strain background (129). Likewise, for this study we employed TALEN pairs designed to target recognition sequences within the *exloqs* gene to disrupt translation of the endogenous ExLoqs protein. This technique enabled the creation of novel *exloqs*-mutant strains of *Ae. aegypti,* referred to as TALEN-ExLoqs, which can be used to assess phenotypic differences between *Ae. aegypti* with and without a functional ExLoqs protein.

Materials and Methods

Mosquito husbandry

Mosquitoes were reared at 28°C and 60-70% humidity, with a photoperiod of 16 hours light and 8 hours darkness. Eggs were hatched in large pans filled with approximately 4 liters of reverse osmosis (RO) purified water, and larvae were fed ground fish food. Adult mosquitoes were fed 10% sucrose solution.

TALEN-based *exloqs* gene disruption

TALEN pairs were synthesized by PNA Bio Inc (Table 4.1). ExLoqs TALENs were co-injected into 928 *Ae. aegypti (*Lvp strain) embryos at a concentration of 200 ng/ul of each TALEN-encoding plasmid. Embryos were injected by Dr. Sanjay Basu. Female Generation 0 (G0) mosquitoes were mated by parental strain (Lvp) males (Figure 4.3), and separated into individual tubes for egg laying. Egg papers from individual females were hatched in separate

pans to produce the G1 generation. G1 siblings were self-crossed to generate G2 egg papers. G1 individuals were screened for TALEN-Exloqs gene excision (double TALEN cleavage) via PCR followed by agarose gel electrophoresis (described below). Since no double-cleavage mutants were identified, G1 siblings were combined, frozen in liquid nitrogen and stored an -80°C until genomic DNA extraction.

G1 families were screened for *exloqs* mutations resulting from N-term TALEN cleavage using PCR followed by high-resolution melt curve analysis (HRMA) of the amplicon (described below). G2 offspring from three families (labeled II, K, and BB) with variant melt curves were hatched, sorted as pupae, and individually screened as adults.

To establish the TALEN-ExLoqs mutant lines, II, K and BB mutant males were mated by Lvp strain *Ae. aegypti* females (Figure 4.3), allowing at least two days for mating. In an attempt to generate II homozygous and II/K trans-heterozygous mutant offspring, these same II and K mutant males were transferred to cages with II females, creating the following crosses: II males x II females, K males x II females.

DNA extraction, PCR screening and high resolution melt curve analysis

All PCR reactions were performed using the Phire Animal Tissue Direct PCR kit (Thermo Scientific), per the manufacturer's instructions, using PCR primers listed in Table 4.2 at 250 μM concentration. For screening individual mosquitoes, single legs were used as templates per the manufacturer's "dilution protocol." For screening TALEN-ExLoqs G1 families, genomic DNAs from pooled G1 siblings were extracted using the NucleoSpin Tissue kit (Machery Nagel). PCR reactions were performed using 40 ng of genomic DNA for each 20 μl reaction.

To screen for complete excision of the ExLoqs ORF, the PCR assay was designed such than an intact *exloqs* gene would result in a 1.8 kb amplicon, whereas excision of the ExLoqs ORF would result in a 163 bp amplicon. This size difference could be resolved by agarose gel electrophoreses. For HRMA, 1x LC Green (BioFire) dye was included in the PCR reactions and the amplicon melting temperatures were analyzed using a LightScanner System (BioFire) and compared to controls. Additional PCRs for sequencing reactions were performed using the primers listed in Table 4.2. The resulting amplicons were sequenced (primer listed in Table 4.2) and compared to non-mutant control DNA sequences from Lvp strain *Ae. aegypti* mosquitoes.

Table 4.1. TALEN recognition sites

N-term TALEN binding sites:

L1 (left arm)	Spacer	R1 (right arm)
TCAAATGAATGCTGTGAAAA	CGGGGACAACGC	CTTACTAAATGGCTATGTGA

C-term TALEN binding sites:

L2 (left arm)	Spacer	R2 (right arm)
TCAACATACCCAGGTGGATA	TGTTCGTATCGA	GAAAGAAGCAGAAAGCAGGA

Table 4.2. Oligonucleotides used for ExLoqs PCRs and sequencing

Primer Name	Purpose	Sequence 5' to 3'*
ExLoqs ORF F	PCR for screening for gene excision and sequencing	ATGGGTAGAACGAATTCGCCGTCAAATG
ExLoqsPF R2	PCR for screening for gene excision	TCAAAGAGAAGAACATTACG
ExLoqsNTerm-F1	PCR for HRMA Screening	TCGCCGTCAAATGAATGCTGT
ExLoqsNTerm-R1	PCR for HRMA Screening	ATTCGATTCTCCCGGCGAAG
Exloqs 5RACE2	PCR for sequencing	CAGGTTTGTTCGCGCTATCGTTGATATACCCA
ExLoqsEx2 R	Sequencing	GTCTCCATCCGGGTACGAT

Results

TALEN recognition sites were chosen such that TALEN-based cleavage would occur in the 2nd exon, downstream of the initiator codon, and in the final exon, just upstream of the termination codon (Figure 4.1). In reference to the location of the cleavage sites in the ExLoqs protein, these TALEN pairs were referred to as the N-term pair and C-term pair, respectively. This way, if successful recognition and cleavage by both TALEN pairs were to occur, nearly the entire *exloqs* ORF would be excised from the genome, resulting in complete ExLoqs protein knockout (Figure 4.1). However, gene disruption could also occur if single cleavage by the N-term TALENs resulted in imperfect DNA repair leading to a frame-shift in the *exloqs* ORF.

From the 928 embryos injected, a total of 235 G0 individuals survived to adulthood (25%). Female G0s were mated with wild-type *Ae. aegypti* to generate G1 progeny; a subset of which were individually screened for excision of the Exloqs ORF, resulting from combined cleavage by both the N-term and C-term TALEN pairs. ExLoqs excision was not detected in any of the individuals screened (n=92, not shown). However, HRMA of amplicons obtained following PCR of genomic DNA isolated from pooled G1 individuals (n=30 families) revealed three families (labeled II, K and BB) with likely mutations in the N-terminal TALEN recognition site (Figure 4.2A, B), suggesting an editing rate for the N-term TALEN pair of ~10%. G2 eggs collected from these individuals prior to DNA extraction were hatched and the resulting progeny screened for the presence of N-terminal mutations using HRMA (Table 4.3). A total of 48 males and 94 females were screened from the II family, 47 males from the K family, and 48 females from the BB family. These resulted in the recovery of 27.5%, 14.9% and 25% mutants for II, K, and BB families, respectively, for an overall average of 24.5% mutants in the G2 generation.

Sequencing of *exloqs* PCR amplicons from the II, BB, and K families revealed 4 bp, 3 bp, and 1 bp deletions, respectively (Table 4.4).

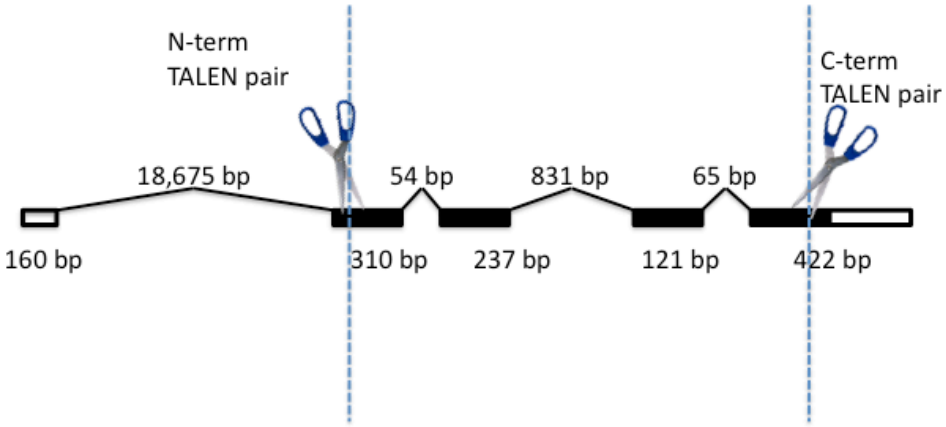

Figure 4.1. Location of TALEN-ExLoqs recognition sequences on *exloqs* gene.
Recognition sites for N-term and C-term TALEN pairs are located near 5' and 3' ends of the ExLoqs ORF. Solid boxes represent ORFs, unfilled boxes represent untranslated regions.

A)

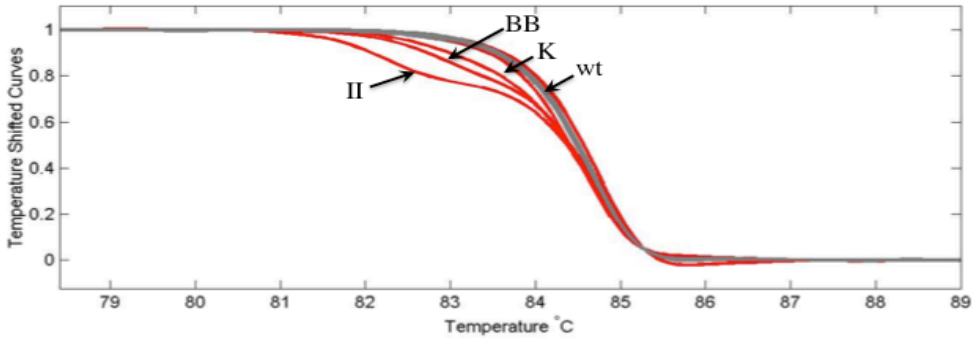

B)

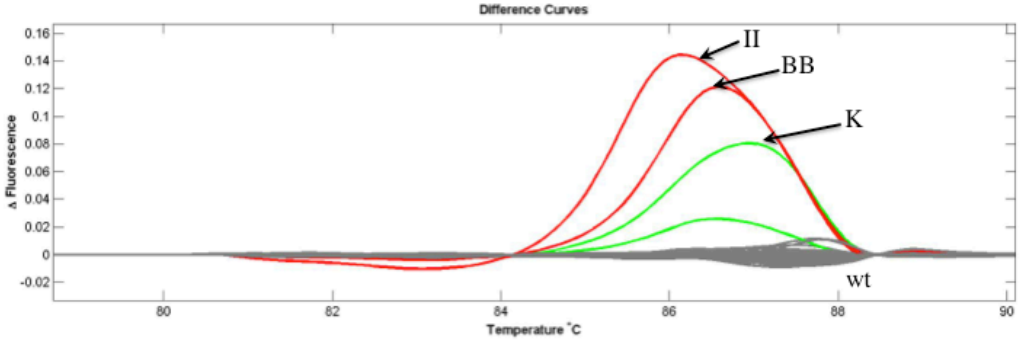

C)

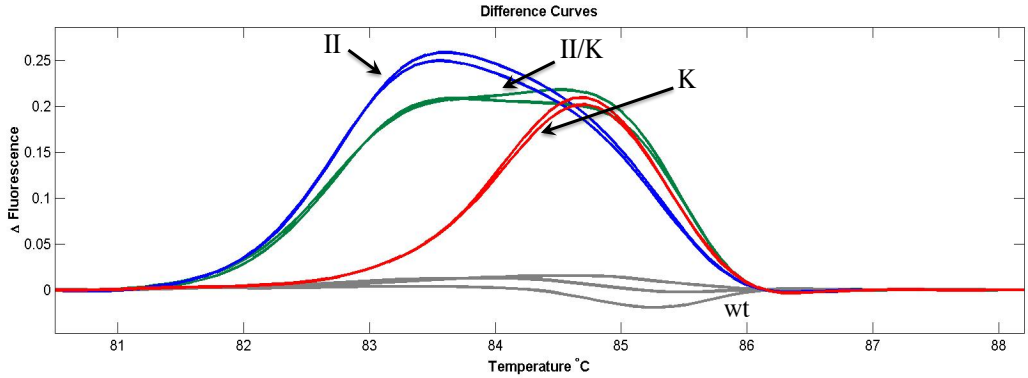

Figure 4.2. High resolution melt curve analysis of TALEN-ExLoqs mosquitoes
Melting point differences in TALEN-ExLoqs mosquitoes were detectable by HRM analysis.
A) Shifted melt curves in TALEN-ExLoqs G1 families. B) Differences in amplicon melting temperatures result in unique peaks in graphed difference curves for TALEN-ExLoqs II, K, and BB families. C) Unique difference curves from II/K trans-heterozygous (m^{II}/m^{K}, green) individuals appear as "hybrids" of the difference curves for II (blue) and K (red) heterozygotes.

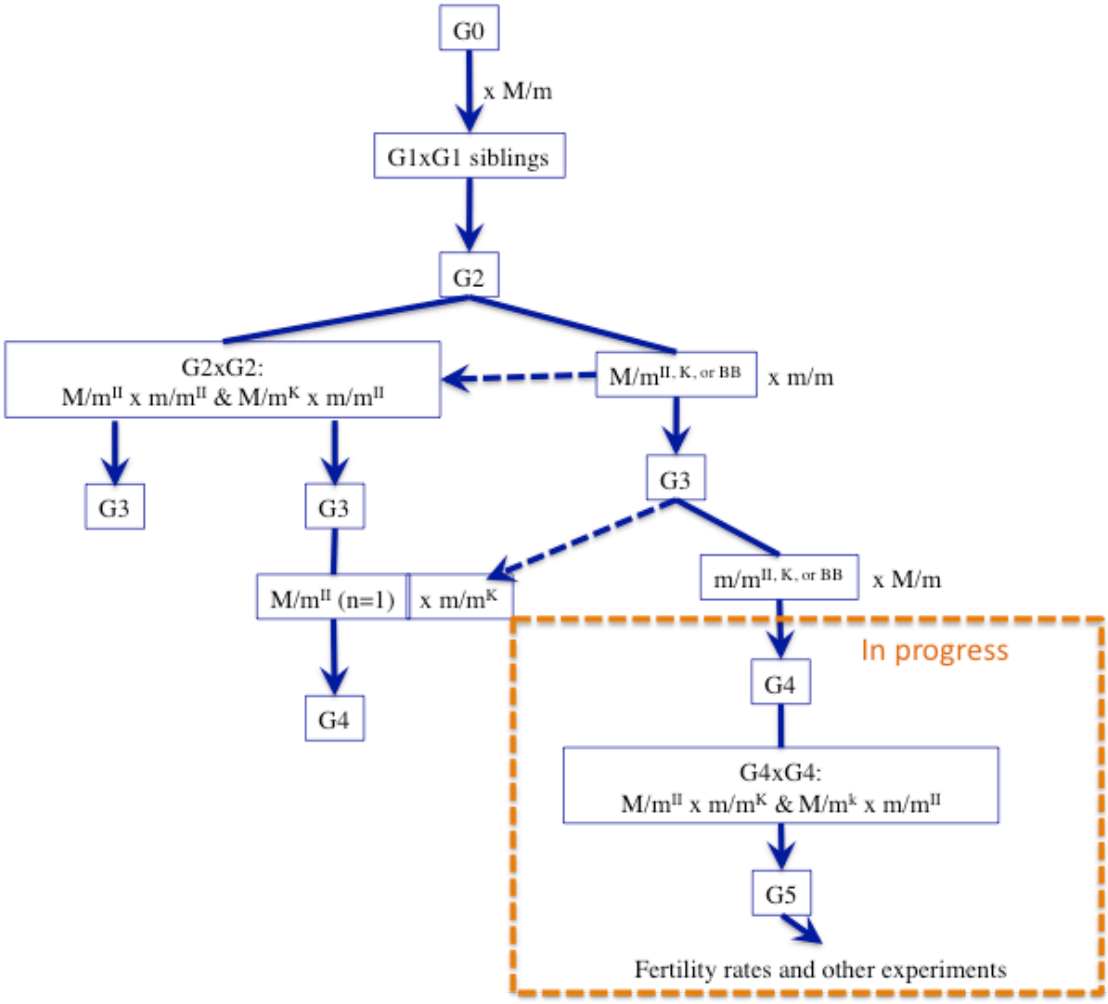

Figure 4.3. TALEN-ExLoqs mating scheme

G0 TALEN-ExLoqs females were mated with wild-type males. G1 siblings were self-crossed. G2 mutant males were mated with wild-type females. The same G2 M/m^{II} an M/m^{K} males were also mated with G2 m/m^{II} females. Less than 1% of eggs from this M/m^{K} x m/m^{II} cross hatched, one of these four offspring, and M/m^{II} male was mated with m/m^{K} females (n=6). G3 mutant females were mated with wild-type males, to generate G4 progeny that could be mated to attempt generation of II/K trans-heterozygous G5 individuals. G5 progeny will be utilized for experiments analyzing fertility and other phenotypic assessments.

Table 4.3. Results from screening G2 TALEN-ExLoqs progeny

Family		#mutant (%)	#wild-type (%)	Total Screened
II	**males**	11 (22.9%)	37 (77.1%)	48
	females	28 (29.8%)	66 (70.2%)	94
	Total	39 (27.5%)	103 (72.5%)	142
		#mutant (%)	**#wild-type (%)**	**Total Screened**
K	**males**	7 (14.9%)	40 (85.1%)	47
	females	-	-	0
		#mutant (%)	**#wild-type (%)**	**Total Screened**
BB	**males**	12 (25.0%)	36 (75.0%)	48
	females	-	-	0

Summary

	#mutant (%)	#wild-type (%)	Total Screened
males	30 (21.0%)	113 (79.0%)	143
females	28 (29.8%)	66 (70.2%)	94
Total	58 (24.5%)	179 (75.5%)	237

Table 4.4. Deletions in TALEN-ExLoqs transgenic lines

Line	Beginning of ExLoqs ORF showing nucleotide deletions (red)
II	**ATG**GGTAGAACGAATTCGCCGTCAAATGAATGCTGTGAAAACGGG**GACA**ACG….
BB	**ATG**GGTAGAACGAATTCGCCGTCAAATGAATGCTGTGAAAACGGGG**ACA**ACG….
K	**ATG**GGTAGAACGAATTCGCCGTCAAATGAATGCTGTGAAAACGGGG**A**CAACG….

Table 4.5. *exloqs* is linked to the sex-determining locus on chromosome 1
Results from screening G3 progeny from heterozygous ($m/m^{II, K \text{ or } BB}$) females mated by wild-type males (M/m)

Parental cross (male x female)		#mutant (%)	#wild-type (%)	Total Screened
M/m x m/m^{II}	**males**	2 (1.4%)	138 (98.6%)	140
	females	62 (98.4%)	1 (1.6%)	61

		#mutant (%)	#wild-type (%)	Total Screened
M/m x m/m^{K}	**males**	0 (0.0%)	138 (100.0%)	138
	females	62 (98.4%)	1 (1.6%)	63

		#mutant (%)	#wild-type (%)	Total Screened
M/m x m/m^{BB}	**males**	1 (0.8%)	128 (99.2%)	129
	females	15 (88.2%)	2 (11.8%)	17

Summary

	#mutant	#wild-type	Total Screened	% recombinant
males	3	404	407	0.7%
females	139	4	143	2.8%
		Average		**1.3%**

Table 4.6. Results from screening G3 and G4 progeny from *exloqs*$^{II\ or\ K}$ x *exloqs*^{II} and *exloqs*^{II} x *exloqs*^{K} crosses

Parental cross (male x female)	Generation		wt/wt	II/wt	II/II	K/wt	II/K	Total Screened
M/m^{II} x m/m^{II}	G3	males	16 (42.1%)	22 (57.9%)	0	0	0	38
		females	45 (54.9%)	37 (45.1%)	0	0	0	82
M/m^{II} x m/m^{k}	G3	males	1 (33.3%)	2 (66.7%)	0	0	0	3
		females	0	0	0	1 (100%)	0	1
M/m^{II} x m/m^{k}	G4	males	12 (50.0%)	0	0	12 (50.0%)	0	24
		females	0	9 (50.0%)	0	0	9 (50.0%)	18

Table 4.7. Results from screening *exloqs*$^{II\ or\ K}$ x wt G4 progeny

Parental cross (male x female)		#mutant (%)	#wild-type (%)	Total Screened
M/m x m/m^{II}	males	15 (62.5)	9 (37.5%)	24
	females	8 (36.4%)	14 (63.6%)	22
	Total	23 (50.0%)	23 (50.0%)	46

		#mutant (%)	#wild-type (%)	Total Screened
M/m x m/m^{K}	males	21 (52.5%)	19 (47.5%)	40
	females	29 (49.2%)	30 (50.8%)	59
	Total	50 (50.5%)	49 (49.5%)	99

Summary

	#mutant (%)	#wild-type (%)	Total Screened
males	36 (56.3%)	28 (43.7%)	64
females	37 (45.7%)	44 (54.3%)	81
Total	73 (50.3%)	72 (49.7%)	145

Sex-linkage of TALEN-ExLoqs mutations

Unlike other Diptera, *Aedes* mosquitoes do not have sex chromosomes, but rather a sex-determining locus on chromosome 1 (130). Results from screening G3 TALEN-ExLoqs individuals indicated that the *exloqs* gene is tightly linked with the *Ae. aegypti* sex determining locus (Table 4.5). Progeny from crosses of TALEN-ExLoqs mutant males (genotype $M/m^{II\ or\ K}$) with wild-type females (m/m) resulted in 97.2% mutant females ($m/m^{II\ or\ K}$) and only 0.7% mutant males. The overall recombination distance between *exloqs* and the sex-determining locus (m) was determined to be approximately 1.3% (Table 4.5).

Generation of TALEN-ExLoqs trans-heterozygous individuals

exloqs^{II} and *exloqs*^{K} males (genotypes M/m^{II} and M/m^{K}) from the G2 generation were mated by II females (m/m^{II}) in attempt to generate II homozygous (m^{II}/m^{II}) and II/K trans-heterozygous (m^{II}/m^{K}) G3 individuals (Figure 4.3). However, these attempts were largely unsuccessful. Based on Mendelian inheritance, we hypothesized that these crosses would result in overall 50% heterozygous, 25% wild-type, and 25% homozygous/trans-heterozygous progeny. However, based on the HRM analysis, both male and female progeny from the *exloqs*^{II} x *exloqs*^{II} cross were approximately 50% heterozygous *exloqs*^{II} and 50% wild-type (Table 4.6). Only four larvae hatched out of 396 *exloqs*^{II} x *exloqs*^{K} eggs, giving a less than 1% hatch rate. Of these four larvae, two were *exloqs*^{II} heterozygous males (M/m^{II}) and one was an *exloqs*^{K} heterozygous female (m/m^{K}) (Table 4.6). We were able to mate one of the M/m^{II} males by m/m^{K} females (n=6) to attempt generation of m^{II}/m^{K} progeny (Figure 4.3). The other M/m^{II} was deemed infertile after failing to mate with wild-type (m/m) females.

Progeny from the single M/m^{II} male mated to wild-type females resulted in an approximately 50:50 ratio of m/m^{II} and m^{K}/m^{II} females (Figure 4.2C and Table 4.6), as would be expected from this cross . This result further suggests that the infertility observed in the previous generation's *exloqs*^{II} x *exloqs*^{K} cross was most likely due to unforeseen founder effects in the generation of the TALEN-ExLoqs transgenic lines which may have been amplified through inbreeding in the G1 generation. The genotypic bottlenecking may also have caused the unexpected genotypic proportions observed from the *exloqs*^{II} x *exloqs*^{II} cross. Since the m^{K}/m^{II} individuals obtained at this point were the progeny from a single M/m^{II} who may harbor unknown deleterious inbreeding genotype, these trans-heterozygous individuals were not used for further experiments after genotyping.

Therefore, attempts at creating additional *exloqs*^{II}/*exloqs*^{K} trans-heterozygotes were revisited after out-crossing heterozygous TALEN-ExLoqs lines with wild-type mosquitoes for an additional generation to improve genetic diversity in the population. Thus, G3 progeny from the TALEN-ExLoqs x wild-type *Ae. aegypti* crosses were screened for heterozygous mutants using HRMA (Table 4.5). Females identified as m/m^{II} or m/m^{K} were mated by wild-type *Ae. aegypti* (Figure 4.3), to generate male and female *exloqs*^{II} and *exloqs*^{K} heterozygous G4 progeny ($M/m^{II\text{ or }K}$ and $m/m^{II\text{ or }K}$). As expected, these G4 progeny were 50% mutant, based on HRMA (Table 4.7). These mutants were crossed (M/m^{II} x m/m^{K} and M/m^{K} x m/m^{II}) to obtain m^{II}/m^{K} females in the G5 generation (Figure 4.3). These trans-heterozygous females will be utilized for experiments assessing the affect of ExLoqs knockout on *Ae. aegypti* mosquitoes.

Discussion

By using TALEN-based gene disruption, we were able to generate three TALEN-Exloqs mutant *Ae. aegypti* lines with unique nucleotide deletions in the *exloqs* gene. The TALEN-based gene-editing rate was approximately 10%, which is lower than the previously reported rate ~23% for KMO gene disruption (129).

One and four base pair deletions in the *exloqs*^{K} and *exloqs*^{II} lines, respectively, are expected to introduce frameshifts to the ExLoqs ORF. Since the frameshifts occur at the N-terminus of the ExLoqs protein, any translation products would lack both DRMs and most likely disrupt ExLoqs' function. The third TALEN-ExLoqs line, BB, has a 3 bp deletion and thus, does not introduce a frameshift to the ExLoqs ORF, but rather the deletion of a single amino acid, N17. Furthermore, screening for TALEN-ExLoqs mutant progeny revealed that *exloqs* is linked with the sex-determining locus, with a recombination distance of approximately 1.3%.

This study was the first successful use of HRMA technology for detection of TALEN-mediated nucleotide deletions in *Ae. aegypti*. HRMA-based screening enabled highly sensitive detection of even single nucleotide deletions and trans-heterozygous deletion combinations. Combined with the Phire Animal Tissue Direct PCR (Thermo Scientific), HRMA also facilitated relatively rapid screening of mosquitoes, such that individuals could be genotyped and mated on the same day (up to ~200 individuals per workday using a single 96-well plate thermocycler). This eliminated the need to await DNA sequencing results prior to setting up crosses; however sequencing was still used to confirm genotypes, when possible. This rapid turnover is especially important given the short lifespan of mosquitoes, and the need to identify sufficient numbers of mutants for successful crosses and ample egg-collection.

The purpose of generating *exloqs* knockout mosquitoes is to ultimately assess the function of ExLoqs in *Ae. aegypti*. Since ExLoqs is most robustly expressed in the gonads of *Ae. aegypti* mosquitoes (see previous chapter), we hypothesized that ExLoqs is most likely important to mosquito fertility. In females, ovarian expression of ExLoqs is most concentrated in nurse cells, suggesting it may play a role in ovarian development, vitellogenesis or germ-line integrity. Thus, our intention is to compare fertility rates (egg counts and hatch rates) and ovarian development of trans-heterozygous TALEN-ExLoqs mosquitoes with wild-type mosquitoes.

Preliminary results comparing hatch rates from existing G4 m^{II}/m^{K} females (n=9) with those from m/m females indicate that *exloqs* knockout mosquitoes are fertile (data not shown). However, this experiment needs to be repeated with a greater number of m^{II}/m^{K} individuals from the G5 generation for greater statistical and biological relevance, as previously mentioned. Normal fertility of ExLoqs knockout mosquitoes could still occur if ExLoqs depletion was compensated by another protein or mechanism with a redundant function. It is also possible that ExLoqs functions in inhibition of transposable elements. The latter could be detected by sequencing mRNA and small RNA libraries to examine differences in the number of sequences mapping to transposons. If ExLoqs functions in silencing transposable elements, the number of transposon-derived small RNAs would decrease, while transposon transcript levels would increase. Likewise, transcriptome silencing would enable identification of specific transposable elements that have been up or down-regulated. This transcriptome based-analysis would be similar to transcriptome screens that have been used to identify piRNA targets in *Drosophila* ovaries (131). Accumulation of deleterious effects from transposons could also be identified by fitness costs in subsequent generations.

Sequencing of mRNA and small RNA libraries from trans-heterozygous TALEN-ExLoqs and control mosquitoes will also enable analysis of a potential role for ExLoqs in small RNA biogenesis or transcript regulation. Differences in the size and origins of small RNAs could provide indications regarding the inhibition or activation of RNAi pathways. For example, sequencing of *Aedine* cell lines reveals that those without functional siRNA pathways (C6/36 and C7-10) have markedly fewer 21 nt small RNAs as compared to those with functional siRNA pathways (Aag2 and U4.4) (132). Viral-infected C6/36 and C7-10 cells also have significantly more 20-30 nt viral-derived piRNAs, than siRNA-competent cells, indicating that the piRNA pathway can compensate for anti-viral defense in the absence of a functional anti-viral siRNA pathway (132). Additionally, transcriptome and small RNA sequencing has been used to determine that drosophilid Loqs-A is essential to miRNA biogenesis, while Loqs-D functions in endo-siRNA biogenesis (23,42). Additionally, transcriptome mapping can facilitate identification of potential up- or down-regulated genes or transposons (131,133).

Since *Aedes* mosquitoes are susceptible to a number of arboviruses that it may be exposed to during blood meals (134-136), another possibility is that ExLoqs evolved to function in anti-viral defense within the germ-line to inhibit vertical transmission. This would be especially significant in regards to propagation and persistence of arboviruses in endemic regions (137,138). Thus, additional experiments with TALEN-ExLoqs mosquitoes may include quantification of differences in the vertical transmission of viruses from infected mosquitoes to their offspring.

Conclusion

Using TALEN-based gene disruption, we were able to create several mutant TALEN-ExLoqs strains of *Ae. aegypti*. Our results indicate that the *exloqs* gene is located near the sex-determining locus. Experiments utilizing this strain to examine the function of the ExLoqs protein are currently underway. Based on gene characterization experiments described in the previous chapter, we hypothesize this protein is important to *Ae. aegypti* fertility, ovarian development, or germline integrity. Thus, future experiments include comparison of egg counts and hatch rates from TALEN-ExLoqs trans-heterozygous females to those of wild-type controls. Sequencing mRNA and small RNA libraries from infected and uninfected mosquitoes will also provide insight as to ExLoqs' potential function in gene regulation, RNA interference, or anti-viral defense.

Chapter 5 - A new sensor for assessing function of the exo-siRNA pathway, using a Nodamura viral expression system

Introduction

RNA interference (RNAi) is a highly conserved mechanism of post-transcriptional gene regulation in eukaryotic organisms. There are several variations of RNAi pathways, all of which are initiated by a protein complex recognizing double stranded RNA (dsRNA) and ultimately result in the degradation of homologous mRNA and inhibition of cognate gene expression. In *Ae. aegypti* mosquitoes, the exo-siRNA pathway directly affects vector competence by limiting arboviral replication during infection (85). In order for a vector mosquito to successfully transmit an arbovirus, the virus must establish a persistent level of infection and dissemination within the mosquito without generating pathogenesis that could limit the mosquito's blood-feeding ability. Thus, a balance must be achieved between viral replication and the vector's innate immunity (30).

The exo-siRNA pathway functions by targeting double-stranded RNA intermediates that form during the replication of RNA viruses. During replication in the cytoplasm, viral dsRNAs are cleaved by a Dicer-2 initiator complex to generate 21 nt exo-siRNAs (139). These siRNAs are loaded into an RNA-induced silencing complex (RISC), along with an Argonaute 2 (AGO2) protein. Once in RISC, the exo-siRNA is unwound, such that the one strand can guide the RISC complex to homologous viral mRNAs and induce cleavage by AGO2 (27).

Nodamura virus (NoV) belongs to the family *Nodaviridae* and the genus *Alphanodavirus*. Its genome consists of bipartite, single stranded, positive sense RNA, with 5' caps and no 3'

poly-adenylation (Figure 5.1). The genomic RNA segments are known as RNA1 and RNA2, and encode for the structural and non-structural proteins, respectively (95). The 3.2kb RNA1 segment encodes an RNA-dependant RNA polymerase (RdRp) protein, known as protein A. The 3' region of RNA1 is also transcribed into a subgenomic mRNA, known as RNA3, which encodes for two additional non-structural proteins known as B1 (same ORF as protein A) and B2 (+2 reading frame) (95,96). The function of B1 is unknown, while B2 functions as an RNAi suppressor protein (96,97). In the absence of B2, viral replication is significantly compromised by RNAi (140). NoV is the only known Nodavirus that can infect both arthropod and mammalian cells (95,141). Despite its wide range of hosts, it is not a known human pathogen, and no reports of NoV infection in human have been reported to date. Nodamura virus's unique characteristics make it a valuable laboratory tool for expressing heterologous RNAs and assessing their effect on RNAi.

The objective for this study was to utilize a NoV-expression system to create a "sensor" for the exo-siRNA pathway, enabling rapid assessment of the functionality of this pathway via conditional expression of a reporter gene. We named this exo-siRNA sensor the NoV-Sensor. Once established, this sensor would provide an efficient method for testing the effects of knockdown or over-expression of target genes on the exo-siRNA pathway. Thus the exo-siRNA sensor would be a valuable tool for further studies involving genes potentially involved in RNAi and anti-viral defense.

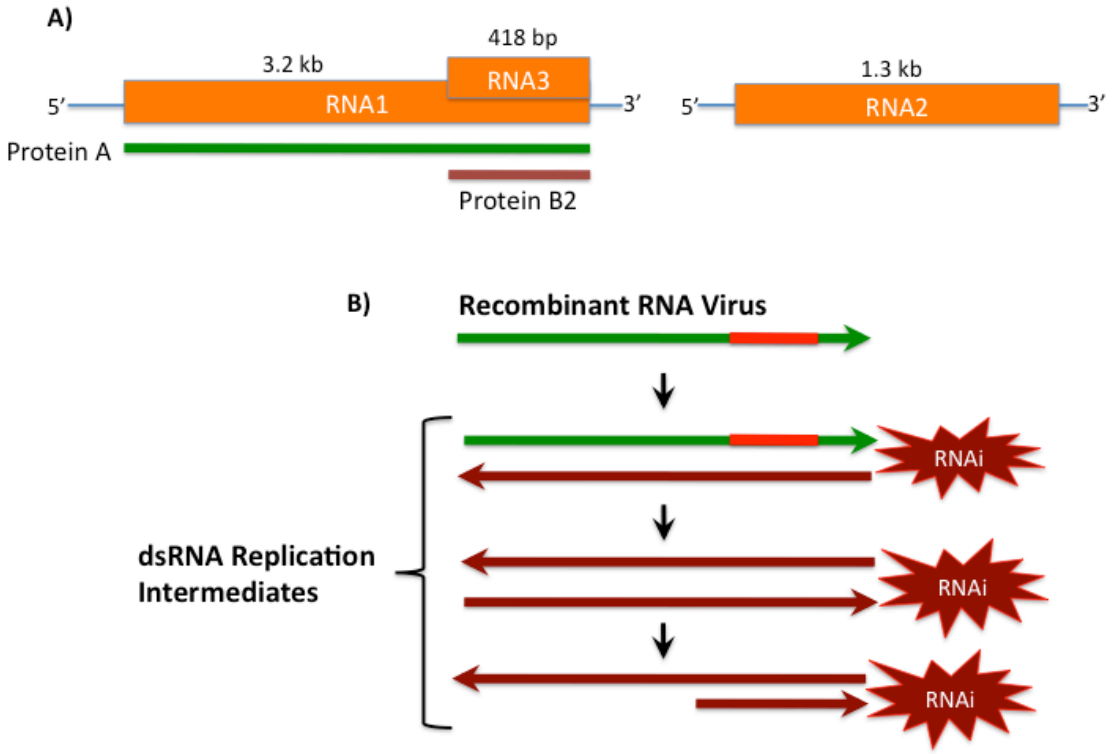

Figure 5.1. Nodamura viral expression system for exo-siRNA induced gene knockdown.
A) Nodamura virus has a bipartite genome. The genomic RNA1 segment encodes the viral replicase, Protein A. The subgenomic RNA3 segment encodes the viral RNAi-suppressor, Protein B2. B) Replication of a recombinant RNA virus encoding a target sequence generates dsRNA intermediates that activate exo-siRNA-based silencing.

Generation of an exo-siRNA sensor was attempted both *in-vivo* (in transgenic mosquitoes), as well as *in-vitro* (in cultured mosquito cells). For the *in-vivo* experiments, the Nov-Sensor mosquito was generated similar to an existing strain known as the "3xP3-sensor" strain, which enables visual assessment of the functionality of the endo-siRNA pathway using a conditionally expressed Enhanced Green Fluorescent Protein (EGFP) marker gene (102). The 3xP3-sensor transgene consists of a series of 3 artificial gene cassettes. The first and the second genes in the series code for the red and green fluorescent proteins, DsRed and EGFP, respectively, while the third cassette consists of an inverted repeat sequence (EGFPir) designed to express hairpin RNA homologous to a portion of the EGFP gene. Separate 3xP3 artificial promoters individually control the expression of each of these genes, thus enabling easily detectable, eye-specific gene expression using a fluorescent microscope. Thus, in mosquitoes with a functional endo-siRNA pathway, EGFP expression should be suppressed, whereas those with a compromised RNAi pathway will express EGFP. The presence of the 3xP3 sensor transgene is verifiable by DsRed expression. Therefore, this sensor mosquito can be used to identify genes important to the endo-siRNA pathway, through knockdown of target genes and observing the effect on EGFP expression (102). Similarly, the purpose of the NoV-Sensor was to identify genes involved in the exo-siRNA pathway (Figure 5.6).

Likewise, the *in-vitro* experiments were designed to enable quantifiable evaluation of exo-siRNA function using a conditionally expressed NanoLuc luciferase (Promega) reporter gene. For both sets of experiments, NoV-viral expression systems were designed to express exo-siRNAs targeting the marker gene (Figure 5.1).

Materials and Methods

Plasmid construction

All oligonucleotide primer sequences used for plasmid construction are listed in Table 5.1. A pBlueScript (pBSK) plasmid containing the sequence for NoVRNA1 was synthesized de novo. The plasmid also included a phage T7 promoter sequence upstream of NoVRNA1, and the Hepatitis Delta Virus (HDV) ribozyme sequence followed by a T7 terminator sequence downstream of NoVRNA1, as described (142). The 3xP3 promoter sequence was cloned into *PacI* to *KpnI* sites located upstream of the T7 promoter sequence, creating the construct 3xP3-NoVRNA1. *PUb*-NoVRNA1 and IE1-NoVRNA1 constructs were generated by Dr. Michael Wiley, as described (142).

The 3xP3-NoVRNA1-GFP and 3xP3-NoVRNA1-GFPas constructs were created by replacing the B2 ORF in the RNA3 subgenomic transcription region with either the GFP ORF or a 505 bp fragment of antisense GFP. The GFP ORF and GFPas sequences were amplified using Platinum Pfx (Qiagen) and primers designed to add *BamHI* and *PflMI* recognition sequences to the 5' and 3' ends, respectively. After restriction enzyme digestion, the PCR products were purified by agarose gel extraction and ligated into *BamHI* and *PflMI* restriction enzyme sites in the RNA3 sequence.

The full NoVRNA1 and RNA3 ORFs were later recovered by amplifying the 3' terminal sequence and cloning it into the *BamHI* restriction site. The sequence was amplified between the endogenous *BamHI* site and the 3' terminus using Platinum Pfx and a primer designed to add a *BglII* restriction site to the 3' end. Thus, the resulting plasmids consisted of 3xP3 driving the expression of the full Protein A product, including the full B2 ORF fused to either GFP or

GFPas. We named these plasmids pBSK-3xP3-NoVRNA1ORF-GFP and pBSK-3xP3-NoVRNA1ORF-GFPas. The SV40 3'UTR (early) was amplified by Pfx PCR using primers designed to add *MluI* and *AscI* recognition sites to the 5' and 3' ends, respectively. This SV40 3'UTR was ligated into the *AscI* site, downstream of the HDV sequence in the 3xP3-NoVRNA1, 3xP3-NovRNA1ORF-GFP, and 3xP3-NoVRNA1ORF-GFP505 constructs.

For the initial Renilla knockdown-constructs, a 575 bp fragment of Renilla luciferase was amplified by Platinum Pfx (Invitrogen) with primers designed to add the *PflMI* recognition site to the 3' end and *SacII* recognition sites to the 5' end. This Renilla luciferase fragment was then ligated in the antisense direction into the *PflMI* and *SacII* restriction sites near the 3' terminus of RNA3 in the 3xP3-NoVRNA1 plasmid, thus creating the 3xP3-NoVRNA1-RenAs plasmid. The full NoVRNA1 and RNA3 ORFs were restored by designing a synthetic construct consisting of the same antisense fragment of Renilla luciferase fused to the B2 ORF and cloning into *BamHI* and *SacII* restriction enzyme sites in the RNA3 region of the 3xP3-NoVRNA1 and PUb-NoVRNA1 plasmids. Thus, the resulting constructs were named 3xP3-NoVRNA1ORF-RenAs and PUb-NoVRNA1ORF-RenAs. For the NanoLuc luciferase (NanoLuc) expression plasmid, the NanoLuc ORF was amplified by Pfx PCR with primers designed to include *SpeI* and *SacII* recognition sites at the 5' and 3' ends, respectively. The digested amplicon was then ligated in the corresponding restriction enzyme sites to replace RenAs in the PUb-NoVRNA1ORF-RenAs-SV40 plasmid, thus creating PUb-NoVRNA1-NL. To create PUb-FSNoVRNA1-NL, a +4 bp frame-shift was introduced to the Protein A ORF of this construct by digesting the plasmid with *NcoI*, blunting the resulting cleavage sites using Klenow DNA polymerase I, and self-ligating the plasmid. Lastly the *PUb*-NoVRNA1ΔB2-NL plasmid was created by using *BamHI* and *NotI*

restriction enzymes to replace the three intact B2 start codons with mutated ones from a *PUb*-NoVRNA1ΔB2 plasmid.

The NoV-Sensor mosquito construct was built using the original "sensor" mosquito template (102), which consisted of 3xP3 promoter sequences driving the expression of DsRed, GFP and a GFP inverted repeat (GFPir), thus the construct was 3xP3-DsRed-3xP3-GFP-3xP3-GFPir. For the Nov-Sensor, the 3xP3-GFPir cassette was replaced by a multiple cloning site (MCS) flanked by *loxP* inverted repeat recognition sites and an *attP* site at the 3'end. This *loxP*-MCS-*loxP*-*attP* sequence was amplified from the pMosDsRED-5HE-MCS-5HE plasmid, using primers designed to add *BamHI* and sites to both the 5' and 3' ends. The entire 3xP3-NoVRNA1ORF-GFPas cassette was excised from the 3xP3-NoVRNA1ORF-GFPas plasmid using *PacI* and *AscI* restriction enzymes, followed by purification via phenol/chloroform extraction from low melt agarose. This cassette was then cloned into *PacI* and *AscI* multiple cloning site, flanked by *loxP* sites. The resulting sequence for the NoV-Sensor was 3xP3-DsRed-3xP3-GFP-3xP3-NoVRNA1ORF-GFPas (Figure 5.6).

Table 5.1. Oligonucleotide sequences used for construction of NoVRNA1 plasmids

Primer Name	*Sequence 5' to 3'
EGFP BamHI F	ttttggatccAATGGTGAGCAAGGGCGAGGAGC
EGFP PflMI R	ttttccacttgttggTTACTTGTACAGCTCGTCCATGCC
EGFP505 BamHI R	ttttggatccAGGATCTTGAAGTTCACCTTGATGCC
EGFP505 PflmI F	tttccacttgttggTTGGTGAGCAAGGGCTAGGAGCTG
NoVRNA1 BamHI F	AACGCTCATGATCGCGGATCCCAACGTCAACAAG
RNA1 BglII R	ttttagatctATGAATCACTCATTTACCACGCCCACGCGA
SV40 MluI F	ttttacgcgtTCATAATCAGCCATACCACATTTGTAGAG
SV40 AscI R	ttttggcgcgccTAAGATACATTGATGAGTTTGGAC
Rluc SacII F	ttttccgcggGCTCGAAAGTTTATGATCCAGAAC
Rluc PflMI R	ttttccaacaagtggCGGCCGCTCTAGAATTATTGTTCATT
NanoLuc SpeI F	ttttactagtATGGTCTTCACACTCGAAGATT
NanoLuc1 R SacII	ttttccgcggTTACGCCAGAATGCGTTCGCA
BamHI LoxP F	ttttggatccCGCGTATAACTTCGTATAGCATACATTATACG
MCS AttP R	tttggatccGGCCGGCCTAGGCTACGCCCCCAA

*lower case letters denote added restriction enzyme recognition sites

Cell culture

BHK-21 and Vero cells were maintained at 37°C, 5% CO_2 in Dulbecco's Modified Eagle Media (Cellgro), supplemented with 10% FBS, 1% penicillin-streptomycin, and 1% L-glutamine. Aag2 cells were maintained at 28 °C in Schneider's *Drosophila* medium (Lonza BioWhittaker) supplemented with 10% FBS, 1% penicillin-streptomycin, and 1% L-glutamine.

For RNA-based cell culture experiments, NoV constructs were transcribed *in-vitro* using T7 polymerase. BHK-21 cells were electroporated with the *in-vitro* transcribed RNA and harvested 4 days post transfection.

The *PUb*-NoVRNA1-NL, *PUb*-FSNoVRNA1-NL, or *PUb*-NoVRNA1ΔB2 were co-transfected with PUb-RenillaFF (control) into Aag2 cells. Cells were transfected in 24 well plates using Effectene transfection reagent (Qiagen). For each well, 200 ng of the NoV plasmid and 50 ng of the control were first mixed with 1.6 µl Enhancer and 48.4 µl Buffer EC. After incubating 5 minutes at room temperature, 5 µl Effectene transfection reagent was added. After an additional 10-minute incubation, the transfection complex was mixed with 350 µl media and added drop-wise to the flask.

Cells were lysed in Promega Passive Lysis Buffer 24 hours post-transfection and luciferase expression was measured using Promega Firefly and NanoGlo Luciferase assay kits (Promega). Luminescence was quantified in a GlowMax plate reader (Promega).

Mosquito husbandry and generation of the NoV-Sensor mosquito strain

Mosquitoes were reared at 28°C and 60-70% humidity, with a photoperiod of 16 hours light and 8 hours darkness. The NoV-Sensor plasmid was injected into 907 kh^w embryos at a

concentration of 500 ng/µl along with 300 ng/µl of pGL3-*PUb*-mos1 helper plasmid in 1x injection buffer (113). Embryos were injected by Dr. Sanjay Basu. Adult mosquitoes were merged into four pools of about 30 individuals per pool, and then mated with kh^w mosquitoes. The resultant G_1 offspring were screened as larvae for DsRed and GFP expression in the eyes, using a Leica MZ-16FL stereofluorescence microscope. Peak excitation and emission wavelengths for DsRed and EGFP are 488 nm / 507 nm and 557 nm /592 nm, respectively.

RNA isolation and northern blotting

Total RNA was isolated from cells using TRIzol Reagent, per the manufacturer's instructions, and detected by northern blot. Agarose gel-purified NoVRNA1 restriction digestion products were used as templates for creating ^{32}P-labeled DNA probes, which labeled using the Amersham Megaprime™ DNA labeling system (GE Healthcare).

Results

Replication of NoV expression systems in mammalian and arthropod cell lines

The objective of this study was to create a new sensor mosquito to assess the function of the exo-siRNA pathway. We initiated this process by first creating a Nodamura viral expression system. Our initial plasmid designs were based on previous experiments by Li in 2003 (32), in which most of the B2 subgenomic ORF of Flock House Virus (also *Nodaviridae*) was replaced by the EGFP ORF. This resulted in EGFP expression driven by the NOV replicase, protein A, in place of the RNAi suppressor protein, B2.

Similarly, we created two plasmids expressing NoVRNA1, driven by the 3xP3 promoter. The majority of the B2 ORF was replaced by either the EGFP ORF, or by a 505 bp antisense fragment of EGFP (GFPas). Thus, when transfected, the 3xP3 promoter would control initial transcription of the NoVRNA1 (Protein A) mRNA. However, once translated and mature, Protein A could drive further replication of the viral mRNA, including both the genomic RNA1 and subgenomic RNA3-EGFP/GFPas mRNAs. The NoV-expression system is designed such that replication of the viral RNA also results in the generation of dsRNA intermediates of the EGFP or GFPas transcripts, thus leading to in exo-siRNA based degradation of GFP mRNA. It is important to note that, since the B2 ORF overlaps the 3' terminus of the Protein A ORF, replacing the B2 sequence also shortened the Protein A sequence, truncating the translated protein by 101 amino acids. Since the viral structural proteins are not included in the construct, the viral genome cannot be encapsulated and exported from the cell. Thus, even though the viral replicon replicates within the cell, no infectious particles are made.

We assessed the replication competency of each NoV construct via electroporation of *in-vitro* transcribed RNA into BHK-21 cells, which lack an exo-siRNA pathway. RNA was extracted 4 days post-transfection, and NoV replication was assessed by Northern analysis via detection of both RNA1 (3200 nt) and RNA3 (480 nt) transcripts. Since the subgenomic RNA3 mRNAs, are dependent on the viral replicon, the RNA3 bands would only be present with successful viral replication.

Transfection of NoVRNA1wt and NoVRNA1-GFP RNA in BHK cells resulted in robust RNA3 or RNA3-GFP expression (Figure 5.2A), consistent with the experiments by Li *et al* (32). However, we were not able to detect RNA3-GFPas after transfection of NoVRNA1-GFPas RNA, indicating that this construct was replication-deficient (Figure 5.2A). These results were

repeated several times, with new *in-vitro* transcription products and reagents. Thus, it appears that Protein A stability was compromised when its C-terminal was truncated with the sequence encoded by the GFPas transcript, though not with the GFP ORF sequence. Thus, we restored the terminal portion of the Protein A reading frame, creating NoVRNA1ORF-GFP and NoVRNA1ORF-GFPas. Both were able to replicate in BHK-21 cells (Figure 5.2A). We also created an additional construct designed to knockdown expression of the Renilla luciferase (RenLuc) reporter gene. This time, an antisense fragment of RenLuc was cloned into the *PflMI* restriction site in NoVRNA1, truncating Protein A by only 26 amino acids, instead of the previous 101 (Table 5.2). Electroporation of this construct in BHK-21 cells resulted in very weak NoV replication, visible only after longer exposure times (Figure 5.2B). Thus, it appears that Protein A 3' terminal stability could be maintained by the EGFP ORF sequence, but not GFPas, or RenAs (Figure 5.2B, Table 5.2).

A)

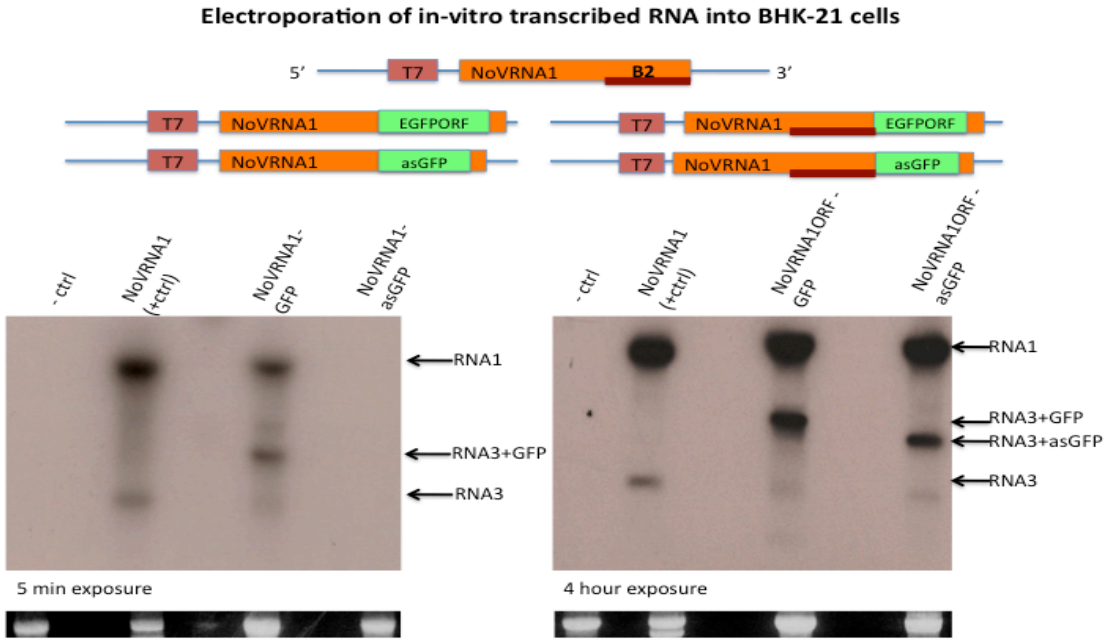

B)

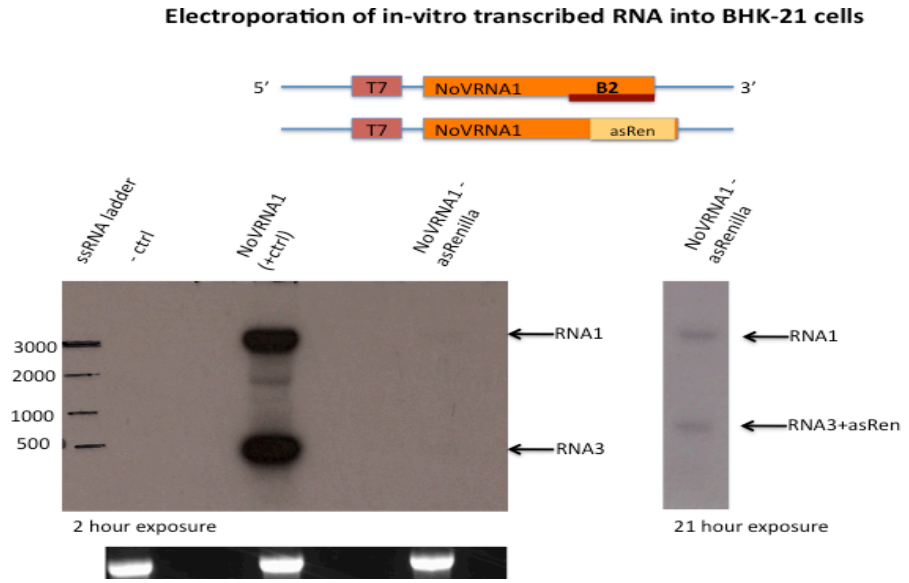

Figure 5.2. Replication of NoVRNA1 constructs in BHK-21 cells

In-vitro transcribed RNA from the NoVRNA1 constructs was electroporated in BHK-21 cells. Replication was assessed by northern blots to detect genomic (RNA1) and subgenomic (RNA3) transcripts. A) Electroporation of BHK-21 cells with NoVRNA1, NoVRNA1-GFP and NoVRNA1-GFPas. B) Electroporation of BHK-21 cells with NoVRNA1, NoVRNA1ORF-GFP and NoVRNA1ORF-GFPas. B) Weak replication of NoVRNA1-RenAs is visible after a longer exposure time. Note: NoVRNA1-RenAs from the same blot is shown after a 2 hour exposure and after a 21 hour exposure to radiographic film. Arrows indicate expected sizes for RNA1 and RNA3/RNA3-fusion bands.

Table 5.2. Protein A terminal stability can be maintained with the EGFP ORF sequence, but not GFPas or RenAs

Construct	Replication in BHK-21 cells	Protein A C-terminal truncation
NoVRNA1	****	(wt)
NoVRNA1-EGFPORF	****	-101 aa
NOVRNA1-GFPas	-	-101 aa
NoVRNA1-RenAs	*	-26 aa

Next, we tested each construct in RNAi-deficient (*A. albopictus C6/36* (36,132)) or RNAi-competent (*Ae. aegypti* Aag2 (36,132)) cell lines, respectively. As previous studies have successfully used the *Drosophila* S2 cell line for DNA-based expression of NoVRNA1(32), we also included this cell line as a control first to document successful DNA-based launch of replication. Three test plasmids were transfected into S2 cells, 3xP3-NoVRNA1, 3xP3-NoVRNA1-SV40, and IE-NoVRNA1 (Figure 5.3A). The second plasmid was the same as the first, but with the addition of the SV40 3'UTR polyadenylation sequence downstream of the HDV ribozyme, after the 3' terminus of NoVRNA1. For third plasmid, initial NoVRNA1 transcription was driven by *baculovirus IE1* promoter. As before, Northern blots were used to assess expression of NoVRNA1 and RNA3 replication products, 3 days post-transfection (Figure 5.3B). Overall, NoVRNA1 expression driven by the *IE1* promoter resulted in much more robust RNA1 and RNA3 bands, as compared with the two 3xP3-driven expression systems. As expected, addition of the SV40 3'UTR appeared to strengthen viral replication for the 3xP3 promoter driven system.

Next we tested the same three plasmids in Aag2 and C6/36 mosquito cells. Cells were harvested 1, 2, and 3 days post-transfection and NoV replication was assessed (Figure 5.3C and D). Unexpectedly, NoV replication was significantly compromised in both of these cell lines. In C6/36 cells, we were able to detect a faint band approximately at the expected size for RNA3 for cells transfected with 3xP3-NoVRNA-SV40 or IE1-NoVRNA1, indicating that low level replication may have been occurring.

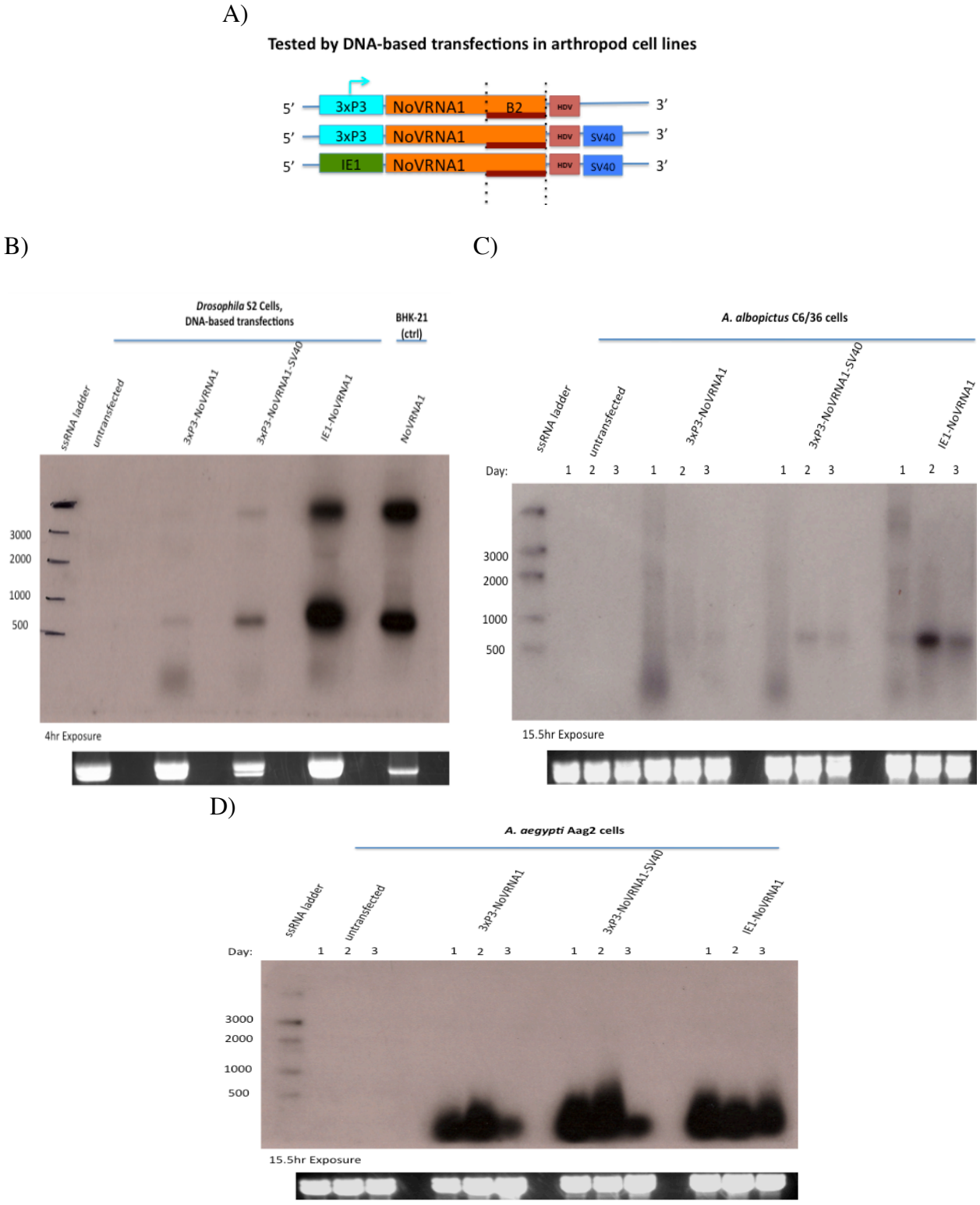

Figure 5.3. Transfection of wild-type NoVRNA1 constructs in arthropod cell lines
A) 3xP3-NoVRNA1, 3xP3-NoVRNA1-SV40 and IE-NoVRNA1 plasmids were transfected into B) *Drosophila* S2 cells, C) *Ae. albopictus* C6/36 cells, and D) *Ae. aegypti* Aag2 cells.

Neither RNA1 nor RNA3 hybridization signals could be detected in the northern blots for the transfected Aag2 cells. Instead, drastic smearing appeared at the bottom of the lanes for cells transfected with the NoVRNA1 constructs, but not in untransfected cells (Figure 5.3D). In addition to performing several replicates transfecting the control plasmids mentioned above, Aag2 transfections using 3xP3-NoVRNA1ORF-GFP, 3xP3-NoVRNA1ORF-GFPas, 3xP3-NoVRNA1ORF-RenAs, and a new construct consisting of the *Ae. aegypti polyubiquitin* (*PUb*) promoter driving transcription of NoVRNA1-SV40 were also attempted (Figure 5.4C). As before, smearing appeared at the bottom of the lanes for cells transfected with NoVRNA1-contaning plasmids, but not for untransfected cells. This time, however, RNA1 and RNA3 bands could be detected for cells transfected with the PUb-NoVRNA1-SV40 plasmid (Figure 5.4C). The *PUb* promoter is a very robust in *Ae. aegypti* cells (143). Thus, it is possible that increased NoVRNA1 transcription resulting from the stronger promoter was able to compensate for antiviral defenses that may have been inhibiting RNA1 and RNA3 detection in the other samples. Given that we used a NoV-specific ^{32}P-labeled probe, we predicted that the smearing was the result of NoV transcript degradation, potentially due to RNAi. It is also important to note, that this smearing was only evident through radiographic film detection of the hybridized 32P-labeled probe, and not during visualization of the RNA on the agarose gel or nitrocellulose membrane using ethidium bromide. To determine if this phenomenon also occurred *in-vivo*, *Ae. aegypti* (Lvp) embryos were injected with 3xP3-NoVRNA1-SV40, IE-NoVRNA1-SV40 or *PUb*-NoVRNA1-SV40 plasmids, and harvested at 1, 2, and 3 days post-injection. As with the cell culture experiments, total RNAs from the injected embryos were northern blotted to detect NoV RNA. Once again, smearing was evident at the bottom of the lanes for all NoV-injected embryos (Figure 5.5B).

To assess, if the consistent smears could be viral small interfering RNAs (viRNAs) resultant from RNAi-based degradation of the replicating, we ran a small RNA Northern blot using total RNAs from: Aag2 cells transfected with either 3xP3-NoVRNA1-SV40 or PUb-NoVRNA1-SV40, S2 cells transfected with 3xP3-NoVRNA1-SV40, and Lvp embryos injected with 3xP3-NoVRNA1-SV40 (Figure 5.5C). Contrary to expectations, the small RNA Northern indicated that the RNA fragments seen in the smear were in fact closer to 100 bp in length, and thus far too large to be viRNAs (Figure 5.5C).

At this point, cell culture experiments addressing the expression and replication of NoVRNA1 and RNA3 in the mosquito cell lines were considered inconclusive. Nonetheless, NoV is known to replicate in *Ae. aegypti* cells (141), and it is possible that our cell culture-based experiments were simply insufficient to accurately gauge how the NoV-expression system would function in the live mosquito. Thus, we decided to proceed with attempting to create an exo-siRNA sensor mosquito, by moving on to *in-vivo* experiments.

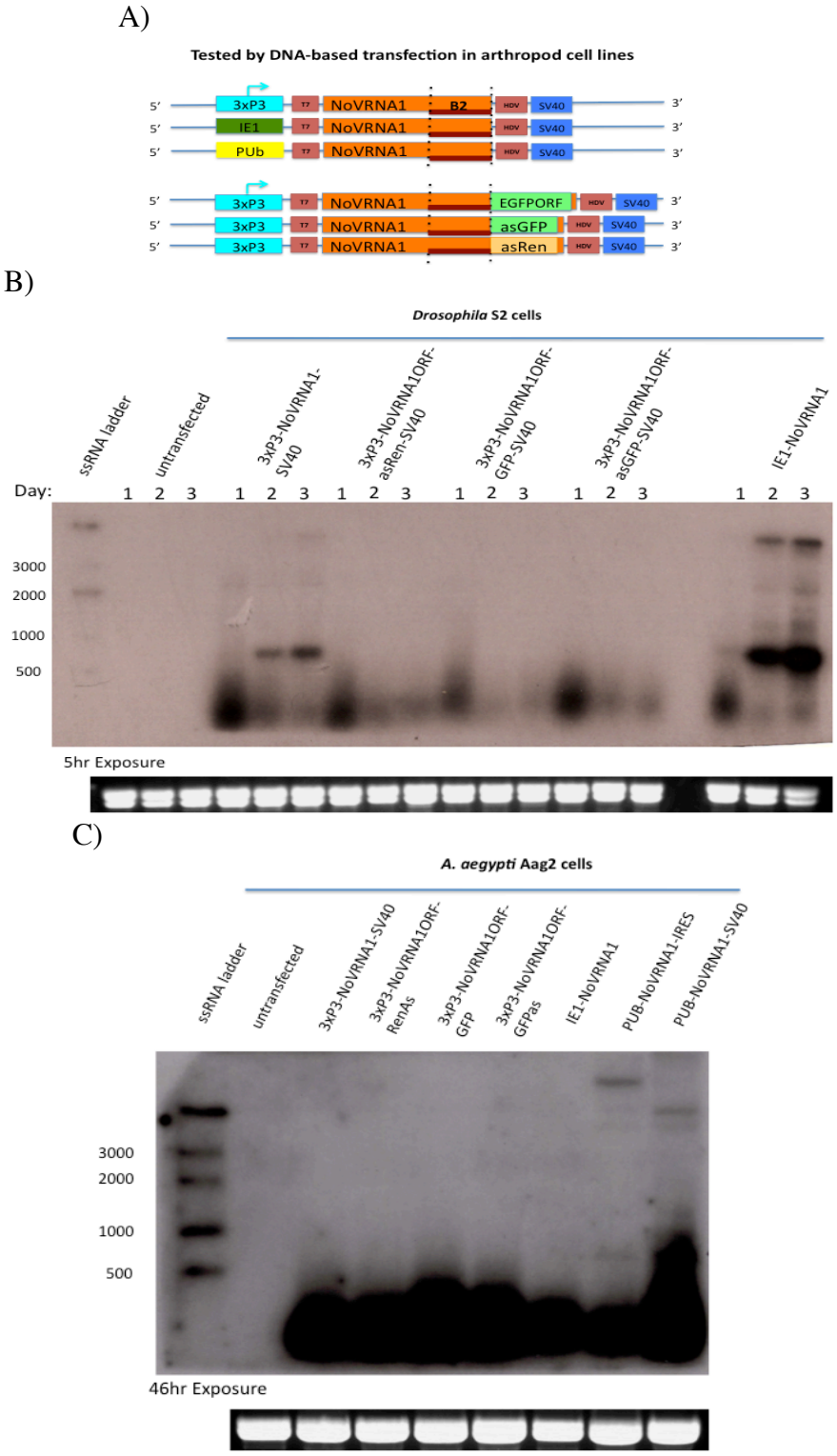

Figure 5.4. Transfection of NoVRNA1-expression plasmids in arthropod cells
A) Plasmids expressing either wild-type or recombinant NoVRNA1 were transfected into B) *Drosophila* S2 and C) *Ae. aegypti* Aag2 cells.

A)

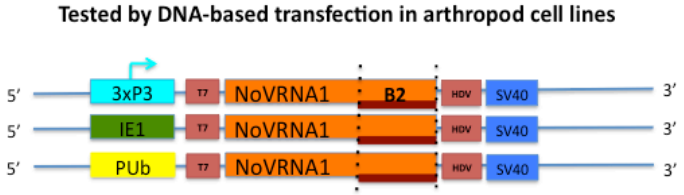

B)

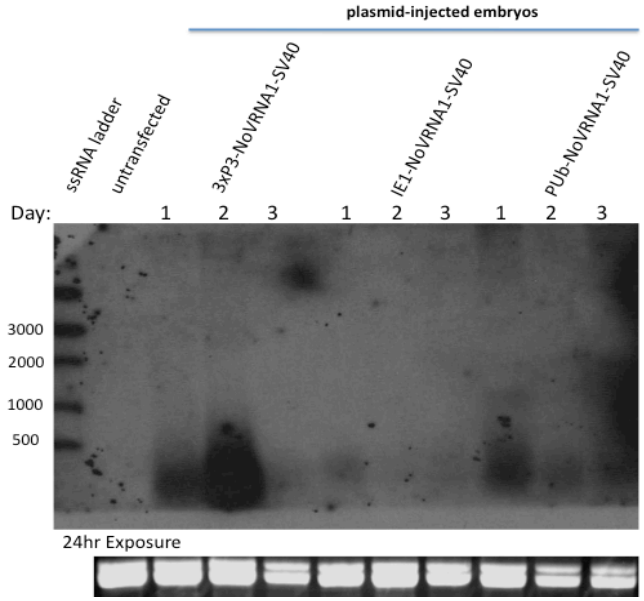

C)

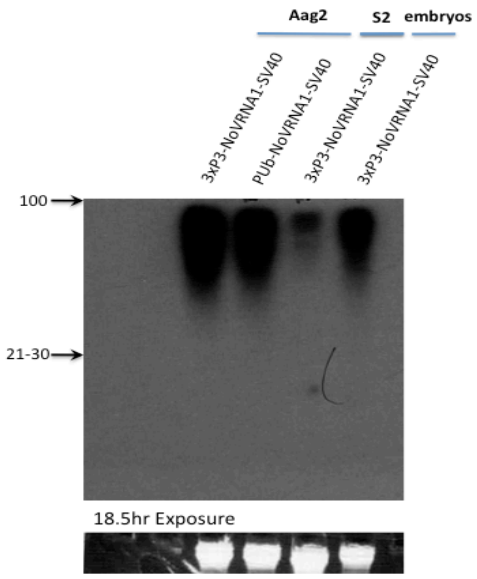

Figure 5.5. Injection of NoVRNA1-expression plasmid in *Ae. aegypti* embryos and small RNA northern blot

A) Plasmids expressing wild-type NoVRNA1 were B) injected in *Ae. aegypti* embryos. C) A small RNA northern assay was run to determine the size of the degradation products. The blot was trimmed at 100 nt. Small RNAs were expected near the center of the blot.

NoV-Sensor mosquito

The exo-siRNA pathway functions in inhibiting viral replication by dicing dsRNA replication intermediates into viral siRNAs, which are then used by the AGO2 RISC to target viral mRNA for degradation. Thus, we designed the NoV-Sensor, such that the EGFP dsRNA would be transcribed by the NoV viral replicase. To accomplish this, we replaced the GFPir sequence from the original sensor plasmid with the NoVRNA1ORF-GFPas construct. Thus, dsRNA homologous to *gfp* mRNA would be generated during transcription and replication of the NoVRNA1 and RNA3 sequences, thereby initiating exo-siRNA-based silencing of GFP expression (Figure 5.6A). Of the 907 embryos injected with the NoV-Sensor plasmid, a total of 127 (14%) G_0 individuals survived to adulthood, and were mated with kh^w mosquitoes. Of the approximately 20,600 G_1 larvae screened, 25 positive individuals were identified in a single pool, #P2 (Table 5.3). These individuals were reared to adulthood and crossed with kh^w mosquitoes.

While endo-siRNA sensor mosquitoes successfully silenced the EGFP transgene, producing a very dim, mosaic GFP phenotype in the adult mosquito eye (102), this was not observed for the NoV exo-siRNA Sensor strain. Rather, the NoV-Sensor displayed robust eye-specific GFP phenotype, as would be expected from uninhibited GFP expression driven by the 3xP3 promoter (Figure 5.6B). To determine if NoV replication was occurring in the NoV-Sensor, we performed a northern analysis using total RNA from adult NoV-Sensor females, and were unable to detect RNA1 or RNA3 transcripts (not shown).

Table 5.3. Results from NoV-Sensor embryo injections and progeny screening

***Mos1* Donor Plasmid**	**# embryos injected**	**# G0 survivors**	**# Pools**	**#G1 progeny screened**	**Pools with DsRed+/GFP+ progeny**	**G2 +/Total (% +)**
pMos-3xP3-DsRed-3xP3-GFP-3xP3-NoVRNA1ORF-GFPas	907	127 (14.0%)	4	~20657	#P2 (25)	204/506 (40.3%)

A)

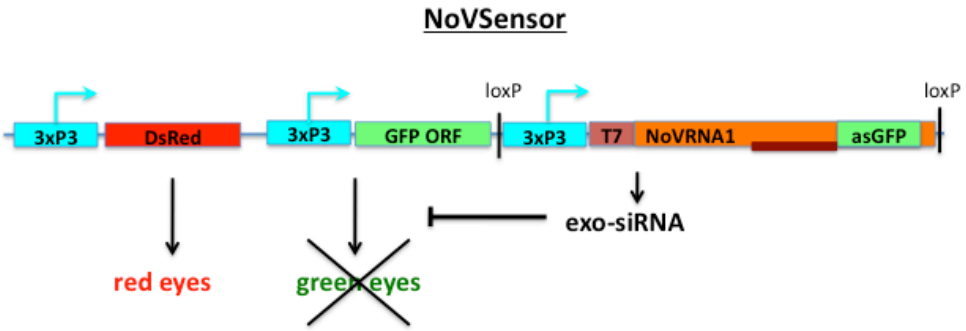

B)

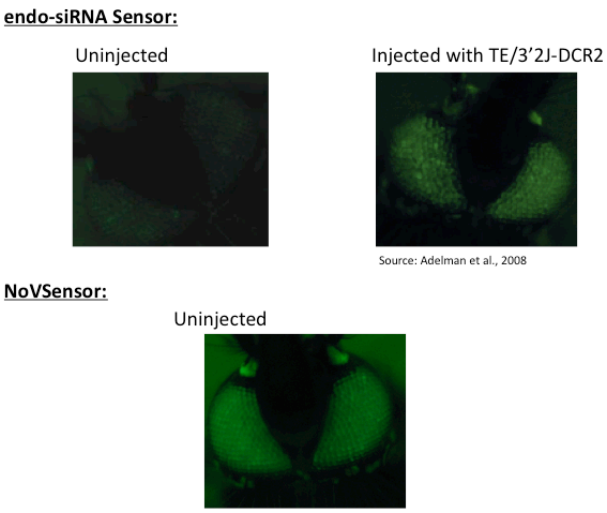

Figure 5.6. Generation of the NoV-Sensor transgenic strain

A) The design of NoV-Sensor construct. Replication by the NoV-viral replicon should result in the *gfp* dsRNA intermediates, initiating exo-siRNA-based degradation of *gfp* mRNA. B) Comparison of GFP expression endo-siRNA sensor and NoV-Sensor mosquitoes.
Images of the endo-siRNA sensor are from Adelman *et al*., 2008.

An *in-vitro* exo-siRNA sensor

Since the previous results in cell culture indicated that the *PUb* promoter was the most promising for expressing NoVRNA1 in Aag2 cells, we focused on this promoter for additional follow-up experiments. We designed a new plasmid consisting of the *PUb* promoter driving transcription of a modified genomic NoVRNA1 sequence, which included the ORF for the NanoLuc Luciferase (Promega) marker gene fused to the subgenomic B2 ORF (B2-NL). This plasmid was named *PUb*-NoVRNA1-NL. Thus, the *PUb* promoter drove initial transcription of the genomic NoVRNA1 mRNA, encoding Protein A. Once translated, Protein A could utilize the NoVRNA1 mRNA as a template for transcribing both the genomic NoVRNA1, as well as the subgenomic RNA3 template. Note that we would only expect the B2-NL expression in the presence of mature Protein A. Subsequently, during robust NoV viral replication we would expect robust NanoLuc expression; however if NoV replication were hindered by RNAi, NanoLuc expression would also be diminished. Thus, if the *PUb*-NoV-NL plasmid were co-transfected with a plasmid that knocks down a gene important to RNAi, we would expect an increase in NanoLuc expression as compared to knocking down a gene with one that has no effect on RNAi. Hence, this system would facilitate identification of genes important to RNAi.

Since the *PUb*-NoVRNA1-NL plasmid encoded the functional B2, RNAi-suppressor protein, we expected this might mask the construct's RNAi "sensor" capabilities. Thus, we created another construct with modified B2 start codons to eliminate the viral RNAi-suppressor protein, creating *PUb*-NoVRNA1ΔB2-NL. Without B2, we expected NanoLuc expression to drastically diminish as compared to the functional B2 construct, but that this expression could be rescued by depleting exo-siRNA proteins. To verify that NanoLuc expression occurred only as a result of protein A-based transcription of the subgenomic transcript, and not as resulting of read-

through from the *PUb* promoter, we also created an identical plasmid with a 4 bp frame-shift, disrupting the protein A ORF. Side-by-side transfection of these three plasmids resulted in robust NanoLuc expression from the intact Protein A /intact B2 construct, diminished NanoLuc expression from the ΔB2 construct, and only background level expression from the frame-shift construct (Figure 5.7). This result confirmed that NanoLuc expression was indeed dependent on the viral RdRp function, and that elimination of the B2 protein negatively affected NanoLuc expression, therefore suggesting that our NoV expression system could function as our exo-siRNA sensor in Aag2 cells.

To determine if this NoV-based sensor system could identify known RNAi genes, we infected Aag2 cells with recombinant Sindbis viruses designed to knockdown DCR2, AGO2 or GFP (as a negative control). At 7 days post-infection (7dpi), we transfected either the *PUb*-NoVRNA1-NL or *PUb*-NoVRNA1ΔB2-NL plasmid into the cells, and measured NanoLuc expression at 8 dpi. Since both DCR2 and AGO2 are important to the exo-siRNA pathway, we expected their knockdown to result in increased NanoLuc expression, especially in the ΔB2 construct, which lacked the viral RNAi-suppressor protein. Contrary to expectations, neither AGO2 nor DCR2 depletion affected NanoLuc expression from the ΔB2 construct (Figure 5.8B). Since both DCR2 and AGO2 are important to siRNA-based silencing (31,102,132), our results indicate that neither the *PUb*-NoVRNA1-NL nor the *PUb*-NoVRNA1ΔB2-NL plasmid functioned as an exo-siRNA sensor.

A)

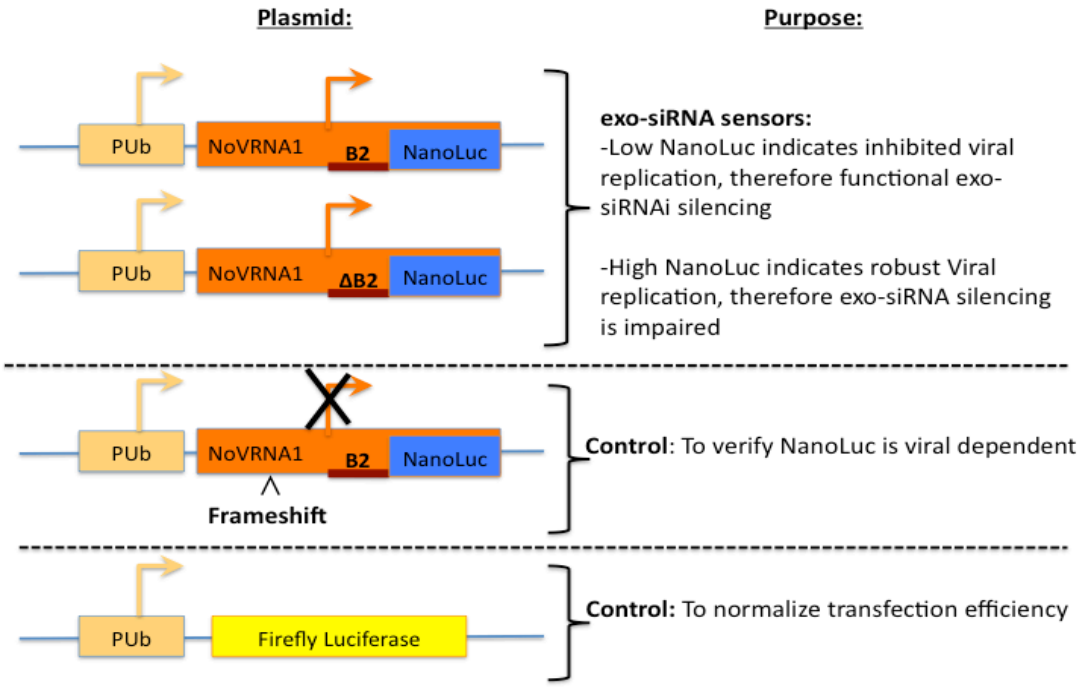

B)

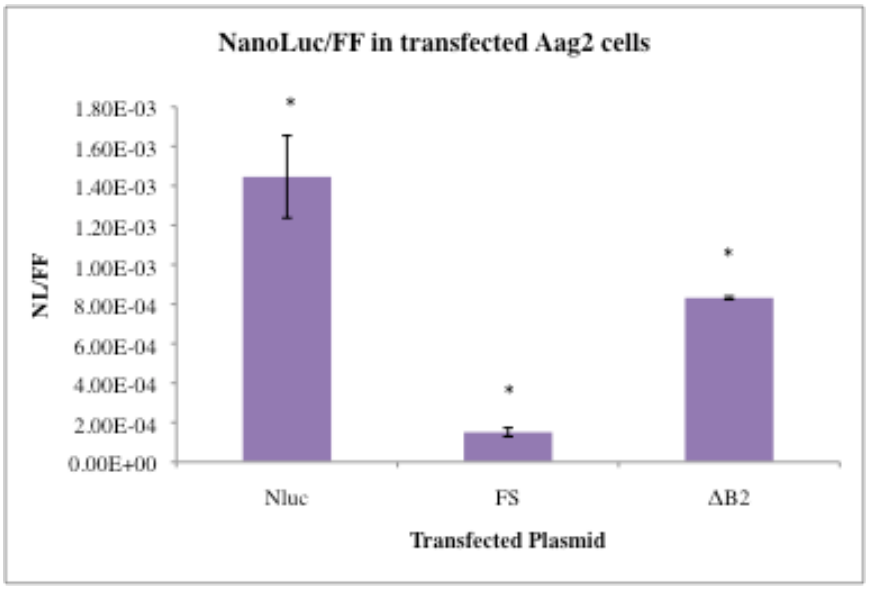

Figure 5.7. NanoLuc expression is Protein A-dependent

A) NoVRNA1 constructs used in testing the NoV exo-siRNA sensor in Aag2 cells. B) Relative NanoLuc expression in Aag2 cells transfected with the PUb-NoVRNA1-NL (Nluc), PUb-NoVRNA1ΔB2-NL(ΔB2), or PUb-FSNoVRNA1-NL (FS) plasmid. Note, all experimental plasmids were co-transfected with PUb-FFluc to normalize for transfection efficiency. Relative luciferase units represent the average ratios of NLuc / FFLuc units between six experimental replicates. Error bars represent the standard deviations (n=6, for each sample). (*P<0.05, based on One-Way ANOVA, followed by a Bonferroni post-test)

A)

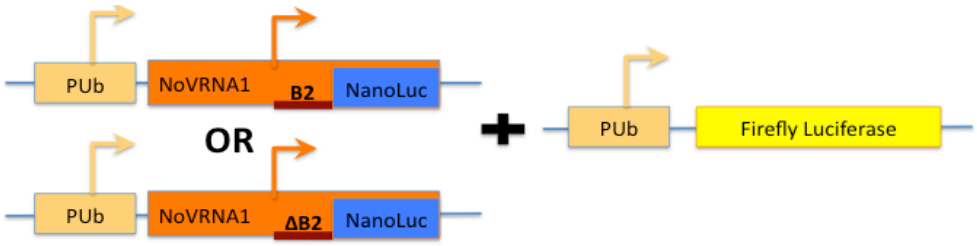

B)

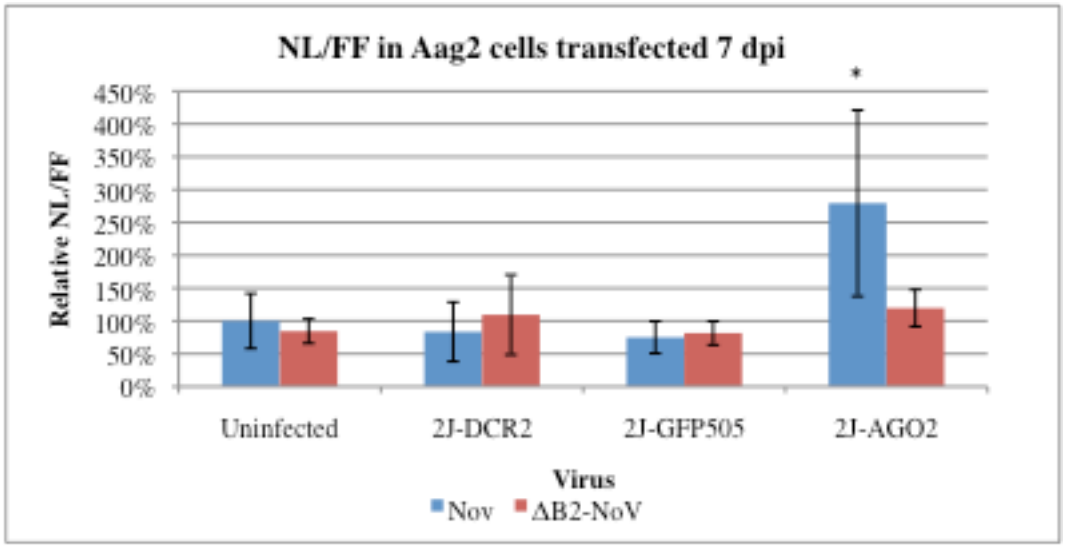

Figure 5.8. Effect of exo-siRNA inhibition on NanoLuc expression

Aag2 cells were infected with recombinant Sindbis virus designed to knockdown DCR2, AGO2, or GFP (ctrl). A) At 7 days post-infection, PUb-NoVRNA1-NL (NoV) or PUb-NoVRNA1ΔB2-NL(B2-NoV) plasmids were co-transfected with PUb-FFLuc to test function of the exo-siRNA sensor constructs. Luciferase expression was measured at 8 dpi (1 day post-transfection). B) Relative NanoLuc expression in experimental samples. Error bars represent the standard deviations (n=6, for each sample). (*P<0.05, based on One-Way ANOVA, followed by a Bonferroni post-test)

Discussion

Upon initiating this project, the simplicity of the NoV genome, low level of pathogenesis, diverse range of hosts, and characterized RNAi-suppressor protein suggested that an NoV replicon would be an ideal tool for creating an exo-siRNA sensor for *Ae. aegypti*. Nonetheless, several challenges impeded progress towards this goal and ultimately rendered the efforts unsuccessful.

In vivo results with the NoV-Sensor transgenic mosquito line revealed that the 3xP3-driven NoV replicon cassette was not functional and therefore not generating sufficient dsRNAs targeting the GFP marker gene in this strain. It is possible that NoV replication would have been improved utilizing the *PUb* promoter, as in cell culture. However, whether or not this would trigger exo-siRNA based silencing of the GFP marker remains unknown.

Successful replication of NoVRNA1 constructs in BHK-21 cells was susceptible to changes to the 3' terminus of the RNA1 sequence. Consist with findings by Li *et al*. (32), replacement of the subgenomic RNA3 transcript (truncating Protein A by 101 amino acids) with the GFP ORF did not hinder replication by the NoV replicon. However, replication could not occur when the same region was replaced by the GFPas sequence. Likewise, truncating Protein A by only 26 amino acids, using RenAs resulted in very weak NoV replication (Figure 5.2B). Thus, it appears that Protein A 3' terminal stability could be maintained by the EGFP ORF sequence, but not GFPas, or RenAs. This lack of stability may be related to configurations in the secondary structure of the mRNA or Protein (Figure 5.2B).

Attempts at expressing heterologous RNA sequences via the NoV replicon in *Drosophila* and Aedine cell lines proved equally challenging. While wild-type NoVRNA1 replication in S2 and C6/36 cells could occur when using the 3xP3 promoter to express NoVRNA1, we were

unable to express heterologous mRNAs when using this promoter to drive initial transcription of the constructs. Furthermore, NoV replication in the *Ae. aegypti* Aag2 cell line could only be achieved using the *PUb* promoter to drive initial NoVRNA1 transcription. NoV replication may therefore require robust expression of the genomic sequence in order to successfully elude innate immunity mechanisms that would hinder further transcription and replication. Attempts at utilizing the NoV expression system as a sensor for the exo-siRNA pathway in Aag2 cells proved unsuccessful, given that expression of a NanoLuc reporter gene fused to the subgenomic viral RNA3 was unaffected by RNAi inhibition *in-vitro*. However, it is important to note that suppression of the exo-siRNA pathway to test the sensor was accomplished by DCR2 knockdown utilizing a dsSINV-expression system. Hence, it is also possible that NoV replication was hindered by the existing SINV infection. Previous studies have demonstrated that mosquito cells with a persistent SINV infection exclude superinfection by other alphaviruses (144). Thus, it is possible that the prior SINV infection may also have limited successful NoV replication, therefore countering any "sensing" capacity. Additional attempts at testing the NoV-based exo-siRNA sensor should employ alternative means of knocking down RNAi factors that do not require the use of dsSINV (such as transfection of DCR2 dsRNA, or plasmids expression inverted repeats targeting DCR2).

The absence of a detectable band for RNA1 in northern blots from transfected arthropod cell lines was intriguing. It is important to note that without translation of the RdRp from this genomic transcript, RNA3 could not be transcribed. Thus, even though the full-length genomic transcript was most likely transcribed and translated, it may have been selectively targeted for degradation and, hence, could not be detected by the northern blot. Furthermore, since small

RNAs could not be detected by northern blot and C6/36 cells do not have a functional Dicer-2 protein, it is possible that another anti-viral pathway was suppressing NoV replication.

Like most eukaryotic organisms, mosquitoes count on a variety of immune responses to stave off potential pathogens. While RNAi is generally accepted as the major antiviral defense pathway modulating arboviral infection and transmission (35), other immune responses may also be up-regulated during viral infection and may be important in limiting the replication of certain viruses (31,145). For example, both the Toll and Janus kinase signal transducer and activator of transcription (JAK-STAT) pathways have been implicated in anti-dengue immune responses in *Ae. aegypti* (145-147) and are known to play roles in anti-viral immunity in *Drosophila* (148,149). Likewise, the immune deficiency (IMD) pathway, which is responsible for the production of anti-microbial peptides, has been shown to suppress SINV replication in *Drosophila* (150). Furthermore, a recent study indicates that, in the absence of a functional siRNA pathway, the piRNA pathway may also function in antiviral defense (132). Thus, it is possible that in the absence of a robust RNAi response, other pathways contributed to regulation of NoV replication from our intended exo-siRNA sensor systems, hence countering their "sensor" purpose. Further experiments involving deactivation of multiple pathways, quantifying viral replication, and analyzing virus-derived small RNAs may help to clarify other immune responses involved.

Conclusion

We were unable to create an exo-siRNA sensor either *in vivo* or *in vitro* using a NoV expression system. A variety of factors likely contributed to both the viability of the NoV replicon as well as its susceptibility to changes in the exo-siRNA pathway. It is possible that

other immune mechanisms also modulated NoV replication when the exo-siRNA pathway was impaired, thus rendering it non-functional as an exo-siRNA sensor. Further studies are needed to analyze the involvement of other immune pathways.

Chapter 6 - Summary

RNAi is important for gene regulation, genomic protection from transposable elements and innate immunity in eukaryotic organisms. Several RNAi mechanisms exist, including the miRNA, endo-siRNA and exo-siRNA pathways. In mosquitoes, the exo-siRNA plays an important role in anti-viral defense, and thus affects the vector competence of the mosquito. Nonetheless, most of what is known about arthropod RNAi is based on studies in *D. melanogaster,* and specific factors involved in the mosquito pathways remain to be defined. Thus, the overall goal of the research presented in this document was to identify genetic factors involved in the RNAi pathways of *Ae. aegypti* mosquitoes.

The first objective was to characterize dsRBPs involved in the various *Ae. aegypti* RNAi pathways. Two of the dsRBPs studied, R2D2 and R3D1, are orthologs of drosophilid proteins known to be important to small RNA biogenesis and RISC loading. The third dsRBP, ExLoqs, was discovered through BLAST queries and phylogenetic analyses of *Ae. aegypti* dsRBPs. Interest in this latter dsRBP arose from its close relationship to R3D1, leading to a suspicion that it may also be involved in RNAi. The *r2d2, r3d1*, and *exloqs* genes were structurally characterized through RACE and cDNA sequencing. Transcript initiation and termination loci were identified for all three genes, and novel exons were discovered in *r3d1* and *exloqs*. Sequencing of *r3d1* cDNA also revealed three unique splice variants, two similar to the drosophilid orthologs, *loqs-a and loqs-b*.

Tissue-specific analysis indicated that *r2d2* and *r3d1* were fairly uniformly expressed in all tissues examined, while *exloqs* was robustly expressed in the gonads, suggesting a role in fertility. *In-situ* hybridization of *Ae. aegypti* ovaries further revealed that *exloqs* is primarily

expressed in ovarian nurse cells. Sub-cellular fractionation assays also enabled intracellular localization of the dsRBPs, as well as AGO and DCR proteins. Localization of certain RNAi factors in the nucleus suggests a potential nuclear role for *Ae. aegypti* RNAi, such as seen in other organisms, but not yet identified in mosquitoes.

Gene-knockdown experiments attempting to assess the importance of R2D2, R3D1, and ExLoqs in RNAi were largely inconclusive. However, co-IP experiments enabled identification of protein-protein interactions between R2D2 and DCR2, as well as R3D1-A and AGO1, AGO2, DCR1, and DCR2. No interaction could be detected between R3D1-B nor ExLoqs and either AGO1, AGO2, DCR1, or DCR2. Interactions were also detected between R2D2 and R3D1A, R2D2 and R3D1A, and R3D1A and R3D1B. These results suggest that R2D2 functions in the siRNA pathway, while R3D1-A is likely involved in multiple small RNA pathways. Future experiments may further examine the nature of the protein complexes, and the specific function of R2D2 and R3D1 in RNAi initiator and effector steps.

While we suspect ExLoqs is involved in *Ae. aegypti* fertility, a phenotype has yet to be associated to this novel dsRBP. Thus, TALEN pairs were injected into *Ae. aegypti* embryos for targeted disruption of the endogenous *exloqs* gene, creating the TALEN-ExLoqs strain. Three unique TALEN-ExLoqs lines were characterized, with 4, 3, and 1 bp deletions near the 5' terminus of the ExLoqs ORF. Thus, two of these mutations introduced frameshifts to the ExLoqs ORF, destroying the translation product, while the third introduced a single amino acid deletion. The close sex-linkage of the *exloqs* mutations also revealed that the *exloqs* gene is located near the sex determining locus. TALEN-ExLoqs mosquitoes will be utilized to study the effects of *exloqs* gene disruption on *Ae. aegypti* fertility, as well as transcription and RNAi.

The final objective of this research was to create an exo-siRNA sensor using a NoV-based expression system. The purpose of the sensor was to facilitate the identification of factors affecting the *Ae. aegypti* exo-siRNA pathway. The NoV replicon was selected to drive conditional expression of a reporter gene that could be used to measure the functionality of the exo-siRNA pathway. We selected the use of the NoV replicon, because the simplicity of NoV's genome, low pathogenesis, diverse host range, and characterized RNAi suppressor protein suggested that it would be an ideal tool for studying the exo-siRNA pathway. However, despite both *in-vivo* and *in-vitro* attempts towards meeting this goal, several challenges blocked progress and rendered the attempts unsuccessful.

Despite initial challenges hindering expression of heterologous mRNAs in arthropod cell lines, we were able to design a plasmid with successful NoV-driven expression of a NanoLuc reporter gene for use in the Aag2 cell line. However attempts at using this NoV expression system as an exo-siRNA sensor were unsuccessful, given that inhibition of the exo-siRNA pathway (via DCR2 knockdown) had little effect on expression of the NanoLuc reporter gene. In the absence of a functional siRNA pathway, other immune responses likely modulate NoV infection in *Ae. aegypti* cells.

Likewise, attempts at creating an *in-vivo* exo-siRNA sensor mosquito were also unsuccessful. The design of the NoV-Sensor mosquito construct was based on that of the existing endo-siRNA sensor *Ae. aegypti* strain. However, results with the NoV-Sensor transgenic mosquito line suggested that the NoV replicon cassette was not functional.

Like most eukaryotic organisms, mosquitoes rely on a variety of immune responses to counter infections by diverse pathogens. Redundancy between various immune pathways likely enables multiple mechanisms to function as secondary forms of defense when primary response

pathways have been compromised. For example, recent studies suggest that, in the absence of a functional siRNA pathway, the piRNA pathway may function in antiviral immunity in *Ae. aegypti* (132).

While we were unable to create the NoV-based exo-siRNA sensor, this research nonetheless furthers our understanding of *Ae. aegypti* RNAi mechanisms. Successful characterization of the structure and expression *Ae. aegypti r2d2, r3d1,* and *exloqs* genes, in conjunction with characterization of protein-protein interactions occurring amongst RNAi factor provides a firm basis for future mechanistic studies of mosquito RNAi. While certain elements of the *Ae. aegypti* RNAi factors appear similar to this described in *Drosophila*, several differences are also present. For example, in *Drosophila*, Loqs-B is essential to the miRNA pathway and Loqs-D is necessary for the endo-siRNA pathway. However, none of the *Ae. aegypti,* R3D1 isoforms resemble the drosophilid Loqs D isoform, while R3D1-A (which resembles drosophilid Loqs-A) interacts with both miRNA and siRNA factors, suggesting it may play a role in both of these mechanisms. Additional experiments may further define these roles as well as assess potential overlaps between the different pathways and anti-viral responses.

References

1. WHO. (2007). WHO, Geneva, Switzerland.
2. Guzman, M.G., Halstead, S.B., Artsob, H., Buchy, P., Farrar, J., Gubler, D.J., Hunsperger, E., Kroeger, A., Margolis, H.S., Martinez, E. *et al*. Dengue: a continuing global threat. *Nat Rev Microbiol*, **8**, S7-S16.
3. Halstead, S.B. (1988) Pathogenesis of dengue: challenges to molecular biology. *Science*, **239**, 476-481.
4. Powers, A.M. and Logue, C.H. (2007) Changing patterns of chikungunya virus: re-emergence of a zoonotic arbovirus. *The Journal of general virology*, **88**, 2363-2377.
5. Townson, H. and Nathan, M.B. (2008) Resurgence of chikungunya. *Trans R Soc Trop Med Hyg*, **102**, 308-309.
6. Staples, J.E., Breiman, R.F. and Powers, A.M. (2009) Chikungunya fever: an epidemiological review of a re-emerging infectious disease. *Clin Infect Dis*, **49**, 942-948.
7. Enserink, M. (2007) Infectious diseases. Chikungunya: no longer a third world disease. *Science*, **318**, 1860-1861.
8. Bean, W.B. (1983) Landmark perspective: Walter Reed and yellow fever. *JAMA : the journal of the American Medical Association*, **250**, 659-662.
9. Gubler, D.J. (2004) The changing epidemiology of yellow fever and dengue, 1900 to 2003: full circle? *Comp Immunol Microbiol Infect Dis*, **27**, 319-330.
10. WHO. (2005), Vol. 80, pp. 249-256.
11. Hardy, J.L., Houk, E.J., Kramer, L.D. and Reeves, W.C. (1983) Intrinsic factors affecting vector competence of mosquitoes for arboviruses. *Annu Rev Entomol*, **28**, 229-262.
12. Blair, C.D., Adelman, Z.N. and Olson, K.E. (2000) Molecular strategies for interrupting arthropod-borne virus transmission by mosquitoes. *Clin Microbiol Rev*, **13**, 651-661.
13. Olson, K.E., Adelman, Z.N., Travanty, E.A., Sanchez-Vargas, I., Beaty, B.J. and Blair, C.D. (2002) Developing arbovirus resistance in mosquitoes. *Insect Biochem Mol Biol*, **32**, 1333-1343.

14. Adelman, Z.N., Jasinskiene, N. and James, A.A. (2002) Development and applications of transgenesis in the yellow fever mosquito, Aedes aegypti. *Mol Biochem Parasitol*, **121**, 1-10.
15. Carlson, J., Olson, K., Higgs, S. and Beaty, B. (1995) Molecular genetic manipulation of mosquito vectors. *Annu Rev Entomol*, **40**, 359-388.
16. Wyss, J.H. (2000) Screwworm eradication in the Americas. *Ann N Y Acad Sci*, **916**, 186-193.
17. Marquardt, W., Black, W., Higgs, S., Freier, J., James, A.A., Hagedorn, H., Kondratieff, B., Hemingway, J. and Moore, C. (2005) *Biology of Disease Vectors*. 2nd ed. Elsevier Academic Press, San Diego, California.
18. Wise de Valdez, M.R., Nimmo, D., Betz, J., Gong, H.F., James, A.A., Alphey, L. and Black, W.C.t. (2011) Genetic elimination of dengue vector mosquitoes. *Proc Natl Acad Sci U S A*, **108**, 4772-4775.
19. Rasgon, J.L. and Scott, T.W. (2003) Wolbachia and cytoplasmic incompatibility in the California Culex pipiens mosquito species complex: parameter estimates and infection dynamics in natural populations. *Genetics*, **165**, 2029-2038.
20. Sinkins, S.P. (2004) Wolbachia and cytoplasmic incompatibility in mosquitoes. *Insect Biochem Mol Biol*, **34**, 723-729.
21. Ritchie, S.A., Montgomery, B.L. and Hoffmann, A.A. (2013) Novel estimates of Aedes aegypti (Diptera: Culicidae) population size and adult survival based on Wolbachia releases. *J Med Entomol*, **50**, 624-631.
22. Turley, A.P., Zalucki, M.P., O'Neill, S.L. and McGraw, E.A. (2013) Transinfected Wolbachia have minimal effects on male reproductive success in Aedes aegypti. *Parasit Vectors*, **6**, 36.
23. Forstemann, K., Tomari, Y., Du, T., Vagin, V.V., Denli, A.M., Bratu, D.P., Klattenhoff, C., Theurkauf, W.E. and Zamore, P.D. (2005) Normal microRNA maturation and germ-line stem cell maintenance requires Loquacious, a double-stranded RNA-binding domain protein. *PLoS Biol*, **3**, e236.
24. Lee, Y.S., Nakahara, K., Pham, J.W., Kim, K., He, Z., Sontheimer, E.J. and Carthew, R.W. (2004) Distinct roles for Drosophila Dicer-1 and Dicer-2 in the siRNA/miRNA silencing pathways. *Cell*, **117**, 69-81.

25. Zhou, R., Hotta, I., Denli, A.M., Hong, P., Perrimon, N. and Hannon, G.J. (2008) Comparative analysis of argonaute-dependent small RNA pathways in Drosophila. *Mol Cell*, **32**, 592-599.

26. Elbashir, S.M., Martinez, J., Patkaniowska, A., Lendeckel, W. and Tuschl, T. (2001) Functional anatomy of siRNAs for mediating efficient RNAi in Drosophila melanogaster embryo lysate. *Embo J*, **20**, 6877-6888.

27. Czech, B., Malone, C.D., Zhou, R., Stark, A., Schlingeheyde, C., Dus, M., Perrimon, N., Kellis, M., Wohlschlegel, J.A., Sachidanandam, R. *et al*. (2008) An endogenous small interfering RNA pathway in Drosophila. *Nature*, **453**, 798-802.

28. Aliyari, R., Wu, Q., Li, H.W., Wang, X.H., Li, F., Green, L.D., Han, C.S., Li, W.X. and Ding, S.W. (2008) Mechanism of induction and suppression of antiviral immunity directed by virus-derived small RNAs in Drosophila. *Cell Host Microbe*, **4**, 387-397.

29. Lu, R., Maduro, M., Li, F., Li, H.W., Broitman-Maduro, G., Li, W.X. and Ding, S.W. (2005) Animal virus replication and RNAi-mediated antiviral silencing in Caenorhabditis elegans. *Nature*, **436**, 1040-1043.

30. Myles, K.M., Michael R. Wiley, Elaine M. Morazzani, and Zach N. Adelman. (2008) Alphavirus-derived small RNAs modulate pathogenesis in disease vector mosquitoes. *PNAS*, **105**, 19938-19943.

31. Sánchez-Vargas, I., Scott, J.C., Poole-Smith, B.K., Franz, A.W., Barbosa-Solomieu, V., Wilusz, J., Olson, K.E. and Blair, C.D. (2009) Dengue virus type 2 infections of Aedes aegypti are modulated by the mosquito's RNA interference pathway. *PLoS Pathog*, **5**, e1000299.

32. Li, W.X., Li, H., Lu, R., Li, F., Dus, M., Atkinson, P., Brydon, E.W., Johnson, K.L., Garcia-Sastre, A., Ball, L.A. *et al*. (2004) Interferon antagonist proteins of influenza and vaccinia viruses are suppressors of RNA silencing. *Proc Natl Acad Sci U S A*, **101**, 1350-1355.

33. Lingel, A., Simon, B., Izaurralde, E. and Sattler, M. (2005) The structure of the flock house virus B2 protein, a viral suppressor of RNA interference, shows a novel mode of double-stranded RNA recognition. *EMBO Rep*, **6**, 1149-1155.

34. Lambrechts, L., Quillery, E., Noel, V., Richardson, J.H., Jarman, R.G., Scott, T.W. and Chevillon, C. (2013) Specificity of resistance to dengue virus isolates is associated with

genotypes of the mosquito antiviral gene Dicer-2. *Proceedings. Biological sciences / The Royal Society*, **280**, 20122437.

35. Sanchez-Vargas, I., Travanty, E.A., Keene, K.M., Franz, A.W., Beaty, B.J., Blair, C.D. and Olson, K.E. (2004) RNA interference, arthropod-borne viruses, and mosquitoes. *Virus Res*, **102**, 65-74.
36. Scott, J.C., Brackney, D.E., Campbell, C.L., Bondu-Hawkins, V., Hjelle, B., Ebel, G.D., Olson, K.E. and Blair, C.D. (2010) Comparison of dengue virus type 2-specific small RNAs from RNA interference-competent and -incompetent mosquito cells. *PLoS neglected tropical diseases*, **4**, e848.
37. Caplen, N.J., Zheng, Z., Falgout, B. and Morgan, R.A. (2002) Inhibition of viral gene expression and replication in mosquito cells by dsRNA-triggered RNA interference. *Mol Ther*, **6**, 243-251.
38. Franz, A.W., Sanchez-Vargas, I., Adelman, Z.N., Blair, C.D., Beaty, B.J., James, A.A. and Olson, K.E. (2006) Engineering RNA interference-based resistance to dengue virus type 2 in genetically modified Aedes aegypti. *Proc Natl Acad Sci U S A*, **103**, 4198-4203.
39. Franz, A.W.E., Sanchez-Vargas, I., Piper, J., Smith, M.R., Khoo, C. C. H., James, Olson, K. E. Stability and loss of a virus resistance phenotype overtime in transgenic mosquitoes harbouring an antiviral effector geneimb_908 661..672. *Insect Molecular Biology*, **18**, 661-672.
40. Travanty, E.A., Adelman, Z.N., Franz, A.W., Keene, K.M., Beaty, B.J., Blair, C.D., James, A.A. and Olson, K.E. (2004) Using RNA interference to develop dengue virus resistance in genetically modified Aedes aegypti. *Insect Biochem Mol Biol*, **34**, 607-613.
41. Liu, Q., Rand, T.A., Kalidas, S., Du, F., Kim, H.E., Smith, D.P. and Wang, X. (2003) R2D2, a bridge between the initiation and effector steps of the Drosophila RNAi pathway. *Science*, **301**, 1921-1925.
42. Zhou, R., Czech, B., Brennecke, J., Sachidanandam, R., Wohlschlegel, J.A., Perrimon, N. and Hannon, G.J. (2009) Processing of Drosophila endo-siRNAs depends on a specific Loquacious isoform. *RNA*, **15**, 1886-1895.
43. Hartig, J.V. and Forstemann, K. (2011) Loqs-PD and R2D2 define independent pathways for RISC generation in Drosophila. *Nucleic Acids Res*, **39**, 3836-3851.

44. Marques, J.T., Kim, K., Wu, P.H., Alleyne, T.M., Jafari, N, Carthew, R.W. (2010) Loqs and R2D2 act sequentially in the siRNA pathway in Drosophila. *Nat Struct Mol Biol*, **17**, 24-30.

45. Miyoshi, K., Miyoshi, T., Hartig, J.V., Siomi, H. and Siomi, M.C. (2010) Molecular mechanisms that funnel RNA precursors into endogenous small-interfering RNA and microRNA biogenesis pathways in Drosophila. *RNA*, **16**, 506-515.

46. St Johnston, D., Brown, N.H., Gall, J.G. and Jantsch, M. (1992) A conserved double-stranded RNA-binding domain. *Proc Natl Acad Sci U S A*, **89**, 10979-10983.

47. Saunders, L.R. and Barber, G.N. (2003) The dsRNA binding protein family: critical roles, diverse cellular functions. *FASEB journal : official publication of the Federation of American Societies for Experimental Biology*, **17**, 961-983.

48. Ramos, A., Grunert, S., Adams, J., Micklem, D.R., Proctor, M.R., Freund, S., Bycroft, M., St Johnston, D. and Varani, G. (2000) RNA recognition by a Staufen double-stranded RNA-binding domain. *EMBO J*, **19**, 997-1009.

49. Sen, G.L. and Blau, H.M. (2006) A brief history of RNAi: the silence of the genes. *FASEB journal : official publication of the Federation of American Societies for Experimental Biology*, **20**, 1293-1299.

50. Lampson, G.P., Tytell, A.A., Field, A.K., Nemes, M.M. and Hilleman, M.R. (1967) Inducers of interferon and host resistance. I. Double-stranded RNA from extracts of Penicillium funiculosum. *Proc Natl Acad Sci U S A*, **58**, 782-789.

51. Farrell, P.J., Sen, G.C., Dubois, M.F., Ratner, L., Slattery, E. and Lengyel, P. (1978) Interferon action: two distinct pathways for inhibition of protein synthesis by double-stranded RNA. *Proc Natl Acad Sci U S A*, **75**, 5893-5897.

52. Leuschner, P.J., Obernosterer, G. and Martinez, J. (2005) MicroRNAs: Loquacious speaks out. *Curr Biol*, **15**, R603-605.

53. Liu, X., Jiang, F., Kalidas, S., Smith, D. and Liu, Q. (2006) Dicer-2 and R2D2 coordinately bind siRNA to promote assembly of the siRISC complexes. *RNA*, **12**, 1514-1520.

54. Tomari, Y., Du, T. and Zamore, P.D. (2007) Sorting of Drosophila small silencing RNAs. *Cell*, **130**, 299-308.

55. Okamura, K., Robine, N., Liu, Y., Liu, Q. and Lai, E.C. (2011) R2D2 organizes small regulatory RNA pathways in Drosophila. *Mol Cell Biol*, **31**, 884-896.
56. Marques, J.T., Kim, K., Wu, P.H., Alleyne, T.M., Jafari, N. and Carthew, R.W. (2010) Loqs and R2D2 act sequentially in the siRNA pathway in Drosophila. *Nat Struct Mol Biol*, **17**, 24-30.
57. Miyoshi, K., Miyoshi, T., Hartig, J.V., Siomi, H. and Siomi, M.C. Molecular mechanisms that funnel RNA precursors into endogenous small-interfering RNA and microRNA biogenesis pathways in Drosophila. *RNA*, **16**, 506-515.
58. Wang, X.H., Aliyari, R., Li, W.X., Li, H.W., Kim, K., Carthew, R., Atkinson, P. and Ding, S.W. (2006) RNA interference directs innate immunity against viruses in adult Drosophila. *Science*, **312**, 452-454.
59. Marques, J.T., Wang, J.P., Wang, X., de Oliveira, K.P., Gao, C., Aguiar, E.R., Jafari, N. and Carthew, R.W. (2013) Functional specialization of the small interfering RNA pathway in response to virus infection. *PLoS Pathog*, **9**, e1003579.
60. Hartig, J.V., Esslinger, S., Bottcher, R., Saito, K. and Forstemann, K. (2009) Endo-siRNAs depend on a new isoform of loquacious and target artificially introduced, high-copy sequences. *EMBO J*, **28**, 2932-2944.
61. Castel, S.E. and Martienssen, R.A. (2013) RNA interference in the nucleus: roles for small RNAs in transcription, epigenetics and beyond. *Nature reviews. Genetics*, **14**, 100-112.
62. Pikaard, C.S., Haag, J.R., Ream, T. and Wierzbicki, A.T. (2008) Roles of RNA polymerase IV in gene silencing. *Trends in plant science*, **13**, 390-397.
63. Djupedal, I., Portoso, M., Spahr, H., Bonilla, C., Gustafsson, C.M., Allshire, R.C. and Ekwall, K. (2005) RNA Pol II subunit Rpb7 promotes centromeric transcription and RNAi-directed chromatin silencing. *Genes & development*, **19**, 2301-2306.
64. Buker, S.M., Iida, T., Buhler, M., Villen, J., Gygi, S.P., Nakayama, J. and Moazed, D. (2007) Two different Argonaute complexes are required for siRNA generation and heterochromatin assembly in fission yeast. *Nat Struct Mol Biol*, **14**, 200-207.
65. Wierzbicki, A.T., Haag, J.R. and Pikaard, C.S. (2008) Noncoding transcription by RNA polymerase Pol IVb/Pol V mediates transcriptional silencing of overlapping and adjacent genes. *Cell*, **135**, 635-648.

66. Cao, X., Aufsatz, W., Zilberman, D., Mette, M.F., Huang, M.S., Matzke, M. and Jacobsen, S.E. (2003) Role of the DRM and CMT3 methyltransferases in RNA-directed DNA methylation. *Curr Biol*, **13**, 2212-2217.

67. Enke, R.A., Dong, Z. and Bender, J. (2011) Small RNAs prevent transcription-coupled loss of histone H3 lysine 9 methylation in Arabidopsis thaliana. *PLoS genetics*, **7**, e1002350.

68. Yigit, E., Batista, P.J., Bei, Y., Pang, K.M., Chen, C.C., Tolia, N.H., Joshua-Tor, L., Mitani, S., Simard, M.J. and Mello, C.C. (2006) Analysis of the C. elegans Argonaute family reveals that distinct Argonautes act sequentially during RNAi. *Cell*, **127**, 747-757.

69. Guang, S., Bochner, A.F., Burkhart, K.B., Burton, N., Pavelec, D.M. and Kennedy, S. (2010) Small regulatory RNAs inhibit RNA polymerase II during the elongation phase of transcription. *Nature*, **465**, 1097-1101.

70. Gu, S.G., Pak, J., Guang, S., Maniar, J.M., Kennedy, S. and Fire, A. (2012) Amplification of siRNA in Caenorhabditis elegans generates a transgenerational sequence-targeted histone H3 lysine 9 methylation footprint. *Nature genetics*, **44**, 157-164.

71. Aravin, A.A., Hannon, G.J. and Brennecke, J. (2007) The Piwi-piRNA pathway provides an adaptive defense in the transposon arms race. *Science*, **318**, 761-764.

72. Brennecke, J., Aravin, A.A., Stark, A., Dus, M., Kellis, M., Sachidanandam, R. and Hannon, G.J. (2007) Discrete small RNA-generating loci as master regulators of transposon activity in Drosophila. *Cell*, **128**, 1089-1103.

73. Rozhkov, N.V., Hammell, M. and Hannon, G.J. (2013) Multiple roles for Piwi in silencing Drosophila transposons. *Genes & development*, **27**, 400-412.

74. Brower-Toland, B., Findley, S.D., Jiang, L., Liu, L., Yin, H., Dus, M., Zhou, P., Elgin, S.C. and Lin, H. (2007) Drosophila PIWI associates with chromatin and interacts directly with HP1a. *Genes & development*, **21**, 2300-2311.

75. Cernilogar, F.M., Onorati, M.C., Kothe, G.O., Burroughs, A.M., Parsi, K.M., Breiling, A., Lo Sardo, F., Saxena, A., Miyoshi, K., Siomi, H. *et al*. (2011) Chromatin-associated RNA interference components contribute to transcriptional regulation in Drosophila. *Nature*, **480**, 391-395.

76. Taliaferro, J.M., Aspden, J.L., Bradley, T., Marwha, D., Blanchette, M. and Rio, D.C. (2013) Two new and distinct roles for Drosophila Argonaute-2 in the nucleus: alternative pre-mRNA splicing and transcriptional repression. *Genes & development*, **27**, 378-389.

77. Taylor, R.M., Hurlbut, H.S., Work, T.H., Kingsbury, J.R. and Frothingham, T.E. (1955) Sindbis virus: A newly recognized arthropod-transmitted virus. *Am. J. Trop. Med. Hyg.*, **4**, 844-846.

78. Strauss, J.H. and Strauss, E.G. (1994) The alphaviruses: gene expression, replication, and evolution [published erratum appears in Microbiol Rev 1994 Dec;58(4):806]. *Microbiol Rev*, **58**, 491-562.

79. Kurkela, S., Ratti, O., Huhtamo, E., Uzcategui, N.Y., Nuorti, J.P., Laakkonen, J., Manni, T., Helle, P., Vaheri, A. and Vapalahti, O. (2008) Sindbis virus infection in resident birds, migratory birds, and humans, Finland. *Emerging infectious diseases*, **14**, 41-47.

80. Sammels, L.M., Lindsay, M.D., Poidinger, M., Coelen, R.J. and Mackenzie, J.S. (1999) Geographic distribution and evolution of Sindbis virus in Australia. *J. Gen. Virol.*, **80**, 739-748.

81. Kurkela, S., Manni, T., Myllynen, J., Vaheri, A. and Vapalahti, O. (2005) Clinical and laboratory manifestations of Sindbis virus infection: prospective study, Finland, 2002-2003. *The Journal of infectious diseases*, **191**, 1820-1829.

82. Sane, J., Guedes, S., Ollgren, J., Kurkela, S., Klemets, P., Vapalahti, O., Kela, E., Lyytikainen, O. and Nuorti, J.P. (2011) Epidemic sindbis virus infection in Finland: a population-based case-control study of risk factors. *The Journal of infectious diseases*, **204**, 459-466.

83. Storm, N., Weyer, J., Markotter, W., Kemp, A., Leman, P.A., Dermaux-Msimang, V., Nel, L.H. and Paweska, J.T. (2013) Human cases of Sindbis fever in South Africa, 2006-2010. *Epidemiology and infection*, 1-5.

84. Doherty, R.L., Bodey, A.S. and Carew, J.S. (1969) Sindbis virus infection in Australia. *The Medical journal of Australia*, **2**, 1016-1017.

85. Myles, K.M., Wiley, M.R., Morazzani, E.M. and Adelman, Z.N. (2008) Alphavirus-derived small RNAs modulate pathogenesis in disease vector mosquitoes. *Proc Natl Acad Sci U S A*, **105**, 19938-19943.

86. Rice, C.M., Levis, R., Strauss, J.H. and Huang, H.V. (1987) Production of infectious RNA transcripts from Sindbis virus cDNA clones: mapping of lethal mutations, rescue of a temperature-sensitive marker, and in vitro mutagenesis to generate defined mutants. *J Virol*, **61**, 3809-3819.

87. Xiong, C., Levis, R., Shen, P., Schlesinger, S., Rice, C.M. and Huang, H.V. (1989) Sindbis virus: an efficient, broad host range vector for gene expression in animal cells. *Science*, **243**, 1188-1191.

88. Olson, K.E., Carlson, J.O. and Beaty, B.J. (1992) Expression of the chloramphenicol acetyltransferase gene in *Aedes albopictus* (C6/36) cells using a non-infectious Sindbis virus expression vector. *Insect Mol Biol*, **1**, 49-52.

89. Olson, K.E., Higgs, S., Hahn, C.S., Rice, C.M., Carlson, J.O. and Beaty, B.J. (1994) The expression of chloramphenicol acetyltransferase in *Aedes albopictus* (C6/36) cells and *Aedes triseriatus* mosquitoes using a double subgenomic recombinant Sindbis virus. *Insect Biochem Mol Biol*, **24**, 39-48.

90. Gardner, J.P., Frolov, I., Perri, S., Ji, Y., MacKichan, M.L., zur Megede, J., Chen, M., Belli, B.A., Driver, D.A., Sherrill, S. *et al*. (2000) Infection of human dendritic cells by a Sindbis virus replicon vector is determined by a single amino acid substitution in the E2 glycoprotein. *J. Virol*., **74**, 11849-11857.

91. Hay, J.G. (2004) Sindbis virus--an effective targeted cancer therapeutic. *Trends in biotechnology*, **22**, 501-503.

92. Tseng, J.-C., Levin, B., Hirano, T., Yee, H., Pampeno, C. and Meruelo, D. (2002) In Vivo Antitumor Activity of Sindbis Viral Vectors. *J. Natl. Cancer Inst*., **94**, 1790-1802.

93. Sawai, K., Ikeda, H., Ishizu, A. and Meruelo, D. (1999) Reducing cytotoxicity induced by Sindbis viral vectors. *Molecular genetics and metabolism*, **67**, 36-42.

94. Seabaugh, R.C., Olson, K.E., Higgs, S., Carlson, J.O. and Beaty, B.J. (1998) Development of a chimeric sindbis virus with enhanced *per Os* infection of *Aedes aegypti*. *Virology*, **243**, 99-112.

95. Johnson, K.L., Price, B.D. and Ball, L.A. (2003) Recovery of infectivity from cDNA clones of nodamura virus and identification of small nonstructural proteins. *Virology*, **305**, 436-451.

96. Johnson, K.L., Price, B.D., Eckerle, L.D. and Ball, L.A. (2004) Nodamura virus nonstructural protein B2 can enhance viral RNA accumulation in both mammalian and insect cells. *J Virol*, **78**, 6698-6704.

97. Sullivan, C.S. and Ganem, D. (2005) A virus-encoded inhibitor that blocks RNA interference in mammalian cells. *J Virol*, **79**, 7371-7379.

98. Scherer, W.F. and Hurlbut, H.S. (1967) Nodamura virus from Japan: a new and unusual arbovirus resistant to diethyl ether and chloroform. *Am J Epidemiol*, **86**, 271-285.

99. Gallagher, T.M., Friesen, P.D. and Rueckert, R.R. (1983) Autonomous replication and expression of RNA 1 from black beetle virus. *J Virol*, **46**, 481-489.

100. Olson, K.E., Myles, K.M., Seabaugh, R.C., Higgs, S., Carlson, J.O. and Beaty, B.J. (2000) Development of a Sindbis virus expression system that efficiently expresses green fluorescent protein in midguts of *Aedes aegypti* following per os infection. *Insect Mol Biol*, **9**, 57-65.

101. WHO. (2009) Dengue and dengue haemorrhagic fiver - Fact Sheet.

102. Adelman, Z.N., Anderson, M.A., Morazzani, E.M. and Myles, K.M. (2008) A transgenic sensor strain for monitoring the RNAi pathway in the yellow fever mosquito, Aedes aegypti. *Insect Biochem Mol Biol*, **38**, 705-713.

103. Bian, G., Shin, S.W., Cheon, H.M., Kokoza, V. and Raikhel, A.S. (2005) Transgenic alteration of Toll immune pathway in the female mosquito Aedes aegypti. *Proc Natl Acad Sci U S A*, **102**, 13568-13573.

104. Erdelyan, C.N., Mahood, T.H., Bader, T.S. and Whyard, S. (2012) Functional validation of the carbon dioxide receptor genes in Aedes aegypti mosquitoes using RNA interference. *Insect Mol Biol*, **21**, 119-127.

105. Finn, R.D., Mistry, J., Tate, J., Coggill, P., Heger, A., Pollington, J.E., Gavin, O.L., Gunasekaran, P., Ceric, G., Forslund, K. *et al*. The Pfam protein families database. *Nucleic Acids Res*, **38**, D211-222.

106. Tamura, K., Peterson, D., Peterson, N., Stecher, G., Nei, M. and Kumar, S. (2011) MEGA5: Molecular Evolutionary Genetics Analysis Using Maximum Likelihood, Evolutionary Distance, and Maximum Parsimony Methods. *Mol Biol Evol*, **28**, 2731-2739.

107. Saitou, N. and Nei, M. (1987) The Neighbor-Joining Method - a New Method for Reconstructing Phylogenetic Trees. *Mol Biol Evol*, **4**, 406-425.
108. Haley, B., Hendrix, D., Trang, V. and Levine, M. (2008) A simplified miRNA-based gene silencing method for Drosophila melanogaster. *Dev Biol*, **321**, 482-490.
109. Juhn, J. and James, A.A. (2012) Hybridization in situ of salivary glands, ovaries, and embryos of vector mosquitoes. *Journal of visualized experiments : JoVE*.
110. Myles, K.M., Kelly, C.L., Ledermann, J.P. and Powers, A.M. (2006) Effects of an opal termination codon preceding the nsP4 gene sequence in the O'Nyong-Nyong virus genome on Anopheles gambiae infectivity. *J Virol*, **80**, 4992-4997.
111. Lawson, D., Arensburger, P., Atkinson, P., Besansky, N.J., Bruggner, R.V., Butler, R., Campbell, K.S., Christophides, G.K., Christley, S., Dialynas, E. *et al*. (2007) VectorBase: a home for invertebrate vectors of human pathogens. *Nucleic Acids Res*, **35**, D503-505.
112. Zuker, M. and Stiegler, P. (1981) Optimal computer folding of large RNA sequences using thermodynamics and auxiliary information. *Nucleic Acids Res*, **9**, 133-148.
113. Coates, C.J., Jasinskiene, N., Miyashiro, L. and James, A.A. (1998) Mariner transposition and transformation of the yellow fever mosquito, *Aedes aegypti*. *Proc Natl Acad Sci U S A*, **95**, 3748-3751.
114. St Johnston, D., Beuchle, D. and Nusslein-Volhard, C. (1991) Staufen, a gene required to localize maternal RNAs in the Drosophila egg. *Cell*, **66**, 51-63.
115. Clements, A.N. and Boocock, M.R. (1984) Ovarian Development in Mosquitos - Stages of Growth and Arrest, and Follicular Resorption. *Physiol Entomol*, **9**, 1-8.
116. van Rij, R.P., Saleh, M.C., Berry, B., Foo, C., Houk, A., Antoniewski, C. and Andino, R. (2006) The RNA silencing endonuclease Argonaute 2 mediates specific antiviral immunity in Drosophila melanogaster. *Genes & development*, **20**, 2985-2995.
117. Ghildiyal, M., Seitz, H., Horwich, M.D., Li, C., Du, T., Lee, S., Xu, J., Kittler, E.L., Zapp, M.L., Weng, Z. *et al*. (2008) Endogenous siRNAs derived from transposons and mRNAs in Drosophila somatic cells. *Science*, **320**, 1077-1081.
118. Okamura, K., Chung, W.J., Ruby, J.G., Guo, H., Bartel, D.P. and Lai, E.C. (2008) The Drosophila hairpin RNA pathway generates endogenous short interfering RNAs. *Nature*, **453**, 803-806.

119. Kugler, J.M., Chen, Y.W., Weng, R. and Cohen, S.M. (2013) miR-989 is required for border cell migration in the Drosophila ovary. *PloS one*, **8**, e67075.
120. Huang, Y.C., Smith, L., Poulton, J. and Deng, W.M. (2013) The microRNA miR-7 regulates Tramtrack69 in a developmental switch in Drosophila follicle cells. *Development*, **140**, 897-905.
121. Pancratov, R., Peng, F., Smibert, P., Yang, S., Jr., Olson, E.R., Guha-Gilford, C., Kapoor, A.J., Liang, F.X., Lai, E.C., Flaherty, M.S. *et al*. (2013) The miR-310/13 cluster antagonizes beta-catenin function in the regulation of germ and somatic cell differentiation in the Drosophila testis. *Development*, **140**, 2904-2916.
122. Kalidas, S., Sanders, C., Ye, X., Strauss, T., Kuhn, M., Liu, Q. and Smith, D.P. (2008) Drosophila R2D2 mediates follicle formation in somatic tissues through interactions with Dicer-1. *Mech Dev*, **125**, 475-485.
123. Ferrandon, D., Elphick, L., Nusslein-Volhard, C. and St Johnston, D. (1994) Staufen protein associates with the 3'UTR of bicoid mRNA to form particles that move in a microtubule-dependent manner. *Cell*, **79**, 1221-1232.
124. St Johnston, D., Driever, W., Berleth, T., Richstein, S. and Nusslein-Volhard, C. (1989) Multiple steps in the localization of bicoid RNA to the anterior pole of the Drosophila oocyte. *Development*, **107 Suppl**, 13-19.
125. Gerbasi, V.R., Preall, J.B., Golden, D.E., Powell, D.W., Cummins, T.D. and Sontheimer, E.J. (2011) Blanks, a nuclear siRNA/dsRNA-binding complex component, is required for Drosophila spermiogenesis. *Proc Natl Acad Sci U S A*, **108**, 3204-3209.
126. Boch, J., Scholze, H., Schornack, S., Landgraf, A., Hahn, S., Kay, S., Lahaye, T., Nickstadt, A. and Bonas, U. (2009) Breaking the code of DNA binding specificity of TAL-type III effectors. *Science*, **326**, 1509-1512.
127. Mousson, L., Zouache, K., Arias-Goeta, C., Raquin, V., Mavingui, P. and Failloux, A.B. (2012) The native Wolbachia symbionts limit transmission of dengue virus in Aedes albopictus. *PLoS neglected tropical diseases*, **6**, e1989.
128. Joung, J.K. and Sander, J.D. (2013) TALENs: a widely applicable technology for targeted genome editing. *Nat Rev Mol Cell Biol*, **14**, 49-55.
129. Aryan, A., Anderson, M.A., Myles, K.M. and Adelman, Z.N. (2013) TALEN-Based Gene Disruption in the Dengue Vector Aedes aegypti. *PloS one*, **8**, e60082.

130. Craig, G.B., Jr. and Hickey, W.A. (1967) In Wright, J. W. and R., P. (eds.), *Genetics of Insect Vectors of Disease*. Elsevier, New York, pp. 67-131.
131. Czech, B., Preall, J.B., McGinn, J. and Hannon, G.J. (2013) A transcriptome-wide RNAi screen in the Drosophila ovary reveals factors of the germline piRNA pathway. *Mol Cell*, **50**, 749-761.
132. Morazzani, E.M., Wiley, M.R., Murreddu, M.G., Adelman, Z.N. and Myles, K.M. (2012) Production of virus-derived ping-pong-dependent piRNA-like small RNAs in the mosquito soma. *PLoS Pathog*, **8**, e1002470.
133. Akbari, O.S., Antoshechkin, I., Amrhein, H., Williams, B., Diloreto, R., Sandler, J. and Hay, B.A. (2013) The developmental transcriptome of the mosquito Aedes aegypti, an invasive species and major arbovirus vector. *G3*, **3**, 1493-1509.
134. Black, W.C.t., Bennett, K.E., Gorrochotegui-Escalante, N., Barillas-Mury, C.V., Fernandez-Salas, I., de Lourdes Munoz, M., Farfan-Ale, J.A., Olson, K.E. and Beaty, B.J. (2002) Flavivirus susceptibility in Aedes aegypti. *Arch Med Res*, **33**, 379-388.
135. Enserink, M. (2006) Infectious diseases. Massive outbreak draws fresh attention to little-known virus. *Science*, **311**, 1085.
136. Igarashi, A. (1978) Isolation of a Singh's *Aedes albopictus* cell clone sensitive to Dengue and Chikungunya viruses. *The Journal of general virology*, **40**, 531-544.
137. Adams, B. and Boots, M. (2010) How important is vertical transmission in mosquitoes for the persistence of dengue? Insights from a mathematical model. *Epidemics*, **2**, 1-10.
138. Miller, B.R., DeFoliart, G.R. and Yuill, T.M. (1977) Vertical transmission of La Crosse virus (California encephalitis group): transovarial and filial infection rates in *Aedes triseriatus* (Diptera: Culicidae). *J Med Entomol*, **14**, 437-440.
139. Galiana-Arnoux, D., Dostert, C., Schneemann, A., Hoffmann, J.A. and Imler, J.L. (2006) Essential function in vivo for Dicer-2 in host defense against RNA viruses in drosophila. *Nature immunology*, **7**, 590-597.
140. Li, H., Li, W.X. and Ding, S.W. (2002) Induction and suppression of RNA silencing by an animal virus. *Science*, **296**, 1319-1321.
141. Bailey, L., Newman, J.F. and Porterfield, J.S. (1975) The multiplication of Nodamura virus in insect and mammalian cell cultures. *The Journal of general virology*, **26**, 15-20.

142. Wiley, M.R. (2012) Doctoral Dissertation, Virginia Polytechnic Institute and State University, Proquest/UMI.
143. Anderson, M.A., Gross, T.L., Myles, K.M. and Adelman, Z.N. (2010) Validation of novel promoter sequences derived from two endogenous ubiquitin genes in transgenic Aedes aegypti. *Insect Mol Biol*, **19**, 441-449.
144. Karpf, A.R., Lenches, E., Strauss, E.G., Strauss, J.H. and Brown, D.T. (1997) Superinfection exclusion of alphaviruses in three mosquito cell lines persistently infected with Sindbis virus. *J Virol*, **71**, 7119-7123.
145. Xi, Z., Ramirez, J.L. and Dimopoulos, G. (2008) The Aedes aegypti toll pathway controls dengue virus infection. *PLoS Pathog*, **4**, e1000098.
146. Souza-Neto, J.A., Shuzhen Sim, George Dimopoulos. (2009) An evolutionary conserved function of the JAK-STAT pathway in anti-dengue defense. *Proc Natl Acad Sci*, **106**, 17841-17846.
147. Sim, S. and Dimopoulos, G. (2010) Dengue virus inhibits immune responses in Aedes aegypti cells. *PloS one*, **5**, e10678.
148. Dostert, C., Jouanguy, E., Irving, P., Troxler, L., Galiana-Arnoux, D., Hetru, C., Hoffmann, J.A. and Imler, J.L. (2005) The Jak-STAT signaling pathway is required but not sufficient for the antiviral response of drosophila. *Nature immunology*, **6**, 946-953.
149. Zambon, R.A., Nandakumar, M., Vakharia, V.N. and Wu, L.P. (2005) The Toll pathway is important for an antiviral response in Drosophila. *Proc Natl Acad Sci U S A*, **102**, 7257-7262.
150. Avadhanula, V., Weasner, B.P., Hardy, G.G., Kumar, J.P. and Hardy, R.W. (2009) A novel system for the launch of alphavirus RNA synthesis reveals a role for the Imd pathway in arthropod antiviral response. *PLoS Pathog*, **5**, e1000582.